Scuola di Dottorato di Ricerca in Scienze Biochimiche, Nutrizionali e Metaboliche

Dottorato di Ricerca in Scienze Biochimiche - XXVIII Ciclo

UNIVERSITÀ DEGLI STUDI DI MILANO

DIPARTIMENTO DI SCIENZE BIOMEDICHE
E CLINICHE "LUIGI SACCO"

THE ENDOCANNABINOID ENZYME MONOACYLGLYCEROL LIPASE: DEVELOPMENT OF A NEW FLUORESCENT ASSAY AND NOVEL INHIBITORS

Dott. Simone LAURIA

Matricola R10198

Tutor: Prof.ssa Pierangela CIUFFREDA

Direttore: Prof. Sandro SONNINO

Coordinatore del Dottorato: Prof. Francesco BONOMI

Anno Accademico 2014-2015

TABLE OF CONTENTS

LIST OF FIGURES

LIST OF TABLES

LIST OF SCHEMES

ABBREVIATIONS

2-AG *sn*-2-arachidonoyl glycerol
2-OG 2-oleyl glycerol
7-HCA 7-arachidonoyl-4-methyl-coumarin
7-HRA 7-hydroxyresorufinylarachidonate
AA arachidonic acid
AcCN acetonitrile
AEA anandamide, *N*-arachidonoyl ethanolamine
BSA bovine serum albumin
CB rec. cannabinoid receptor
CBD cannabidiol
CBN cannabinol
CDI carbonyl diimidazole
$CDCl_3$ deuterated chloroform
CD_3OD deuterated methanol
COX cyclooxygenase
DAG *sn*-1-acyl-2-arachidonoylglycerol
DCM dichloromethane
DMAP 4-dimethylaminopyridine
DMSO *N*,*N*-dimethyl sulfoxide
d_6-DMSO deuterated *N*,*N*-dimethyl sulfoxide
ECs endocannabinoids
ECS endocannabinoid system
EDTA ethylendiaminetetraacetic acid
EMT endocannabinoids membrane transporter
EtOAc ethyl acetate
FAAH fatty acid amide hydrolase
F.U fluorescence units
GDE1 glycerophosphodiesterase 1
GPCR G-protein coupled receptor
GP-NAE glycerophospho-*N*-acyl ethanolamine
HPLC high performance liquid chromatography
MAGL monoacylglycerol lipase
hMAGL human recombinant monoacylglycerol lipase
lyso-PI *sn*-1-lysophospholipid
lyso-PLC lysophosphatidylinositol-selective phospholipase C
MAFP methyl arachidonyl fluorophosphonate
MeOH methanol
NAAA *N*-acylethanolamine-hydrolysing acid amidase
NADA *N*-arachidonoyl dopamine
NAEs *N*-acyl ethanolamines
NAPE *N*-acyl-phophatidyl ethanolamine

NAPE-PLD NAPE-phospholipase D
NAT *N*-acyl trasferase
OEA *N*-oleoyl ethanolamine
pAEA phospho-*N*-arachidonoyl ethanolamine
PEA *N*-palmitoyl ethanolamine
PBS phosphate buffered saline
PA phosphatidic acid
PE phosphatidyl ethanolamine
PI phosphatidylinositol
PLA1 phospholipase A1
PLC phospholipase C
PTPN22 phosphatase protein tyrosine phosphatase 22
SEA *N*-stearoyl ethanolamine
THC tetrahydrocannabinol

INTRODUCTION

1. THE ENDOCANNABINOID SYSTEM

The history of the endocannabinoid system (ECS) started very far away in the time: in fact, the Indian and Chinese populations, for the treatment of pain and anxiety, reported the use of *Cannabis Sativa* plants more than three thousand years ago[1].

In addition to cannabis fibres, also seeds, leaves, flowers and extracts have been used in medicine and in social or religious rituals of different cultures for thousands of years.

Over the centuries, cannabis has also been used as anaesthetic and anthelmintic, in the treatment of diarrhoea, migraine, spasmodic asthma and to treat opiates' and alcohol's withdrawal symptoms.

More recently in history (1964), the structure of the main active component Δ^9-THC (tetrahydrocannabinol) was described[2], opening the field for the comprehension of action's mechanism of this molecule and its related analogues, which are a pool of more than 80 compounds.

Among these molecules, that are the so - called "Cannabinoids" (**fig. 1**), the most important in terms of activity are tetrahydrocannabinol (Δ^9-THC), cannabinol (CBN) and cannabidiol (CBD).

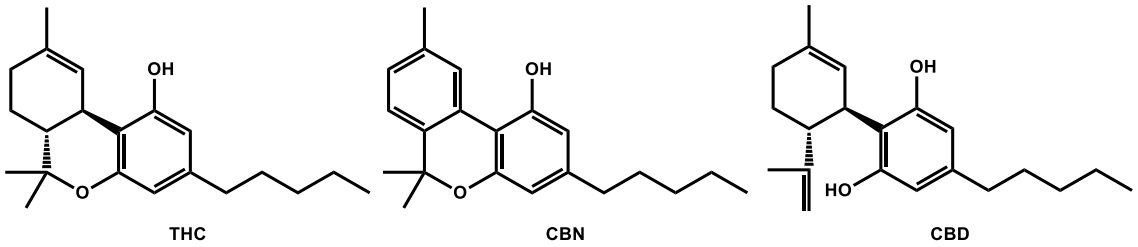

Fig. 1: Cannabis Sativa's main components

The description of Δ^9-THC structure and the understanding that its activity was stereochemistry-dependent[3] led to the hypothesis of a receptor-driven mechanism of action[4].

In early 90's, an orphan G-protein coupled receptor (GPCR) that bound cannabinoids (with the expected affinity and stereo selectivity) was discovered and named CB_1 cannabinoid receptor[5], followed very soon by another receptor with peripheral localisation - the CB_2 cannabinoid receptor[6].

Since then, researchers have made major progress due to the discovery of their endogenous ligands and the enzymes responsible for the synthesis and inactivation of these molecules.

This complex signalling system is known as endocannabinoid system (ECS).

The core of endocannabinoid system functioning are derivatives of unsaturated fatty acids with ethanolamine, glycerol, or glycerol ether head groups and are known as "Endocannabinoids" (ECs).

[1] Russo, E. B. et al.; Chem. *Biodivers.* 4, **2007**, 1614-1648. History of cannabis and its preparations in saga, science, and sobriquet.
[2] Gaoni, Y. et al.; *J. Am. Chem. Soc.*, 86, **1964**, 1646-1647. Isolation, structure and partial synthesis of an active constituent of hashish
[3] Mechoulam, R. et al.; *Prog. Med. Chem.*, 24, **1987**, 159-207. Towards cannabinoid drugs.
[4] Little, P. J. et al.; *J. Pharmacol. Exp. Ther.*, 247, **1988**, 1046-1051. Pharmacology and stereoselectivity of structurally novel cannabinoids in mice.
[5] Matsuda, L. A. et al.; *Nature*, 346, **1990**, 561-564. Structure of a cannabinoid receptor and functional expression of the cloned cDNA.
[6] Munro, S. et al.; *Nature*, 365, **1993**, 61-65. Molecular characterization of a peripheral receptor for cannabinoids.

The structures of the most important endocannabinoids are shown in **fig. 2**: the first to be isolated was anandamide (*N*-arachidonoyl ethanolamine, AEA)[7], followed by other ethanol amine derivatives. such *N*-homo-γ-linolenoyl ethanolamine and N-docosatetraenoyl ethanolamine[8].

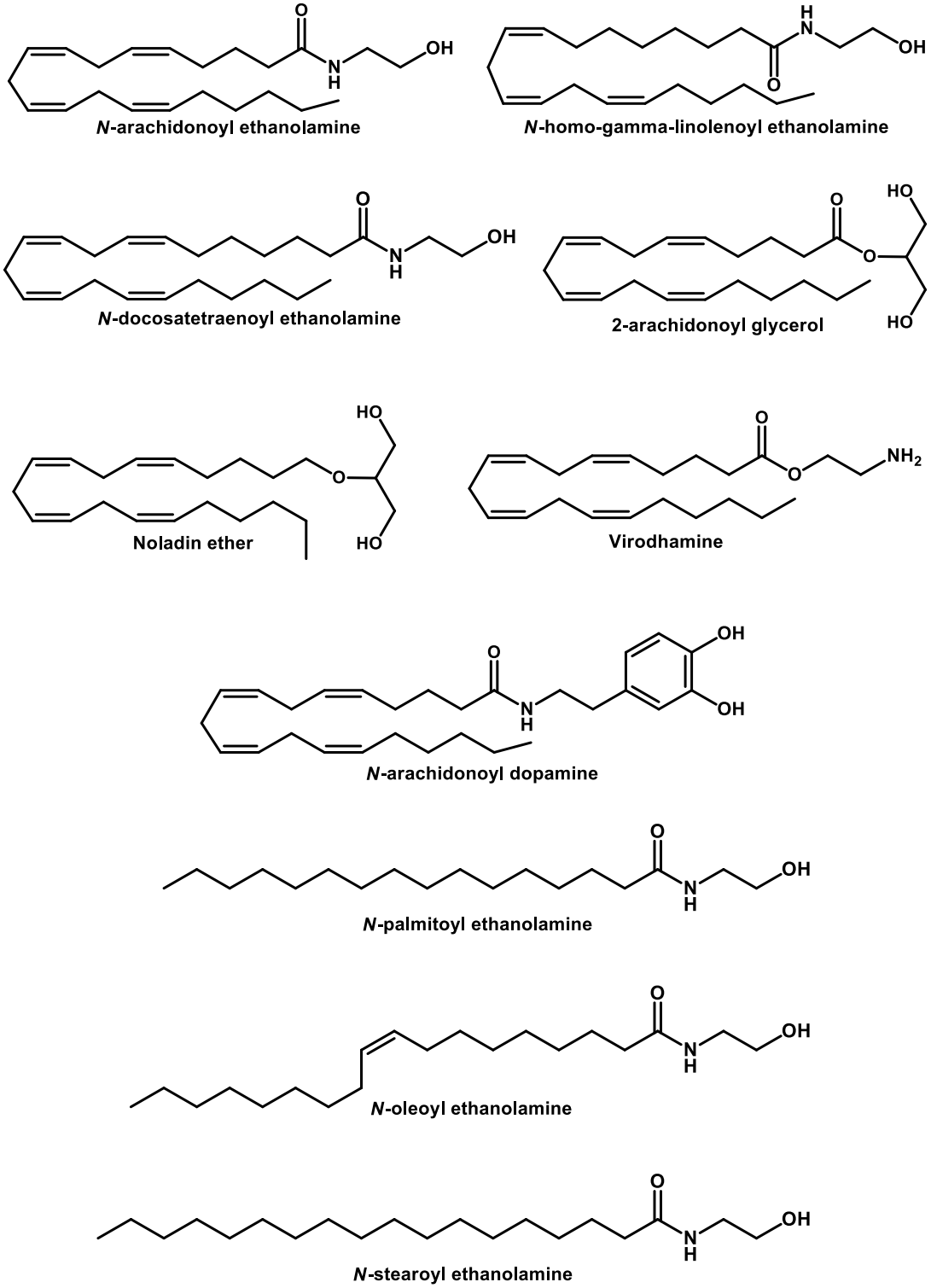

Fig. 2: Endocannabinoids structures

[7] Devane, W. A. et a.; *Science*, 258 (5090), **1992**, 1946-1949. Isolation and structure of a brain constituent that binds to the cannabinoid receptor.
[8] Hanus, L. et al.; *J. Med. Chem*., 36 (20), **1993**, 3032-3034. Two new unsaturated fatty acid ethanolamides in brain that bind to the cannabinoid receptor.

Afterwards, the second most important endogenous compound *sn*-2-arachidonylglycerol (2-AG)[9] was described, and showed to be present in the brain in much higher concentration than AEA (170-fold)[10]. An additional glycerol-related compound, 2-eicosa-5',8',11',14'-tetraenylglycerol (2-AG ether, noladin ether) was identified[11], followed by other endogenous cannabinoids such *N*-arachidonoyl dopamine (NADA)[12] and virodhamine[13].

The identification of endogenous ligands for CB receptors brought to light the enzymes that are responsible for the inactivation of these molecules.

The Fatty Acid Amide Hydrolase (FAAH)[14] acting prevalently on AEA; the Monoacylglycerol Lipase (MAGL)[15], dedicated to the block of monoacylglycerols; the *N*-Acylethanolamine-hydrolysing Acid Amidase (NAAA)[16] responsible for the hydrolysis of different *N*-acyl ethanolamines (NAEs), such *N*-palmitoyl ethanolamine (PEA), *N*-oleoyl ethanolamine (OEA) and *N*-stearoyl ethanolamine (SEA).

The complexity of the system, the large number of molecules implied in its functioning and the deep involvement of Ecs in many physiological and pathological conditions[17], justify the great interest around this field, about which – at the moment – we are far from a complete understanding.

[9] Mechoulam, R. et al.; *Biochem. Pharmacol.*, 50, **1995,** 83-90. Identification of an endogenous 2-monoglyceride, present in canine gut, that binds to cannabinoid receptors.

[10] Stella, N. et al.; *Nature*, 388 (6644), **1997**, 773-778. A second endogenous cannabinoid that modulates long-term potentiation.

[11] Hanus, L. et al.; *Proc. Natl. Acad. Sci. USA,* 98 (7), **2001,** 3662-3665. 2-arachidonyl glyceryl ether, an endogenous agonist of the cannabinoid CB1 receptor.

[12] Bezuglov, V. et al*.; Bioorg Med Chem Lett,* 11 (4), **2001**, 447-449. Synthesis and biological evaluation of novel amides of polyunsaturated fatty acids with dopamine.

[13] Porter, A. C. et al.*; J Pharmacol Exp Ther*, 301 (3), **2002**, 1020-1024. Characterization of a novel endocannabinoid, virodhamine, with antagonist activity at the CB1 receptor.

[14] Cravatt, F. et al.; *Proc. Natl. Acad. Sci. USA,* 94, **1997**, 2238-2242. Molecular characterization of human and mouse fatty acid amide hydrolases.

[15] Boyer, J. et al.; *J. Clin. Endocrinol. Metab.* 53, **1981**, 143-148. Human Erythrocyte Monoester Lipase: Characterization and Radiochemical Assay of the Cell-Bound Enzyme in Normal Subjects.

[16] Tsuboi, K. et al.*; CHEMISTRY & BIODIVERSITY*, 4, **2007**, 1914-925. The N-Acylethanolamine Hydrolyzing Acid Amidase (NAAA).

[17] Di Marzo, V. et al.; *Curr Opin Lipidol*, 18, **2007**, 129-140. Endocannabinoids and the regulation of their levels in health and disease.

1.1 Biosynthesis and release of endocannabinoids

The biosynthesis of endocannabinoids is a complex process which occur at the level of post-synaptic cells only after the arrival of an adequate signal; in fact, the Ecs are known to be post-synaptic retrograde mediators – thing that justify, for example, their implication in synaptic plasticity modulating the signals mediated by other transmitters[18].

The depolarisation of the post-synaptic cell is mediated by the release, from the pre-synaptic one, of different neurotransmitters in the synaptic space.

The interaction between the transmitter and its post-synaptic receptor can trigger different effects (inhibition, excitation, second messenger cascade's activation) and – basing on the type of cell – it can produce the on-site synthesis and release of 2-AG, AEA or other Ecs[19], through the elevation of intracellular calcium.

1.1.1 Endocannabinoid signalling via Anandamide

Anandamide (AEA) was the first endogenous cannabinoid isolated and characterized, acting as agonist on the same receptors of THC.

AEA is predominantly generated *in vivo* from phospholipid precursors (**scheme. 1**): and subsequently degraded intracellularly by fatty acid amide hydrolase (FAAH).

The depolarisation-induced influx of calcium into the post-synaptic neuron causes the activation of an enzyme called *N*-acyl trasferase (NAT); this enzyme catalyses the first conversion necessary for Ecs biosynthesis, transforming membrane's phosphatidyl ethanolamine (PE) into *N*-acyl-phophatidyl ethanolamine (NAPE)[20].

A first direct way leading to the formation of NAEs is NAPE hydrolysis by a Ca^{2+}-sensitive NAPE-phospholipase D (NAPE-PLD), which seems to be kept in a constitutively active form[21].

The evidence that low calcium levels are not correlated to a complete block of NAEs biosynthesis[22], suggests the existence of other different synthetic pathways.

One pathway passes through the formation of Lyso-NAPE and glycerophospho-NAE (GP-NAE) thanks to a double O-deacylation of NAPE[23]; the action of a Lyso-PLD on Lyso-NAPE and of an enzyme called glycerophosphodiesterase 1 (GDE1) on GP-NAE leads to the formation of NAEs.

---

[18] Kano, M. et al.; *Physiol. Rev.,* 89, **2009**, 309-380. Endocannabinoid-mediated control of synaptic transmission.

[19] Pertwee, R. G. et al.; *Br. J. Pharmacol.,* 153 (2), **2010**, 199-215. The diverse CB1 and CB2 receptor pharmacology of three plant cannabinoids: delta9-tetrahydrocannabinol, cannabidiol and delta9-tetrahydrocannabivarin.

[20] Di Marzo, V.et al.; *Nature* 372, **1994**, 686-691. Formation and inactivation of endogenous cannabinoid anandamide in central neurons.

[21] Wang, J. et al.; *Neuropharmacology,* 54, **2008**, 8-15. The stimulatory effect of phosphatidylethanolamine on N-acylphosphatidylethanolamine-hydrolyzing phospholipase D (NAPE-PLD).

[22] Leung, D. et al.; *Biochemistry, 45,* **2006**, 4720-4726. Inactivation of N-acyl phosphatidylethanolamine phospholipase D reveals multiple mechanisms for the biosynthesis of endocannabinoids.

[23] Simon, G.M. et al.; *J. Biol. Chem.,* 281, **2006**, 26465-26472. Endocannabinoid biosynthesis proceeding through glycerophospho-N-acyl ethanolamine and a role for alpha/beta-hydrolase 4 in this pathway.

In particular, the action of GDE1 is higher for C16:0, C18:1, C20:4, which are the substrates least affected by NAPE-PLD activity[24].

Another pathway passes through the action of *phospholipase C* (PLC) that releases 6hosphor-*N*-arachidonoyl ethanolamine (pAEA) from NAPE; the following cleavage by phosphatase protein tyrosine phosphatase (PTPN22) leads to the formation of AEA[25].

The characterization of at least three important pathways through which NAEs are synthesized poses questions about the selectivity of action of each one.

Depending on the acyl chain, the phospholipid membrane composition at the site of synthesis and the tissue conditions, one pathway would be preferred over the others leading to different NAEs; for example, the opposite regulation of NAPE-PLD and PTPN22 expression in macrophages under LPS (lipopolysaccharide) stimulation suggests that PTPN22 is responsible for activity-dependent AEA production rather than NAPE-PLD[26].

Moreover, the block of a synthetic pathway would be compensate by the increased activation of another one, leading to different levels for each NAE[27].

[24] Simon, G.M. et al.; *J. Biol. Chem.,* 283, **2008**, 9341-9349. Anandamide biosynthesis catalyzed by the phosphodiesterase GDE1 and detection of glycerophospho-N-acyl ethanolamine precursors in mouse brain.

[25] Liu, J. et al.; *Neuropharmacology,* 54, **2008**, 1-7. Multiple pathways involved in the biosynthesis of anandamide.

[26] Liu, J. et al.; *Proc. Natl. Acad. Sci. USA, 103,* **2006**, 13345-13350. A biosynthetic pathway for anandamide.

[27] Sun, Y. X. et al.; *Biochem. J.,* 380, **2004**, 749-756. Biosynthesis of anandamide and N-palmitoylethanolamine by sequential actions of phospholipase A2 and lysophospholipase D.

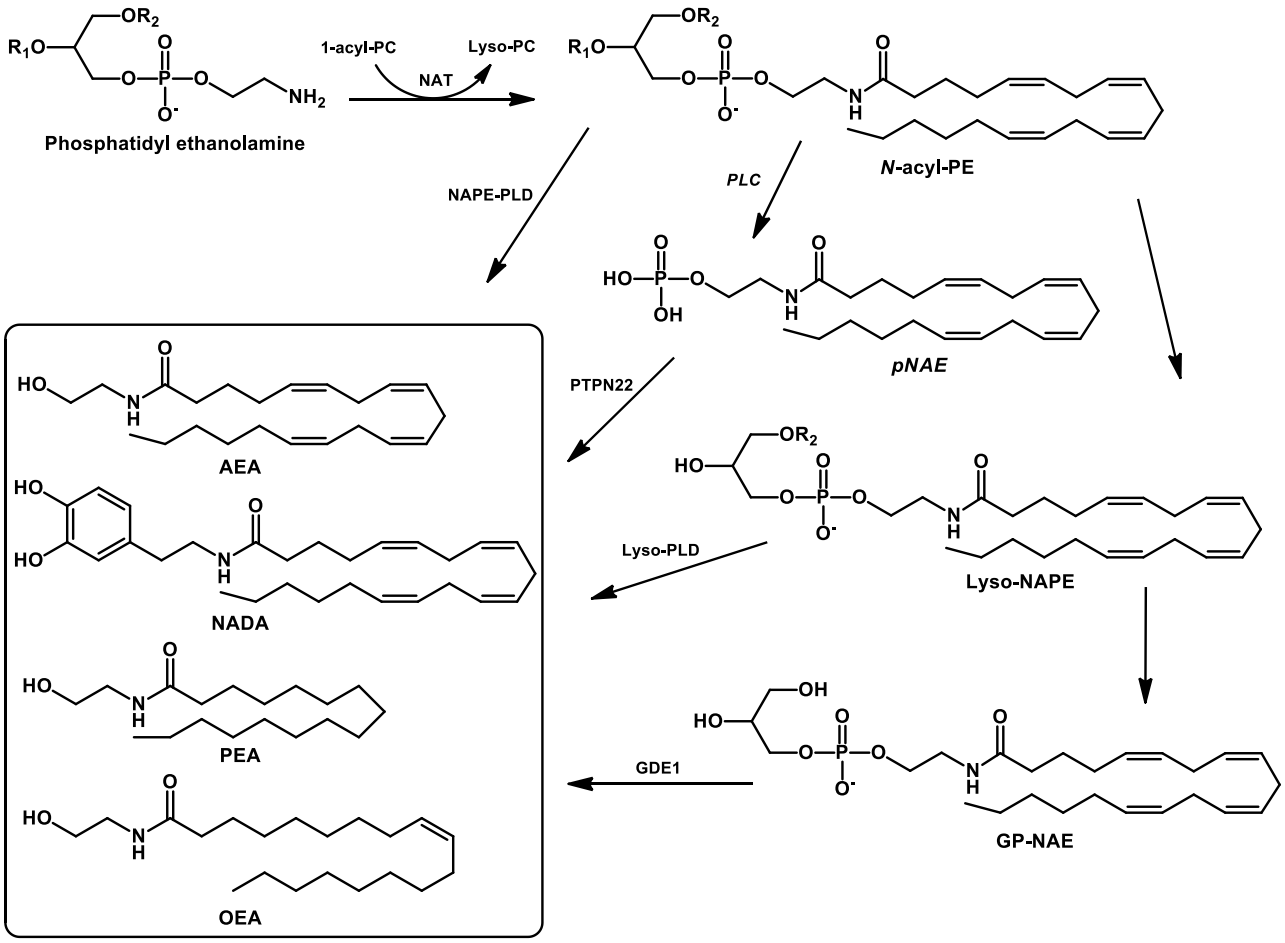

Scheme 1: AEA and other NAEs biosynthesis

1.1.2 Endocannabinoid signalling via 2-arachidonoylglycerol

2-arachidonoylglycerol (2-AG) is an endogenous cannabinoid receptor ligand, which binds to both central and peripheral cannabinoid receptors, eliciting a variety of cannabinergic responses *in vitro* and *in vivo*.

2-AG functions as a retrograde synaptic neurotransmitter modulating both inhibitory GABAergic and excitatory glutamatergic signaling, it is more abundant than AEA in the brain and it is considered the main endocannabinoid signalling molecule.

As shown for NAEs, different synthetic pathways are responsible for the production of 2-AG (**scheme 2**); the first and more direct one gives 2-AG by the action of a classic lipase, cleaving the residues in position 1 and 3 of a triacylglycerol containing the arachidonic acid in position 2.

Another mechanism passes from a two steps pathway, via generation of *sn*-1-acyl-2-arachidonoylglycerol (DAG) from phosphatidylinositol (PI) by PLC activity and subsequent hydrolysis of the produced DAG by a diacylglycerol lipase (*sn*-1-DAG lipase)[28]. It has been

[28] Stella, N. et al.; *Nature,* 388, **1997**, 773-778. A second endogenous cannabinoid that modulates long-term potentiation.

demonstrated that cellular activity of these two enzymes highly correlates with 2-AG production, and their inhibition results in the decreasing of this endocannabinoid mediator[29].

DAG can be obtained from phosphatidic acid (PI) by the action of phosphatidic acid phosphohydrolase (PA-phosphohydrolase), which is an alternative pathway than the PLC one[30].

The third biosynthetic route passes through the *sn*-1-lysophospholipid (lyso-PI) which, with the subsequent action of phospholipase A1 (PLA1) and lysophosphatidylinositol-selective phospholipase C (lyso-PLC) gives 2-AG[31].

It is important to keep in mind that most of these mediators are intermediates of different pathways, and not all of them are involved in the physiological cannabinoid signalling process.

Moreover, the synthesis of 2-AG seems to be related to different stimuli, and it is connected to the activation of the different synthetic pathways.

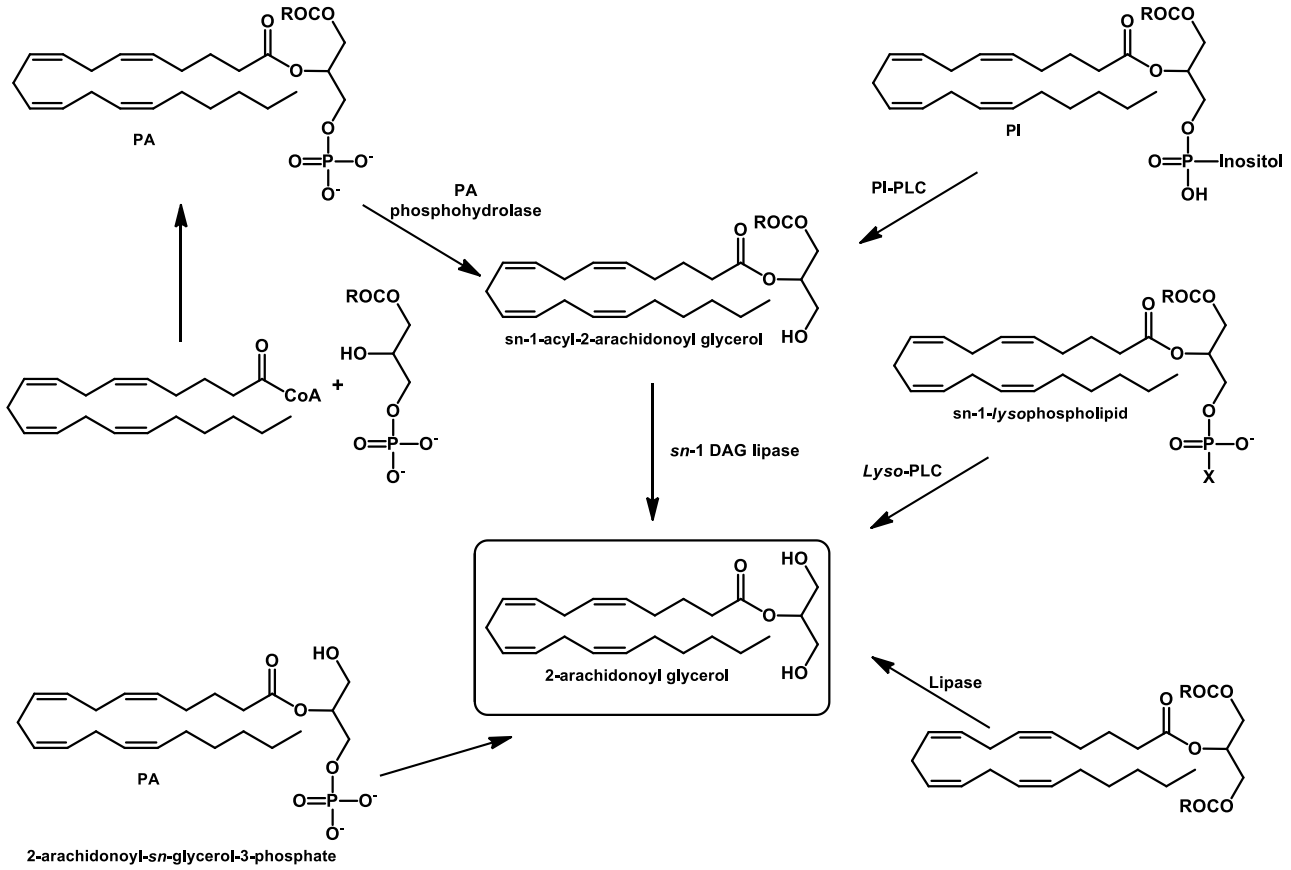

Scheme 2: 2-AG biosynthesis

[29] Bisogno, T. et al.; *J. Cell Biol.*, 163, **2003**, 463-468. Cloning of the first sn1-DAG lipases points to the spatial and temporal regulation of endocannabinoid signaling in the brain.

[30] Bisogno, T. et al.; *J. Neurochem.*, 72, **1999**, 2113-2119. Phosphatidic acid as the biosynthetic precursor of the endocannabinoid 2-arachidonoylglycerol in intact mouse neuroblastoma cells stimulated with ionomycin.

[31] Ueda, H. et al.; *J. Neurochem.*, 61, **1993**, 1874-1881. A possible pathway of phosphoinositide metabolism through EDTA-insensitive phospholipase A1 followed by lysophosphoinositide-specific phospholipase C in rat brain.

1.1.3 Endocannabinoids release

The biosynthesis occurring after the arrival of the appropriate stimuli is immediately followed by the release of Ecs in the synaptic space, through a mechanism that is not completely clear but that seems to be mediated by the action of an "endocannabinoid membrane transporter" (EMT), responsible also for the internalisation at the level of the presynaptic cell.

This idea is supported by different observations:

- loading cells with radiolabelled AEA leads to the release of the compound with a temperature-dependent mechanism which is possible to inhibit pharmacologically[32];
- selective inhibitors of AEA cellular uptake can inhibit the release of *de novo* synthesised AEA, with increase of post-synaptic intracellular AEA levels[33].

[32] Hillard, C. J. Et al.; *J Neurochem*, 69, **1997**, 631-638. Accumulation of N arachidonoylethanolamine (anandamide) into cerebellar granule cells occurs via facilitated diffusion.

[33] Ligresti, A. et al.; *Biochem J*, 380, **2004**, 265-272. Further evidence for the existence of a specific process for the membrane transport of anandamide.

1.2 Cannabinoid receptors CB_1/CB_2 and retrograde mechanism of Ecs

A great advancement in the understanding of the endocannabinoid system was made in the 90's, with the discovery of the endogenous target on which *cannabis sativa*'s extract worked.

In a very short period, two different type of receptors were identified and described: the CB_1 and CB_2 receptors.

Endocannabinoids act, by definition, on these two receptors that are the physiological target for their activity; obviously, they have different affinities and efficacy:

- AEA and NADA are more selective for the CB_1 type, with the following order of affinities AEA > NADA;
- AEA is a partial agonist on CB_1 and is almost inactive on CB_2[34];
- 2-AG has almost the same affinity for both types of receptors and acts as a full agonist on both[35];
- Virhodamine is an antagonist for CB_1 and a partial agonist for CB_2[36];

Other non-CB receptors responding to high level of endocannabinoids – and of AEA in particular – were identified:

- vanillyl fatty acid amide receptors[37], isolated in murine astrocytes;
- AEA/abnormal cannabidiol receptor[38], another GPCR rec. for AEA and the non-psychotropic cannabinoid identified in vascular endothelial cells, which mediate the local vasodilating effect of AEA;
- saturated NAE-receptors[39], proposed to mediate some of the analgesic and anti-inflammatory effects of PEA;
- vanilloid TRPV1 receptor[40], site of action of capsaicin (component of pungent red pepper) activated by the action of AEA and NADA;
- peroxisome proliferator-activated receptor (PPAR), in particular PPARα, mediates the analgesic effect of PEA[41], and other types are bound by AEA and 2-AG[42].

---

[34] McAllister, S. D. et al.; *Prostaglandins Leukot Essent Fatty Acids*, 66, **2002**, 161-171. CB(1) and CB(2) receptor mediated signalling: a focus on endocannabinoids.

[35] Di Marzo, V. et al.; *Prostaglandins Leukot Essent Fatty Acids*, 53, **1995**, 1-11. Anandamide, an endogenous cannabinomimetic eicosanoid: 'killing two birds with one stone'.

[36] Porter, A. C. et al.; *J Pharmacol Exp Ther*, 301, **2002**, 1020-1024. Characterization of a novel endocannabinoid, virodhamine, with antagonist activity at the CB1 receptor.

[37] Sagan, S. et al.; *Eur J Neurosci,* 11, **1999**, 691-699. Anandamide and WIN 55212-2 inhibit cyclic AMP formation through G-protein-coupled receptors distinct from CB1 cannabinoid receptors in cultured astrocytes.

[38] Jarai, Z. et al.; *Proc. Natl. Acad. Sci. USA,* 96, **1999**, 14136-14141. Cannabinoid-induced mesenteric vasodilation through an endothelial site distinct from CB1 or CB2 receptors.

[39] Franklin, A. et al.; *J Neurosci,* 23, **2003**, 7767-7775. Palmitoylethanolamide increases after focal cerebral ischemia and potentiates microglial cell motility.

[40] Szallasi, A. et al.;*Pharmacol Rev,* 51, **1999**, 159-212. Vanilloid (Capsaicin) receptors and mechanisms.

[41] Sun, Y. et al.; *Br J Pharmacol.,* 152 (5), **2007**; 734-743. Cannabinoid activation of PPAR alpha; a novel neuroprotective mechanism.

[42] Lenman, A. et al.; *Br J Pharmacol.*, 151 (8), **2007**; 1343–1351. Interaction of ligands for the peroxisome proliferator-activated receptor gamma with the endocannabinoid system.

Both CB_1 and CB_2 receptors are G-protein coupled receptors, that share little sequence homology, 44% at the protein level or 68% in the transmembrane domains – which are thought to contain the binding sites for the Ecs[43].

As anticipated, Ecs action mechanism is realised through a retrograde signalling: the depolarisation of the post-synaptic neuron caused by Ca^{2+} influx produces the activation of the biosynthetic ways and the formation/liberation of the endocannabinoids; the newly synthesised Ecs travel in the synaptic space, bind the pre-synaptic CB receptors and operate with an inhibitory effect on transmitters' release.

CB receptors couple to the adenylate cyclase through $G_{i/o}$ subtypes of G-proteins, and that causes – after ligand binding – the block of cyclase activity, the reduction of calcium influx and the decrease of transmitters vesicles' release.

The receptors couple also to the system of phosphatidylinositol-3-phosphate kinase, which take a role as second messenger in addition to the adenylate cyclase system.

Overall, this chain of events leads to a temporary or more persistent dimming of inhibitory currents at GABAergic and of excitatory currents glutamatergic synapsis respectively[44].

The different effects observed in the endocannabinoid system are related to the type of ligand, the receptor activated and the tissue localisation, which is a fundamental parameter for the understanding of the system and of the possible druggability.

1.2.1 CB_1 receptors

In general, CB_1 are highly expressed throughout the brain by many classes of neurons, and in lower level are present in glia cells and many peripheral cell lines[45]; they are abundantly expressed in GABAergic interneurons and less in glutamatergic principal neurons[46].

CB_1 couple to $G_{i/o}$ proteins and modulate the activity of different ion channels and second messenger, and the different modulation of cell functions depends by their acute versus sustained activation[47].

For example, neuronal CB_1 receptors acute activation (milliseconds or seconds) inhibits pre-synaptic N-type Ca^{2+}-channels and activate K^+-channels reducing neurotransmission and controlling excitability[48].

[43] Marsicano, G. et al.; *Nature,* 418, **2002**, 530-534. The endogenous cannabinoid system controls extinction of aversive memories.
[44] Rhee, M. H: et al.; *J. Neurochem.,* 71 (4), **1998**, 1525-1534. Cannabinoid Receptor Activation Differentially Regulates the Various Adenylyl Cyclase Isozymes.
[45] Howlett, A. C. et al.; *Pharmacol Rev.*, 54, **2002**; 161-202. International Union of Pharmacology. XXVII. Classification of cannabinoid receptors.
[46] Uchigashima, M. et al.; *J Neurosci.*, 27(14), **2007**; 3663-3676. Subcellular arrangement of molecules for 2-arachidonoyl-glycerol-mediated retrograde signaling and its physiological contribution to synaptic modulation in the striatum.
[47] Straiker, A. et al.; *AAPS J.,* 8 (2), **2006**; 272-276. Cannabinoids, electrophysiology, and retrograde messengers: challenges for the next 5 years.
[48] Marinelli, S. et al.; *Nat Neurosci.*, 12(12), **2009**; 1488–1490. Self-modulation of neocortical pyramidal neurons by endocannabinoids.

CB_1 sustained activation (minutes or hours) results on the other hand, in the stimulation of intracellular signalling, such through ERK, modifying the activity of enzymes and the expression of specific genes[49].

1.2.2 CB_2 receptors

CB_2 receptors display a different pharmacological profile and tissue localisation than the CB_1 type[50]. They are not expressed in healthy brain tissue, with exceptions of a small neurons' population in the brain stem and in the cerebellum[51]; furthermore, CB_2 receptors expression can be induced in many immune cells thus, in particular conditions of neuroinflammation, these receptors could be up-regulated by specific cell populations in the brain[52].

CB_2 receptors population is typical of immune system cells, and was identified in different immune subpopulations with the following ranking related to the expression level: B-cells, natural killer cells, monocytes, neutrophils, CD8 T-cells, CD4 T-cells, tonsils, spleen, thymus cells[53].

With this distribution, it is easy to understand the importance of CB_2 receptors for what concerns immune system functions, the role that can be played by the ECS in inflammation processes and responses to infections and cancers.

[49] Marsicano, G. et al.; *Science*, 302, **2003**, 84-88. CB1 cannabinoid receptors and on-demand defense against excitotoxicity.
[50] Felder, C. C. et al.; *Mol Pharmacol.,* 48 (3), **1995**, 443-450. Comparison of the pharmacology and signal transduction of the human cannabinoid CB1 and CB2 receptors.
[51] Van Sickle, M. D. et al.; *Science*, 310 (5746), **2005**; 329-332. Identification and functional characterization of brainstem cannabinoid CB2 receptors.
[52] Nunez, E. et al.; *Synapse*, 53 (4), **2004**; 208-213. Cannabinoid CB2 receptors are expressed by perivascular microglial cells in the human brain: an immunohistochemical study.
[53] Galiegue, S. et al.; *Eur. J. Biochem.,* 232, **1995**, 54-61. Expression of central and peripheral cannabinoid receptors in human immune tissues and leukocyte subpopulations.

1.3 Endocannabinoids degradation

Once released in the extracellular space (**fig. 3**), Ecs act prevalently – with varying selectivity – on cannabinoid receptors (CB_1 and CB_2); however, AEA and NADA can also act – previously to their release – on intracellular sites, such the vanilloid TRPV1 (transient receptor potential vanilloid type 1) ion channels, or T-type Ca^{2+} ion channels. In these cases, their release in the extracellular compartment seems to be a way to inactivate the action of these endocannabinoids, rather than to facilitate their action.

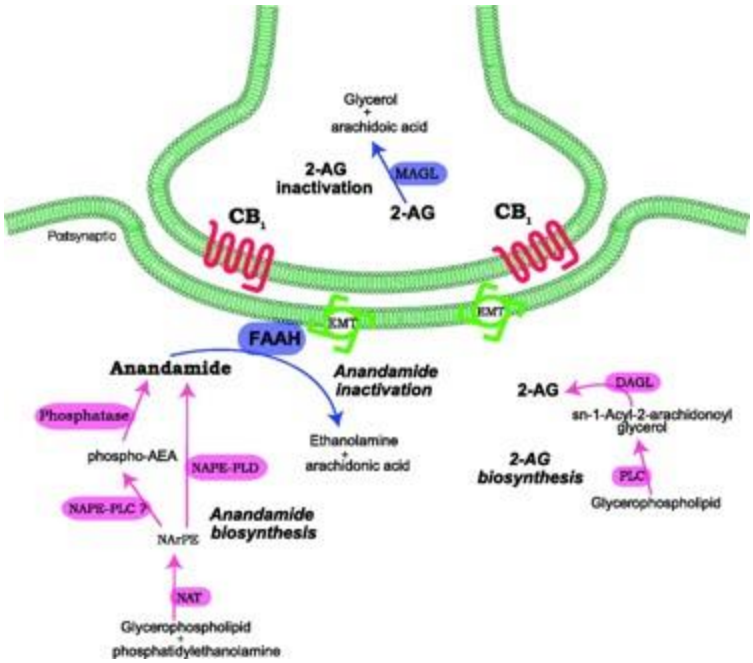

Fig. 3: Synaptic junction (from *Current Medicinal Chemistry 17 (24), 2010*)

The fate of Ecs is strictly correlated to their reuptake by the pre-synaptic and the post-synaptic cells. In fact, after the action on CB receptors their activity is rapidly terminated by the internalisation in the cells, followed by their hydrolytic inactivation by the deputed enzymes: the Fatty acid amide hydrolas*e* (FAAH), the Monoacylglycerol lipase (MAGL) and the *N*-acyl ethanolamine-hydrolysing acid amidase (NAAA).

It has been demonstrated that, when incubated with intact cells, the Ecs are rapidly cleared away from the extracellular medium[54]; as previously said, this process depends on the presence of a membrane transporter (EMT) which is responsible for the uptake of the Ecs from the extracellular to the intracellular spaces.

The evidence that the process is saturable, sensitive to temperature, selective for polyunsaturated long-chain fatty acid derivatives and sensitive to inhibitors, supports the hypothesis[55]

[54] Di Marzo, V. et al.; *Nature*, 372, **1994**, 686-691. Formation and inactivation of endogenous cannabinoid anandamide in central neurons.
[55] Beltramo, M. et al; *Neuroreport*, 11, **2000**, 1231-1235. Carrier-mediated transport and enzymatic hydrolysis of the endogenous cannabinoid 2-arachidonylglycerol.

However, the high lipophilic nature of the Ecs seems to be responsible for their natural reuptake, mediated by a passive diffusion mechanism driven by the intracellular enzymatic activity, which maintains the gradient between the inside and the outside of the cell[56].

Taken together, these data suggest that, even if the intracellular hydrolysis has a great influence on the rate of Ecs facilitated diffusion, the existence of an EMT – subjected to regulation – is fundamental for the fate of the endocannabinoids[57]; in fact, their reuptake is immediately followed by the inactivation by the hydrolytic enzymes, which bring the stop signal to the system.

It is important to remember that in addition to the enzymes strictly correlated to the endocannabinoid system (MAGL, FAAH, NAAA), the presence of long-chain polyunsaturated fatty acid derivatives calls in also other enzymes.

Most of all, part of the Ecs degradation is related to the action of cyclooxygenase-2 (COX-2).

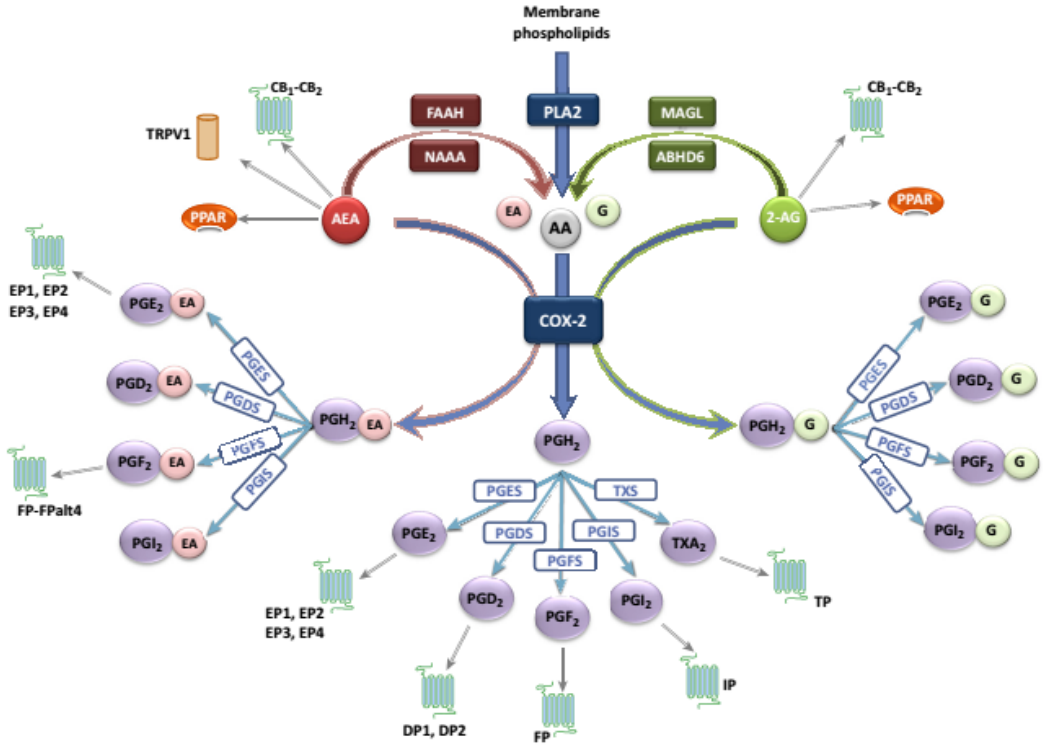

Fig. 4: Possible Ecs degradation pathways (from *Trends in pharmacological sciences, 35, 2014*)

In fact, as shown in **fig. 4,** the production of arachidonic acid (AA) from the Ecs hydrolysing enzymes, leads to the liberation of great amounts of this mediator, which can enter its classical cascade for the synthesis of prostaglandins, leukotrienes and thromboxanes[58].

[56] Deutsch, D. G. et al.; *J Biol Chem* , 276, **2001**, 6967-6973. The cellular uptake of anandamide is coupled to its breakdown by fatty-acid amide hydrolase.

[57] Glaser, S. T. et al.; *Proc. Natl. Acad. Sci. USA*, 100, **2003**, 4269-4274. Evidence against the presence of an anandamide transporter.

[58] Alhouayek, M. et al.; *Trends Pharmacol. Sci,* 35 (6), **2014**, 1925-1938. COX 2-derived endocannabinoid metabolites as novel inflammatory mediators

1.3.1 Fatty Acid Amide Hydrolase

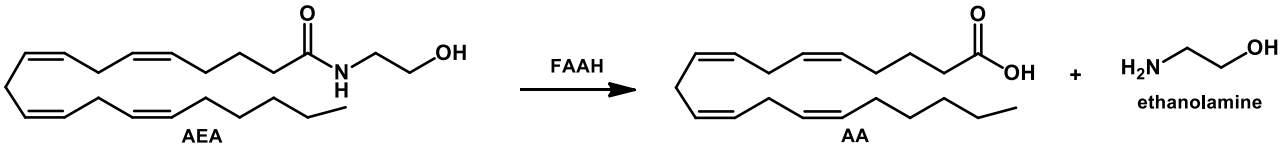

Scheme 3: AEA hydrolysis by FAAH

The Fatty acid amide hydrolase (FAAH) is the enzyme responsible for the cleavage and inactivation of AEA (**scheme 3**).

The action spectra of the enzyme is wider than this; in fact, in addition to AEA it can hydrolase a small amount of 2-AG, PEA and other NAEs[59].

Furthermore, its localisation is specifically post-synaptic, and for this reason, the degradation of AEA occurs at the level of the post-synaptic cell, requiring the intervention of the endocannabinoid membrane transporter to internalise the endogenous ligand[60].

FAAH is an integral membrane enzyme that seems to be able to organise in oligomers at membrane level, forming an over-structure that is necessary to take interaction with its substrates[60]; the enzyme crystallises in a dimeric structure, indicating that it is at least a dimer in solution[61].

Its intricate membrane binding structure may facilitate the movement of its substrates directly from the bilayer to the active site – which is directed toward the intracellular compartment – without the need of transporting these substrates through the aqueous cytosol, but thanks to the existence of different channels in the FAAH structure[61].

These channels grant the enzyme simultaneous access to both the membrane and the cytoplasmic compartments of the cell; at least three channels have been described to be important in substrates recruitment and recognition[62], and one of those has amphipathic features in order to manage both the hydrophobic long acid chains and the hydrophilic head groups

In this model, after substrates' entrance through the membrane to the active site, and following hydrolysis, the liberated fatty acid (hydrophobic) and amine (hydrophilic) products would exit through the membrane-access and cytosolic-access channels, respectively.

The cytoplasmic channel is needed also to provide the entry of a water molecule that is required for deacylation of the FAA-FAAH acyl-enzyme intermediate[63].

---

[59] Cravatt, B.F, et al.; *Nature*., 384 (6604), **1996**, 83-87. Molecular characterization of an enzyme that degrades neuromodulatory fatty-acid amides.

[60] Patricelli, M. P. et al.; *Biochemistry*,37(43), **1998**, 15177-15187. Comparative Characterization of a Wild Type and Transmembrane Domain-Deleted Fatty Acid Amide Hydrolase: Identification of the Transmembrane Domain as a Site for Oligomerization.

[61] Bracey, M.H. et al.; *Science*, 15, **2002**, 1793-1796. Structural Adaptations in a Membrane Enzyme That Terminates Endocannabinoid Signaling.

[62] Cravatt, F.et al.; *Biochemistry*, 40 (20), **2001** 6107-6115. Characterization and Manipulation of the Acyl Chain Selectivity of Fatty Acid Amide Hydrolase.

[63] Patricelli, M.P. et al.; *Biochemistry*, 38 (43), **1999**, 14125-14130. Fatty Acid Amide Hydrolase Competitively Degrades Bioactive Amides and Esters through a Nonconventional Catalytic Mechanism.

FAAH belongs to the α/β serine-hydrolase superfamily, and its catalytic mechanism is very similar to that of this class but, instead of a classical serine-hystidine-aspartic acid catalytic triad, *Lys*-142 appears to play as both a base and acid in the hydrolytic mechanism (**fig. 6**)[64].

Fig. 5: FAAH's catalytic triad (from *Annu. Rev. Biochem. 74, 2005*)

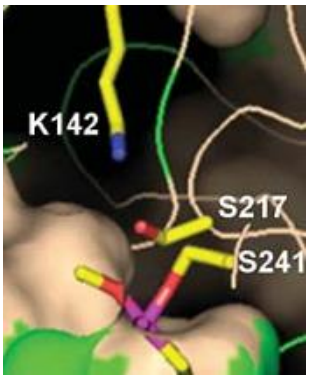

This residue activates nucleophilic Ser-241 for the attack on the substrate carbonyl function , and then seems to participate in the protonation of the substrate's leaving group[64]; the process is helped somehow by the presence of another serine residue (in particular Ser-217), the lack of which produces a high reduction in the catalytic capability[65].

This particular Ser-Ser-Lys catalytic triad (**fig. 5**), with the double action of the Lys-142, justifies the ability of FAAH to hydrolyse at the same rate amides and esters substrates, because of the protonation process induced by the presence of this residue.

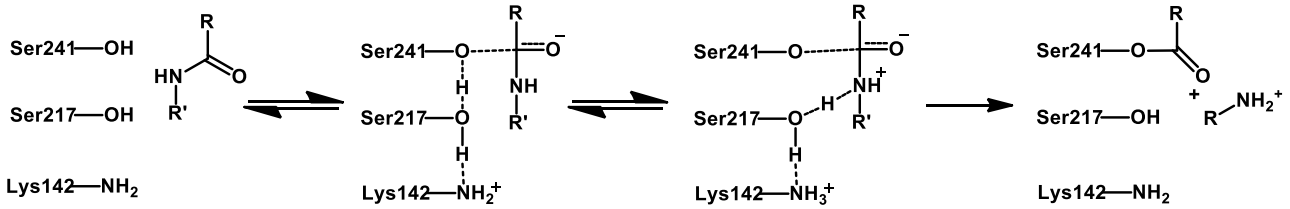

Fig. 6: Hydrolytic mechanism of FAAH

The subsequent intervention of a water molecule completes the hydrolysis with the detachment of the acyl chain from the enzyme.

The impact of Lys-142 on Ser-241 nucleophile strength and leaving group protonation likely occurs indirectly via the bridging Ser-217 of the triad, which may act as a "proton shuttle"[64].

The understanding of the molecular features of FAAH and of its catabolic mechanism, helped in the design of different classes of compounds, with the aim of synthesising inhibitors of this enzyme that is implied in several physiological and pathological conditions.

1.3.2 *N*-Acylethanolamine-hydrolysing Acid Amidase

In contrast to polyunsaturated NAEs, saturated and monounsaturated NAEs appear to be inactive at cannabinoid receptors.

[64] Patricelli, M.P. et al.; *Biochemistry*, 38 (31), **1999**, 9804-9812. Chemical and Mutagenic Investigations of Fatty Acid Amide Hydrolase: Evidence for a Family of Serine Hydrolases with Distinct Catalytic Properties.

[65] McKinney, M. K. Et al.; *J. Biol. Chem*., 278, **2003**, 37393-37399. Evidence for Distinct Roles in Catalysis for Residues of the Serine-Serine-Lysine Catalytic Triad of Fatty Acid Amide Hydrolase.

However, these NAEs show different biological activities: PEA is anti-inflammatory[66], immunosuppressive[67], neuroprotective[68], and analgesic[69].

Furthermore, OEA is anorexic[70], and SEA is pro-apoptotic[71] and anorexic[72]; all these activities are mediated by the action on different receptors: PPAR[73], GPR-55[74].

All these molecules are catabolised for a very small amount by FAAH, and for the major part by an enzyme that has been named NAAA: *N*-acylethanolamine-hydrolysing acid amidase[75].

NAAA does not reveal sequence homology with FAAH and belongs to another class of hydrolase; its predominant characteristic is the catalytic optimum at pH 4.5 – 5, which is consistent with its localisation at lysosomes level.

Another particularity is that NAAA exhibits ~35% homology to the structure of acid ceramidase, the lysosomal enzyme responsible for the hydrolysis of ceramide to fatty acid and sphingosine.

Moreover, the catalytic centre of human NAAA contains Cys-126 and Asp-145, and it is very interesting to note that this cysteine residue corresponds to Cys-143 of human acid ceramidase, confirming the homology between the two enzymes[76].

FAAH and NAAA show several differences in the catalytic properties, which suggest their different roles in vivo.

The most important difference, as said, is the pH dependency of their catalytic activities: FAAH is active in a wide range of pH with the optimal pH value at 8.5 – 10, while NAAA shows a pH optimum at 4.5 – 5 and is almost inactive at alkaline pH and even at neutral pH[77].

The cellular localisation of NAAA is consistent with its acidic optimum of pH 4-5, which is the normal pH of the intralysosomal compartment, and their substrate preferences are different too, with FAAH preferring AEA and NAAA preferring all other NAEs[78].

Thus, NAAA is more similar to acid ceramidase than FAAH, but is strictly related to the catabolism of different atypical endocannabinoids such as NAEs.

---

[66] Facci, L. t al.; *Proc. Natl. Acad. Sci. USA,* 92, **1995**, 3376-3380. Mast cells express a peripheral cannabinoid receptor with differential sensitivity to anandamide and palmitoylethanolamide.

[67] Berdyshev, E. v. et al.*; Eur. J. Pharmacol.,* 330, **1997**, 231-239 Influence of fatty acid ethanolamides and Δ^9-tetrahydrocannabinol on cytokine and arachidonate release by mononuclear cells.

[68] Skaper, S. D. et al.; *Proc. Natl. Acad. Sci. USA,* 93, **1996**, 3984-3989. The ALIAmide palmitoylethanolamide and cannabinoids, but not anandamide, are protective in a delayed postglutamate paradigm of excitotoxic death in cerebellar granule neurons.

[69].Calignano, A. et al.; *Eur. J. Pharmacol.*, 419, **2001**, 191-198. Antinociceptive activity of the endogenous fatty acid amide, palmitylethanolamide.

[70] Rodriguez de Fonseca, F. et al.; *Nature*, 414, **2001**, 209-212. An anorexic lipid mediator regulated by feeding.

[71] Maccarrone, M. et al.; *Biochem. J.*, 366, **2002**, 137-144. Binfind, degradation and apoptotic activity of stearoylethanolamide in rat C6 glioma cells.

[72] Terrazzino, S. et al.; *FASEB J.*, 18, **2004**, 1580-1582. Stearoylethanolamide exerts anorexic effects in mice via down-regulation of liver stearoyl-coenzyme A desaturase-1 mRNA expression.

[73] Fu, J. Et al.; *Nature,* 425, **2003**, 90-93. Oleylethanolamide regulates feeding and body weight through activation of the nuclear receptor PPAR-α.

[74] Baker, D. et al.; *Trends Pharmacol. Sci.,* 27, **2006**, 1-4. In silico patent searching reveals a new cannabinoid receptor.

[75] Tsuboia, K. Et al.; *CHEMISTRY & BIODIVERSITY*, 4, **2007**, 1914-1925. The N-Acylethanolamine-Hydrolyzing Acid Amidase (NAAA).

[76].Bernardo, K. Et al.; *J. Biol. Chem.*, 270, **1995**, 11098-11102. Purification, characterization, and biosynthesis of human acid ceramidase.

[77] Tsuboi, K. Et al.; *J. Biol. Chem.*, 280, **2005**, 11082-11092. Molecular Characterization of N-Acylethanolamine-hydrolyzing Acid Amidase, a Novel Member of the Choloylglycine Hydrolase Family with Structural and Functional Similarity to Acid Ceramidase.

[78] Ueda, N. et al.; *J. Biol. Chem.*, 270, **1995**, 23823-23827. Partial Purification and Characterization of the Porcine Brain Enzyme Hydrolyzing and Synthesizing Anandamide.

1.3.3 Monoacylglycerol Lipase

A special role in the endocannabinoid system functioning is played by 2-arachidonoyl glycerol; anyway, its activity has to be blocked after its action on the appropriate target, to avoid the over activation that is typical of direct agonists/antagonists use.

The termination of 2-AG signalling occurs intracellularly by an enzyme called Monoacylglycerol Lipase (MAGL)[79], which acts hydrolysing the molecule of 2-AG to free arachidonic acid and glycerol (**scheme 4**) after the transport from the extracellular space.

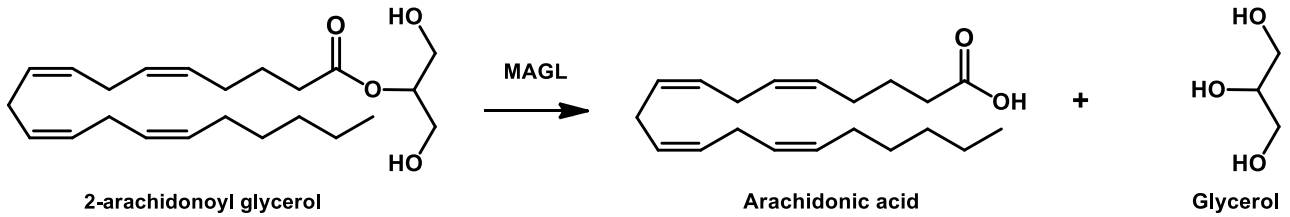

Scheme 4: 2-AG hydrolysis by MAGL

MAGL was purified in 1975 from rat-adipocyte tissue, its molecular weight was estimated to be 32.9 kDa and it was found to work best at a pH 8.0[80]; the enzyme specifically catalyses the hydrolysis of monoacylglycerols and is unable to operate the same reaction on either di- or tri-acyl glycerols.

Interestingly, MAGL has no effect on AEA levels, while FAAH is able to catalyze the breakdown of 2-AG.

The inhibition of this enzyme leads to higher 2-AG levels in the brain and therefore holds significant therapeutic potential; it was studied in depth and described to be involved in a very wide range of physiological and pathological conditions[81].

For these reasons, the interest around MAGL has spread out and the synthesis of active molecules able to act at this level of the endocannabinoid system has become more and more interesting, opening the field to different pharmacological approaches for MAGL modulation.

Detailed information about MAGL will be given in chapter two.

[79] Somma Delpero, C. et al.; *Biochem. J.*, 312, **1995**, 519-525. Purification and properties of a monoacylglycerol lipase in human erythrocytes.

[80] Tornqvist, H. et al.; *J. Biol. Chem.*, 251, **1976**, 813-819. Purification and some properties of a monoacylglycerol-hydrolyzing enzyme of rat adipose tissue.

[81] Fowler C. J. Et al.; *Br. J. Pharmacol.,* 166, **2012**, 1568-1585. Monoacylglycerol lipase - a target for drugdevelopment?

1.4 Role of ECS in disease

The ubiquity of ECS poses the necessity to study in depth every component of this system to understand each specific role; the quantification of anandamide and 2-AG levels in various tissues under physiological and pathological conditions provided important information as to the possible functions of these mediators.

Ecs are abundant in the brain, particularly in the basal ganglia and cerebellum where they control movement and posture[82]; their actions on autonomic nervous system result in the regulation of circulatory and gastrointestinal functions[83] and the hypothalamic-pituitary-adrenal axis – underlying their role on reproduction)[84], bone formation[85] and adipocyte functioning[86].

Ecs signalling often undergoes dramatic tissue-specific changes in pathological conditions[87]; in many cases, Ecs levels are controlled through various mechanism that often differ between AEA and 2-AG and are the reflection of different role of FAAH and MAGL enzymes[88].

There are also examples of the same stimulus (e.g. leptin) leading to the same change in the tissue concentrations of AEA and 2-AG, but through different regulatory strategies and it is also known that the levels Ecs precursors are influenced by the diet and by its relative contents in arachidonic and docosahexaenoic acids.

During some acute pathological states or temporary perturbations of the normal homeostasis of the organism, the levels of at least one EC in the tissues specifically involved in the disorder are momentarily elevated to help re-establish the normal levels of other endogenous mediators.

It can happen for example in specific nervous system areas following insults or stress stimuli (food deprivation, aversive memories, pain, and head injury)[89]

The progressive nature of some disorders might results in a permanent over activation of the system; this is an initial help to re-establish the homeostasis, but could be traduced in the development of symptoms typical of the disorder.

It happens in experimental model of Parkinson's disease, in which Ecs levels are elevated in the attempt to reduce glutamatergic and GABAergic signalling, but end up contributing to locomotor impairment viaCB1 receptors[90].

---

[82] Van der Stelt, M. et al.; *Eur. J. Pharmacol.,* 480, **2003**, 133-150. The endocannabinoid system in the basal ganglia and in the mesolimbic reward system: implications for neurological and psychiatric disorders.

[83] Lynch, M. E. et al.; *Pain Res Manag,* 10, **2005**; 7-14. Preclinical science regarding cannabinoids as analgesics: An overview.

[84] Barna, I. et al.; *Life Sci.*, 75, **2004**; 2959-2970. The role of endogenous cannabinoids in the hypothalamo-pituitary-adrenal axis regulation: in vivo and in vitro studies in CB1 receptor knockout mice.

[85] Tam, J. et al.; *Mol Pharmacol,* 70, **2006**, 786-792. Involvement of neuronal cannabinoid receptor CB1 in regulation of bone mass and bone remodeling.

[86] Walter, L. et al.; *Br. J. Pharmacol.*, 141, **2004**; 775-785. Cannabinoids and neuroinflammation.

[87] Van der Stelt, M. et al.; *Cell Mol Life Sci,* 63, **2006**, 1410-1424. .; Endocannabinoids and beta-amyloid-induced neurotoxicity in vivo: effect of pharmacological elevation of endocannabinoid levels.

[88] Witting, A. et al.; *Proc. Natl. Acad. Sci. USA,* 101, **2004**, 3214-3219. P2X7 receptors control 2-arachidonoylglycerol production by microglial cells.

[89] Di Marzo, V. et al.; *Annu Rev Med* ,57, **2006**, 553-574. Plant, synthetic, and endogenous cannabinoids in medicine.

[90] Fernandez-Espejo, E. et al.;. *Neurobiol Dis,* 18, **2005**; 591-601. Cannabinoid CB1 antagonists possess antiparkinsonian efficacy only in rats with very severe nigral lesion in experimental parkinsonism.

Similarly, in Alzheimer's disease models, Ecs protects from microglial cell-driven inflammation but they also participate in CB_1-mediated loss of memory, with particular implication of AEA in this process[91].

Also in lateral sclerosis animal models, elevated level of Ecs in the spinal cord seems to induce protective effects that are mediated by CB_2 receptors[92].

A lot more studies have been made to fully understand the role of ECS in physiology and pathology, and to underlie the possible pharmacological interventions that can be made.

[91] Ramirez, B. G. et al.; *J Neurosci,* 25, **2005**, 1904-1913. Prevention of Alzheimer's disease pathology by cannabinoids: neuroprotection mediated by blockade of microglial activation.

[92] Bilsland, L. G. et al.; *FASEB J,* 20, **2006**, 1003-1005. Increasing cannabinoid levels by pharmacological and genetic manipulation delay disease progression in SOD1 mice.

2. MONOACYLGLYCEROL LIPASE BIOCHEMICAL CHARACTERISATION

2.1 Molecular characterization and structure features

Twenty years after its discovery, MAGL was cloned from a mouse-adipocyte cDNA library and it was determined to be composed by 302 amino acids[93]; later, the cloning of the human MAGL analogue was made, founding to contain 303 residues[94].

The homology's degree in terms of amino acids sequence between mouse-, rat- and human isoforms is very high, with human and mouse MAGL identical for 84%, rat and mouse MAGL identical for 92%[95].

MAGL shows no homology with FAAH or other known amidases, but shares a similar tertiary fold that is typical of many lipases - the α/β-hydrolase fold[96].

Enhancements in MAGL structure comprehension were made when the enzyme was crystallised in 2010 by *Lambert et al*[97] and the structure resolved by X-ray diffraction.

MAGL was found to organise as a biological dimer, and that data was confirmed by another experiment performed by mass spectrometry, in which no monomer's peak was found after gel filtration chromatography.

Furthermore, similarly to what reported after the elucidation of FAAH structure[98], it was found that both catalytic site entries face the same direction, and are oriented in the best way to interact with the membrane for recruiting the substrate.

The enzyme structure presents the features of the α/β-hydrolase superfamily: its central β-sheet is constituted of seven parallel and one antiparallel strands and is surrounded by six α-helices; a cap domain (which varies much more among the members) covers the β-sheet and the active site.

Buried in depth below the cap there is the catalytic triad, composed by residues Ser-122, Asp-239, His-269 and closely superimposed on that of other hydrolases.

Ser-122 is located in the GXSXG consensus sequence between helix-α3 and strand-β5, in the so-called "nucleophilic elbow" sharp turn found within this superfamily; the oxyanion hole is constituted by backbone NH from Ala-51 and Met-123 and stabilizes the tetrahedral anionic intermediate during hydrolysis (as for Lys-142 in FAAH structure during AEA hydrolysis).

[93] Karlsson, M. et al.; *J. Biol. Chem.*, 272, **1997**, 27218-27223. cDNA Cloning, Tissue Distribution, and Identification of the Catalytic Triad of Monoglyceride Lipase.
[94] Dinh, T.P. et al.; *Proc. Natl. Acad. Sci. USA,* 99, **2002**, 10819-10824. Brain monoglyceride lipase participating in endocannabinoid inactivation.
[95] Karlsson, M. et al.; *Gene*, 272, **2001**, 11-18. Exon-intron organization and chromosomal localization of the mouse monoglyceride lipase gene.
[96] T. P. Dinh, T. F. Freund, D. Piomelli,Chem. Phys. Lipids2002, 121, 149-158 A role for monoglyceride lipase in 2-arachidonoylglycerol inactivation
[97] Labar, G. et al.; *ChemBioChem*, 11, **2010**, 218-227. Crystal Structure of the Human Monoacylglycerol Lipase, a Key Actor in Endocannabinoid Signaling.
[98] Bracey, M. H. et al.; *Science*, 298, **2002**, 298, 1793-1796. Structural Adaptations in a Membrane Enzyme That Terminates Endocannabinoid Signaling.

The homology of MAGL to other different enzymes used as model is quite high for what concerns the central core structure and the catalytic triad[99], but it changes significantly considering the cap domain (from residue 151 to 225) and substrate binding site.

In fact, in MAGL the cap domain varies substantially: in the upper part a first α-helix is moved outward then in model enzymes; in the lower part, a longer loop connects α-5 to α-6 helices.

Through these modifications, the four helices pass from a V-shaped organisation (typical of esterases and haloperoxidases) to a wider U-shaped structure, allowing the enzyme to give substrates a broader access to the active site, comparing to other related proteins.

This particular organisation is responsible for substrate recruitment and access to the catalytic site and for the action on different ECs.

Furthermore, it is useful to mention that MAGL - contrary to FAAH that is a post-synaptic membrane's enzyme - was reported to be present both in the cytosolic and in the membranes fractions of pre-synaptic cells (immunohistochemical studies indicate that MAGL is often co-localized with the CB_1 cannabinoid receptor, predominantly on the axon terminals of pre-synaptic neurons[100]).

2.2 Catalytic mechanism, substrate specificity and tissue distribution

The characteristic action of MAGL is the hydrolysis of EC molecule 2-AG; the recruitment of the substrate and the catabolic mechanism are strictly related to the structural features of the enzyme, and in particular of the cap domain, the active site and the exit pores for final products.

Docking studies of 2-AG to MAGL showed the formation of a tetrahedral intermediate (**fig. 7**) covalently bound to Ser-122 (as for FAAH mechanism).

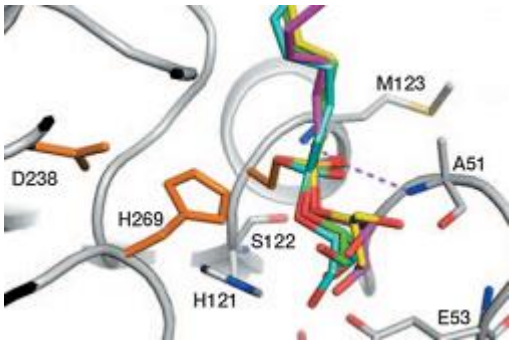

Fig. 7: MAGL's catalytic site (from *ChemBioChem 11, 2010*)

These studies revealed a cavity (wider and wider moving away from the catalytic triad) able to accommodate the long and flexible lipid chain of the substrates; several hydrophobic residues cover the channel leading from the surface to the nucleophilic serine.

Leu-148, Ala-164, Leu-176, Ile-179, Leu-205, Val-207, Ile-211, Leu-213, Leu-214, Val-217 and Leu-241 side chains are properly located to interact with the arachidonoyl moiety of 2-AG, and mediate the MAGL substrate specificity for lipid substrates.

[99] Roussel, A. et al.; *J. Biol. Chem.*, 277, **2002**, 2266-2274. Crystal Structure of the Open Form of Dog Gastric Lipase in Complex with a Phosphonate Inhibitor.

[100] Gulyas, A. I. et al.; *Eur. J. Neurosci., 20,* **2004**, 441-458. Segregation of two endocannabinoid-hydrolyzing enzymes into pre- and postsynaptic compartments in the rat hippocampus, cerebellum and amygdala.

The catalytic environment on the contrary presents a more hydrophilic character: the Tyr-58 hydroxyl group, the NH from the His-121 and His-272 side chains, the guanidinium from Arg-57, the carboxylate from Glu-53, and the backbone carbonyl from Ala-51 delimit a polar cavity that accommodates the polar glycerol head group of 2-AG.

MAGL was reported to hydrolyse 1-OG and 2-OG at similar rates[101], and docking of 2-AG allows to understand this lack of selectivity; in fact, if the acyl chain is bound in the 2-position, the glycerol moiety does not entirely fill up the hydrophilic cavity.

Therefore, the glycerol group of 1-OG can freely be accommodated in the same pocket without encountering a steric hindrance, and stretches to the bottom of the cavity.

A small opening coated by Pro-178, Ser-181, Leu-184, Tyr-194, Asn-195, Arg-202 and Ala-203, connects the active site to the outside of the protein; this channel, perpendicular to the path from the hydrophilic pocket to the membrane binding site is the exit door for the glycerol moiety that is released after the action of the enzyme.

All these molecular observations constitute the logical explanation to the characteristic selectivity of MAGL for its different possible substrate, with the undisputed action on monoacylglycerol derivatives over their di- or tri- substituted analogues, but without the possibility to have a clear preference between *sn*-1 and *sn*-2-substituted derivatives.

In addition, the preferences for different types of acid chains are very wide, with the enzyme able to act on a variegated pool of acyl chains; the only prerequisite is that the acid has to be unsaturated.

MAGL can hydrolyse medium- and long-chain fatty acids: myristic, palmitic, oleic, stearic, and arachidonic acid, from the *sn*-2-position of the monoacylglycerol with the highest hydrolysis rate observed for arachidonic acid[102].

The first localisation of MAGL was made in the adipose tissue, but from that moment it has extended to many other tissues and now it is known that the enzyme is ubiquitous.

In rat it is present in adipose tissue, testis, kidneys, adrenal gland, brain, liver, skeletal muscle, ovary and spleen[103]; the presence of MAGL at brain's level is ubiquitous to, and it is expressed in the cortex, hippocampus, cerebellum, thalamus, striatum and in lower amount in the brainstem and hypothalamus[104].

[101] Tornqvist, H. et al.; *J. Biol. Chem.*, 251, **1976**, 813-819. Identification and some characteristics of the enzyme protein of the hormone-sensitive lipase from rat adipose tissue.

[102] Rindlisbacher, B. et al.; *Biochim. Biophys. Acta*, 905, **1987**, 349-357. Diacylglycerol breakdown in plasma membranes of bovine chromaffin cells is a two-step mechanism mediated by a diacylglycerol lipase and a monoacylglycerol lipase.

[103] Karlsson, M. et al.; *Gene,* 272, **2001**, 11-18. Exon-intron organization and chromosomal localization of the mouse monoglyceride lipase gene.

[104] Gulyas, A. I. et al.; *Eur. J. Neurosci.,* 20, **2004**, 441-458. Segregation of two endocannabinoidhydrolyzing enzymes into pre- and postsynaptic compartments in the rat hippocampus, cerebellum and amygdala.

In many tissues, the cellular distribution of MAGL was reported both in the membrane and in the cytosol: in fact, microsomal and membrane fractions of human platelets possess MAGL activity[105], in the intestinal mucosa it is associated with the microsomal and the mitochondrial fractions[106] and the same happens for pancreas β-cells, chromaffin cells and erythrocytes[107].

2.3 MAGL inhibitors

Since the discovery of MAGL and the understanding of its relations in many physiological and pathological conditions, a lot was made to develop molecules that could act on this enzyme.

In particular the research is focused on the study of MAGL inhibitors, molecules that act blocking the catalytic activity of the enzyme, causing a local increase in the levels of 2-AG and thus, producing a pharmacological effect which could targeted to a specific region of the body and not producing a general activation of the endocannabinoid system.

In fact, one of the major concern with the development of molecules working on the ECS is that they could produce cannabis-like effects - catalepsy, hypothermia, hyperphagia - which would limit their therapeutic use.

When the first selective FAAH inhibitor was discovered and showed no induction of the cannabinoid-tetrad (thermal analgesia, catalepsy, locomotor activity and rectal temperature)[108], this concern was greatly reduced, pushing researchers to go deeper inside the field of endocannabinoid enzyme inhibition.

As for FAAH, also for MAGL there is the need to find potent ad selective inhibitors; the first generation MAGL inhibitors (**fig. 8**) showed modest activity in vivo, but were initially used to indicate that MAGL was a 2-AG hydrolase and that its block caused the increase in brain 2-AG levels in animal models.

[105] Prescott, S. M. et al.; *J. Biol. Chem.*, 258, **1983**, 764-769. Characterization of 1,2-diacylglycerol hydrolysis in human platelets. Demonstration of an arachidonoyl-monoacylglycerol intermediate.

[106] Senior, J. R. et al.; *J. Clin. Invest*., 42, **1963**, 187-192. Utilization of Glycerol-C^{14} for Intestinal Glyceride Esterification: Studies in a Patient with Chyluria.

[107] Somma-Delpero, C. et al.; *Biochem. J*., 313, **1995**, 519-525. Purification and properties of a monoacylglycerol lipase in human erythrocytes.

[108] Kathuria, S. et al.; *Nat. Med.,* 9, **2003**, 76-81. Modulation of anxiety through blockade of anandamide hydrolysis.

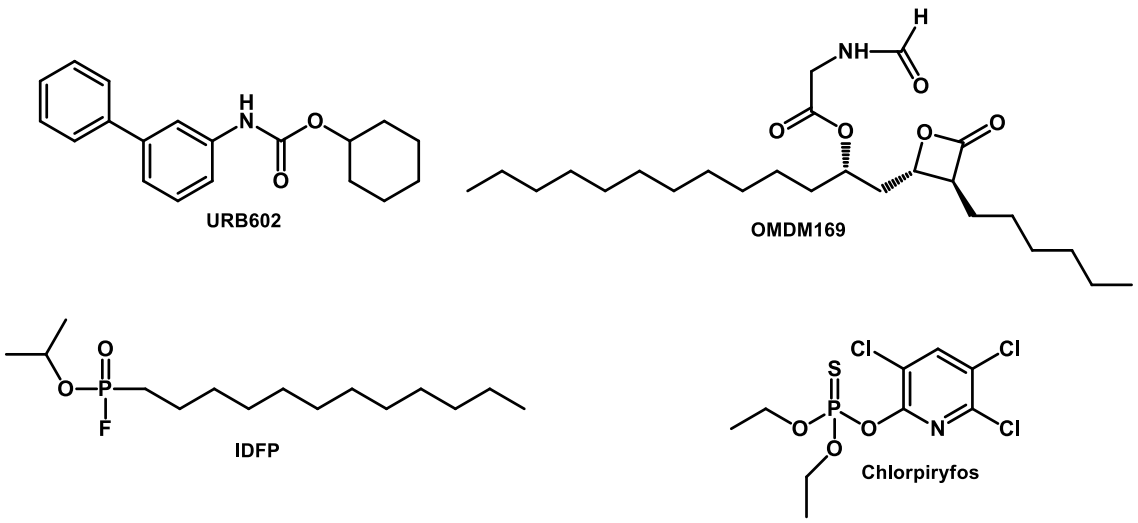

Fig. 8: Examples of MAGL inhibitors

MAGL activity can be attenuated by general non-specific serine hydrolase inhibitors such as methyl arachidonoylfluorophosphonate, phenylmethnsulfonyl fluoride, arachidonoyl trifluoromethylketone and hexadecyl sulfonyl fluoride[109].

The first selective MAGL inhibitors URB602, *N*-archidonoyl maleimide (NAM) and OMDM-169 had modest increase in 2-AG concentration and proved to be effective against rodent model of pain.

2.3.1 Carbamate compounds

URB602 was the first MAGL-preferring inhibitor to be reported[110]; it elevates 2-AG levels without altering that of AEA and mediate peripherally anti-nociceptive effects in various models of pain[111]. The action of URB602 is exerted with a non-competitive, partially reversible mechanism of action and the inhibition is time-independent[112].

From this molecule, many derivatives were synthesised maintaining the structural carbamate core and varying in different ways the side rings and chains: isosteric replacement, incorporation of biphenyl element, insertion of *p*-substituent groups led to the conclusion that the carbamate functionality is a promising scaffold for the development of MAGL inhibitors.

2.3.2 JZL184 and other inhibitors targeting the catalytic site

In 2009, the piperidine carbamate JZL184 (**fig. 9**) was discovered[113]: it blocks MAGL with very high potency (IC_{50} of 8nM) and shows a huge *in vivo* increase in 2-AG levels in the brain.

---

[109] Saario, S. M. et al.; *Biochem. Pharmacol.,* 67, **2004**, 1381-1387. Monoglyceride lipase-like enzymatic activity is responsible for hydrolysis of 2-arachidonoylglycerol in rat cerebellar membranes.

[110] Hohmann, A. G. et al.; *Nature,* 435, **2005**, 1108-1112. An endocannabinoid mechanism for stress-induced analgesia.

[111] Desroches, J. et al.; *Br. J. Pharmacol.,* 155, **2008**, 913-924. Modulation of the antinociceptive effects of 2-arachidonoyl glycerol by peripherally administered FAAH and MGL inhibitors in a neuropathic pain model.

[112] King, A.R. et al.; *Chem. Biol.,* 14, **2007**, 1357-1365. URB602 inhibits monoacylglycerol lipase and selectively blocks 2-arachidonoylglycerol degradation in intact brain slices.

[113] Long, J. Z. et al.;5, *Nat. Chem. Biol.,* **2009**, 37-44. Selective blockade of 2-arachidonoylglycerol hydrolysis produces cannabinoid behavioral effects.

It works through the formation of a covalent complex with the nucleophilic Ser-122[114] with results in the irreversible deactivation of the enzyme; the selectivity for MAGL is very high compared to that on FAAH but it blocks many other carboxylesterases in peripheral tissues, cross reactivity for FAAH after repeated administration and low cross-species activity.

The acute administration of this compound seemed to be positively effective, but the repeated administration caused many negative results: CB_1-receptor desensitisation, cross-tolerance to receptor agonist and tolerance to their anti-nociceptive effects, physical dependence[115].

Trying to overcome cross-species activity, new compound with *O*-hexafluoroisopropyl carbamate[116] or *N*-hydroxysuccinimidyl carbamate functionalities have been studied[117].

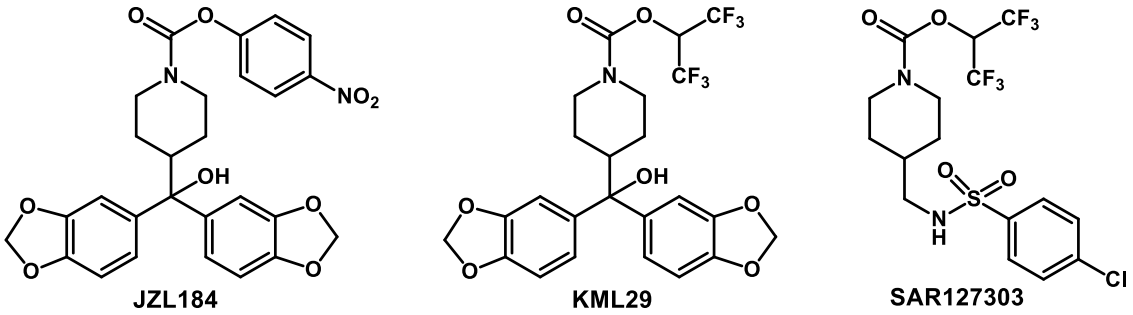

Fig. 9: Catalytic site-targeting inhibitors

The resulting compound KML29[118] (**fig.9**) showed very good selectivity for MAGL, with inhibitory values comparable to that of JZL184; moreover, it showed inhibitory activity both on rat and human MAGL, improving cross-species activity.

The bad side of the KML29 is that it causes cannabimimetic effects when administered in vivo[119].

Another promising compound is SAR127303[120], a potent *O*-hexafluoroisopropyl carbamate (**fig.9**): it shows potent inhibitory activity on mouse and human MAGL, and good selectivity for MAGL over FAAH; it exerts anti-nociceptive effects in inflammatory and visceral pain models and anti-epileptic effects, but it also negatively affects memory formation, causes impairment in cognitive performances.

---

[114] Long, J.Z. et al.; *Chem. Biol.,* 16, **2009**, 744-753. Characterization of monoacylglycerol lipase inhibition reveals differences in central and peripheral endocannabinoid metabolism.

[115] Schlosburg, J. E. et al.; *Nat. Neurosci.,* 13, **2010**, 1113-1119. Chronic monoacylglycerol lipase blockade causes functional antagonism of the endocannabinoid system.

[116] Chang, J. W. et al.; *Chem. Biol*., 19, **2012**, 579-588. Highly selective inhibitors of monoacylglycerol lipase bearing a reactive group that is bioisosteric with endocannabinoid substrates.

[117] Niphakis, M. J. et al.; *ACS Chem.Neurosci.,* 4, **2013**, 1322-1332. Evaluation of NHS carbamates as a potent and selective class of endocannabinoid hydrolase inhibitors.

[118] Chang, J. W. et al.; *ACS Chem. Biol.*8, **2013**, 1590-1615. Proteome-wide reactivity profiling identifies diverse carbamate chemotypes tuned for serine hydrolase inhibition.

[119] Pasquarelli, N. et al.; *Neuropharmacology,* 91, **2015**, 148-156. Comparative biochemical characterization of the monoacylglycerol lipase inhibitor KML29 in brain, spinal cord, liver, spleen, fat and muscle tissue.

[120] Griebel, G. et al.; *Sci. Rep.,* 5, **2015**, 7642-7670. Selective blockade of the hydrolysis of the endocannabinoid 2-arachidonoylglycerol impairs learning and memory performance while producing antinociceptive activity in rodents.

Some other serine-reactive compounds have been described[121] but beside the good potency on MAGL they lack of selectivity for this enzyme.

2.3.3 Cysteine-targeting compounds

MAGL is sensitive to sulfhydryl-specific inhibitors, such mercuric chloride, 4-chloromercuribenzoic acid and *N*-ethylmaleimide, all molecules that act oxidising the –SH residues of Cys-201 and Cys-242, which are known to be in their reduced form for the maintaining of enzyme's activity[122].

Starting from the evidence that MAGL contains some sensitive sulfhydryl sensitive sites, different *N*-ethylmaleimide derivatives were tested as potential MAGL inhibitors[123] and with the aim of understanding the role of these –SH containing residues.

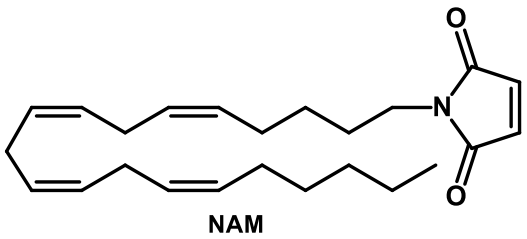

Fig. 10: *N*-arachidonylmaleimide

In this way, NAM (**fig. 10**) was identified as the most potent compound targeting MAGL cysteines[124]; the action of this class of compounds is exerted with a Michael addition mechanism, which results in the formation of a covalent adduct between the enzyme and the compound, causing an irreversible inhibition[125].

2.3.4 Disulphide compounds

Various disulphide compounds were tested to fully understand the role of cysteine residues, including disulfiram analogues - dicyclopentamethylenthiuram disulphide (**fig. 11**) and phenyl disulphide[126].

[121] Ortar, G. et al.; *Eur. J. Med. Chem.,* 63, **2013**, 118-130. Biaryl tetrazolyl ureas as inhibitors of endocannabinoid metabolism: modulation at the N-portion and distal phenyl ring.
[122] Scalvini, L. et al.; *Chem. Phys. Lipids,* **2015**, Monoglyceride lipase: Structure and inhibitors.
[123] Saario, S. M. et al.; *Chem. Biol.*, 12, **2005**, 649-656. Characterization of the sulfhydryl-sensitive site in the enzyme responsible for hydrolysis of 2-arachidonoyl-glycerol in rat cerebellar membranes.
[124] Matuszak, N. et al.; *J. Med. Chem.,* 52, **2009**, 7410-7420. Synthesis and in vivo evaluation of N-substituted maleimide derivatives as selective monoglyceride lipase inhibitors.
[125] Zvonok, N. et al.; *Chem. Biol.,* 15, **2008**, 854-862. Covalent inhibitors of human monoacylglycerol lipase: ligand-assisted characterization of the catalytic site by mass spectrometry and mutational analysis.
[126] Labar, G. et al.;, *ChemBioChem*, 8, **2007**, 1293-1297. Disulfiram is an inhibitor of human purified monoacylglycerol lipase, the enzyme regulating 2-arachidonoylglycerol signalling.

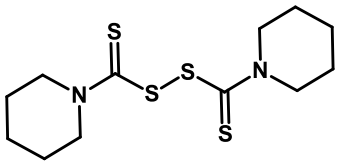

Dicyclopentamethylenethiuram disulphide

Fig. 11: Example of a disulphide compound

The activity of these compounds is comparable to that of carbamate compounds and their activity is made possible through a redox process requiring the formation of a mixed disulphide with Cys-208 and Cys-242.

The use of reducing agents reversed the inhibition[127], supporting the hypothesis that the role of these cysteine residues is fundamental for the activity of the enzyme and could be a potential target for MAGL inhibitors development.

2.3.5 Natural terpenoids

Some natural compounds proved to be active as MAGL inhibitors: pristimerin and euphol[128] (**fig. 12**). These two molecules belongs to the terpenoid class and showed good activity on MAGL; pristimerine can react with cysteine groups giving covalent adduct through a reversible non-competitive mechanism.

Euphol showed to be less potent than pristimerin but with a similar mechanism.

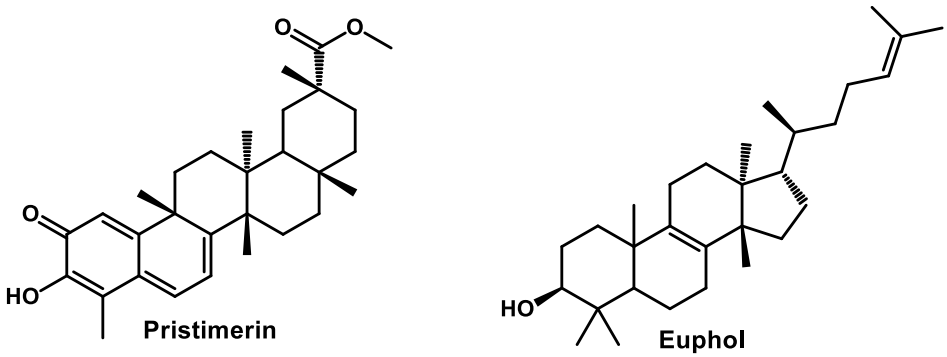

Fig. 12: Natural terpenoids

The effect of these two molecules resulted in an increased level of 2-AG, without effects on those of AEA.

More recently, the pentacyclic terpenoid β-amyrin was discovered as a novel MAGL inhibitor[129] with no effect on the other endocannabinoid system's enzymes; an important observation was that this compound could block also the action of two other 2-AG hydrolysing enzymes - ABHD6 and

[127] Kapanda, C. N. et al.; *J. Med. Chem.,* 52, **2009**, 7310-7314. Bis(dialkylaminethiocarbonyl)disulfides as potent and selective monoglyceridelipase inhibitors.

[128] King, A. R. et al.; *Chem. Biol.*, 16, **2008**, 1045-1052. Discovery of potent and reversible monoacylglycerol lipase inhibitors.

[129] Chicca, A. et al.; *Br. J. Pharmacol.,* 167, **2012**, 1596-1608. The antinociceptive triterpene amyrin inhibits 2-arachidonoylglycerol (2-AG) hydrolysis without directly targeting cannabinoid receptors.

ABHD12 - confirming terpenoids as a promising class of natural compounds for the regulation of 2-AG levels.

2.4 Therapeutic potential of MAGL-metabolizing enzymes inhibitors

As previously said, the endocannabinoid system - and the MAGL in particular - are ubiquitously expressed in the body; this fact, taken together with the proved participation of the catabolic enzymes in a lot of physiological ad pathological conditions, open the field for the development of hydrolysis' inhibitors that can have a therapeutic potential.

The fields of application can be very wide, because of the implications of the ECS in a wide range of systems (**fig. 13**): from the cardiovascular system, to immune system, from the gastrointestinal to the reproductive system; moreover, there is a great interest in the role of ECS in pain and inflammation, cognitive functions and cancer development and therapy.

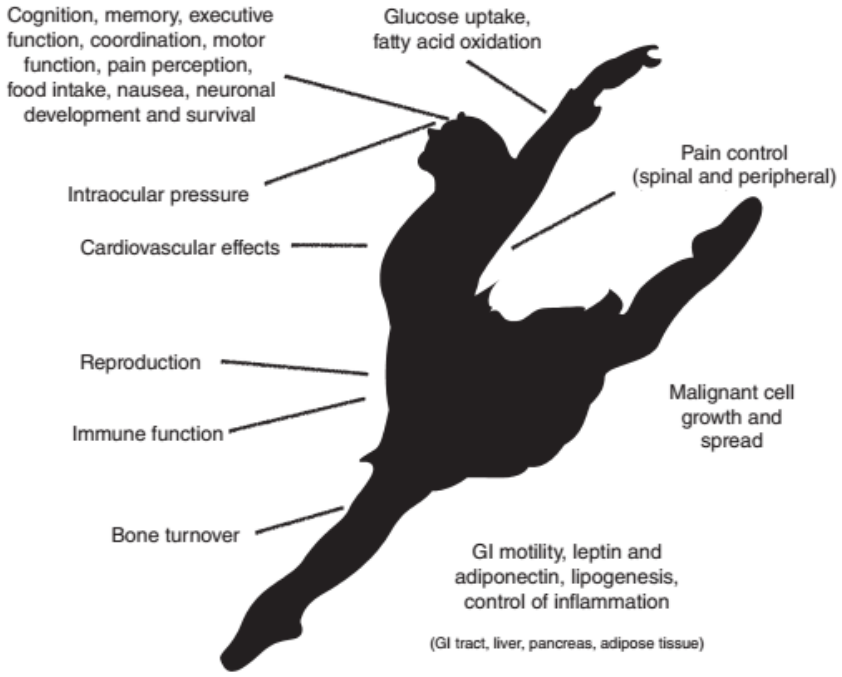

Fig. 13: ECS ubiquity (from *British Journal of Pharmacology, 166, 2012*)

For all these systems, the implication of the ECS was studied and described in depth, and a lot of experimental evidences suggested that the block of the catabolic hydrolysis can be the right way to search treatments concerning endocannabinoid dysfunctions, more than the use of direct receptor agonists or antagonists.

In the following paragraphs, the role of MAGL inhibition will be discussed relatively to its implication in different systems, as examples of the therapeutic possibilities related to the use of synthetic compounds active on MAGL.

2.4.1 In inflammation

A very big deal for MAGL inhibitors possible application is their use in inflammatory and neurodegenerative diseases.

Different studies have shown that MAGL is the primary source of arachidonic acid for the generation of pro-inflammatory eicosanoids in many tissues, including the brain, the liver and the lungs[130], thus its block could be a potential therapeutic strategy.

MAGL blockade proved to reduce mechanical allodynia in mice undergoing sciatic nerves chronic constriction[131] and to be protective in mouse model of inflammatory bowel disease, in which the use of a selective MAGL inhibitor reduced inflammatory cytokine levels and restored the intestinal barrier functions[132].

Chronic MAGL blockade prevented also chronic stress-induced anxiety-like behaviour and long-term depression of GABAergic transmission, preventing the synaptic adaptation to chronic stress that may cause to the worsening of the affective disorders[133].

Pharmacological and genetic ablation of the enzyme showed anti-inflammatory effects in Parkinson's and Alzheimer's disease mouse models[134] and protected from pharmacological-induced dopaminergic neurodegeneration[135]; a recent study[136] showed that MAGL blockade caused the lowering of β-amyloid plaque levels in Alzheimer's disease lowering also eicosanoids' levels.

These positive effects on Alzheimer's disease are sustained by the observation that MAGL block caused a reduction in the cleavage of Amyloid Precursor Protein (APP), responsible for the formation of aggregating peptides Aβ1-40 and 1-42.

It was also shown that the use of MAGL inhibitors reduced neurodegeneration, maintained the integrity of hippocampal synaptic structure and function and improved long-term synaptic plasticity and memory in Alzheimer's disease models.

Concerning peripheral tissue injuries, different studies have shown the positive effects of MAGL blockade in this situation: MAGL inactivation lowered hepatic inflammation caused by ischemia-reperfusion injury by lowering neutrophil infiltration, inflammatory cytokines, and reactive oxygen stress[137].

---

[130] Nomura, D. K. Et al.; *Science*, 334, **2011**, 809-813. Endocannabinoid hydrolysis generates brain prostaglandins that promote neuroinflammation.
[131] Kinsey, S. G. et al.; *J. Pharmacol. Exp. Ther.,* 330, **2009**, 902-910. Blockade of Endocannabinoid-Degrading Enzymes Attenuates Neuropathic Pain.
[132] Alhouayek, M. et al.; *FASEB J.,* 25, **2011**, 2711-2721. Increasing endogenous 2-arachidonoylglycerol levels counteracts colitis and related systemic inflammation.
[133] Sumislawski, J. J. et al.; 36, **2011**, 2750-2761. Reversible Gating of Endocannabinoid Plasticity in the Amygdala by Chronic Stress: A Potential Role for Monoacylglycerol Lipase Inhibition in the Prevention of Stress-Induced Behavioral Adaptation.
[134] Piro, J. R. et al.; *Cell Rep.,* 1, **2012**, 617-623. Dysregulated Endocannabinoid-Eicosanoid Network Supports Pathogenesis in a Mouse Model of Alzheimer's Disease.
[135] Long, J. Z. et al.; *Chem. Biol.,* 16, **2009**, 744-753. Characterization of monoacylglycerol lipase inhibition reveals differences in central and peripheral endocannabinoid metabolism.
[136] Chen, R. Q. et al.; *Cell Rep.,* 2, **2012**, 1329-1339. Monoacylglycerol lipase is a new therapeutic target for Alzheimer's disease.
[137] Cao, Z. et al.; *Gastroenterology,* 144, **2013**, 808-817. Monoacylglycerol Lipase Controls Endocannabinoid and Eicosanoid Signaling and Hepatic Injury in Mice.

Another study showed that MAGL inhibitors could protect against lung injury in a lipopolysaccharide-induced lung injury model; the acute treatment with an inhibitor reduced leukocytes migration into the lungs, vascular permeability and inflammatory chemokine levels in alveolar fluids[138].

2.4.2 In pain

MAGL inhibitors can have therapeutic applications in the field of pain treatment, but for their use some preliminary facts have to be taken into consideration:

- the pain state has to respond to cannabinoid agonists, to confirm that the situation could at least respond to the ECS signalling;
- animal models have to prove that in the studied situation the ECS is out of balance, so that the block of MAGL can have a measurable effect, either to normalise a deficient signal or to potentiate a protective response;
- for repeated dose regimes, there should be no tolerance to the compound in question.

Positive effects have been described: several clinical trials were conducted[139], and led to the conclusion that there are evidences that cannabinoids are safe and effective in neuropathic pain, with efficacy in fibromyalgia and rheumatoid arthritis[140].

Detectable levels of AEA and 2-AG were found in synovial fluid from patient with osteoarthritis and rheumatoid arthritis undergoing total knee surgery against no detectable levels in normal people[141].

In all these studies, the use of MAGL inhibitors was investigated, leading to the conclusion that they can be useful for the treatment of residual pain after certain types of surgery (amputations, thoracotomy, mastectomy, coronary artery bypass)[142].

It was demonstrated that after surgery, there is an increase in the relative proportion of MAGL-positive cells, pointing to a disturbance of the EC system following surgery, in which the use of MAGL inhibitors could be a potential help[143].

Alkaitis et al[144] indicated that "there are suggestions that therapeutic strategies designed to enhance endocannabinoid signalling may prevent patients from developing persistent or chronic pain states

[138] Costola-de-Souza, C. et al.; *PLoS One,* 8, **2013**, 525-532. Monoacylglycerol lipase (MAGL) inhibition attenuates acute lung injury in mice.
[139] Campbell, F. et al.; *Br. Med. J.,* 323, **2001**, 13-16. Are cannabinoids an effective and safe treatment option in the management of pain? A qualitative systematic review.
[140] Lynch, M. E. et al.; *Br. J. Clin. Pharmacol.,* 72, **2011**, 735-744. Cannabinoids for treatment of chronic non-cancer pain; a systematic review of randomized trials.
[141] Richardson, D. et al.; *Arthritis Res. Ther.*, 10, **2008**, R43. Characterisation of the cannabinoid receptor system in synovial tissue and fluid in patients with osteoarthritis and rheumatoid arthritis.
[142] Kehlet, H. et l.; *Lancet,* 367, **2006**, 1618-1625. Persistent postsurgical pain: risk factors and prevention.
[143] Ma, W. X. Et al.; *Int. J. Legal. Med.,* 125, **2011**, 549-558. Time-dependent expression and distribution of monoacylglycerol lipase during the skin-incised wound healing in mice.
[144] Alkaitis, M. S. et al.; *PLoS ONE,* 5, **2010**, 398-409. Evidence for a role of endocannabinoids, astrocytes and p38 phosphorylation in the resolution of postoperative pain.

following surgery"; this conclusion resulted in the validation of the hypothesis that MAGL inhibitors' use could have positive effects on pain treatment.

2.4.3 In cancer and cancer treatment

One of the most interesting possible application of MAGL inhibitors is in cancer treatment.

In fact, tumour cells adapt their metabolism toward a lipogenic phenotype, which is related to high expression of MAGL, a key element in the fatty acid network[145].

The high expression of this enzyme - able to liberate fatty acid chains from their precursors - offers to cancer cells the possibility to find highly energetic molecules with which feed their expensive replicative machinery.

This is a fundamental process for energy generation during deprivation and an essential source of precursors for lipids and membrane synthesis, or lipid signalling mediators[146].

The dysregulated lipogenesis seems to play a key role in cancer development and progression because tumour cells can use the lipolytic pathway to generate essential lipid blocks for their accelerated metabolism and proliferation.

The recent availability of MAGL inhibitors helped to prove that MAGL is highly expressed in different types of human cancer cell; moreover, MAGL activity also correlates with high proliferation, invasiveness and tumour growth[147].

MAGL is elevated, for example, in colon carcinoma and in androgen-independent prostate cancer cells[148]; its tumour-promoting action is due to the degradation of substrates different from 2-AG and the liberation of other free fatty acids, in particular C16:0 and C18:1[149] that enter in a tumorigenic network sustained by their conversion in oncogenic lipid mediators.

In prostate cancer, the antitumor effects of MAGL block are completely abolished by co-treatment with fatty acids, indicating that increased endocannabinoid signalling and a reduced supply of free fatty acids from MAGL contribute to the antitumor effect.

Furthermore, MAGL blockade can be also a strategy for alleviating cancer-associated symptoms: in fact, 2-AG administration and MAGL inhibition attenuate nausea and vomiting and reduce mechanical hyperalgesia in bone cancer pain[150].

---

[145] Pisanti, S. et al.; *Trends in Pharmacol. Sci.,* 34 (5), **2013**, 273-282. The endocannabinoid signaling system in cancer.

[146] Lass, A. et al.; *Prog. Lipid Res.,* 50, **2011**, 14-27. Lipolysis - a highly regulated multi-enzymecomplex mediates the catabolism of cellular fat stores.

[147] Nomura, D. K. et al.; *Cell,* 140, **2010**, 49-61. Monoacylglycerol lipase regulates a fatty acid network that promotes cancer pathogenesis.

[148] Ye, L. et al.; *Cancer Lett*., 307, **2011**, 6-17. Monoacylglycerol lipase (MAGL) knockdown inhibits tumor cells growth in colorectal cancer.

[149] Nomura, D. K. et al.; *Chem. Biol.,* 18, **2011**, 846-856. Monoacylglycerol lipase exerts dual control over endocannabinoid and fatty acid pathways to support prostate cancer.

[150] Khasabova, I. A. et al.; *Pharmacol. Res.*, 64, **2011**, 60-67. Increasing 2-arachidonoyl glycerol signaling in the periphery attenuates mechanical hyperalgesia in a model of bone cancer pain.

On the other hand, brain tumours, such as gliomas, are related to increased endocannabinoid tone and the use of MAGL inhibitors would be detrimental.

All these observations confirm cancer treatment as an interesting field of application for MAGL inhibitors, but a lot more has to be done, both in the development of potent drugs and in the identification of the appropriate diseases on which their use could be positive.

EXPERIMENTAL WORK

1. AIMS OF THE WORK

The real comprehension of the endocannabinoid system - of the role of its endogenous substrates, synthetic and degrading enzymes, receptors and implications in health and diseases - is a major task for the implied scientists[151].

To understand the mechanisms at the base of this system, and how to act in order to develop possible treatments for different pathological situations, it is necessary to have access to easy and reliable methods for the evaluation of potential drugs' use.

Moreover, trying to explore the different mechanisms involved in the ECS, and how modulate them, there is the need of different types of active molecules, which can help in the understanding of the general situation and could be potential therapeutic agents.

The aims of this work are:

- the developing of a fast and reliable fluorescence method for activity screening of potential inhibitors;
- the design and synthesis of new molecules able to act as MAGL (which is our main target) inhibitors;
- the evaluation of new synthetic molecules' activity through our self-developed fluorescence method.

The purpose of this work then is to add a piece in the knowledge of the ECS, and to identify some potentially active compounds, which could be selected for the improvement of therapeutic interactions with this complex - but still very fascinating - system.

[151] Piomelli, D. et al.; *Neuropharmacology,* 76, **2014**, 228-234. More surprises lying ahead. The endocannabinoids keep us guessing.

2. SET UP OF A NEW FLUORESCENCE-BASED ASSAY FOR MAGL INHIBITORS SCREENING

One of the major task in the development of MAGL inhibitors remains the necessity of a fast and reliable method for the evaluation of potentially active compounds, to speed up the process that runs through the design of a new molecule and its evaluation as an active agent on the endocannabinoid system.

At the moment, different methods are described for the evaluation of potential inhibitors' activity, on the isolated enzyme or in *in vitro* assays.

These methods are based on the evaluation of a signal (light at different wavelengths, in particular) that is released when the enzyme hydrolyses a suitable substrate; that signal is then recorded and correlated to the amount of transformed substrate basing on a calibration curve and the value obtained associated to the activity of MAGL.

Each of these methods, however, has several different features in terms of specificity, sensitivity and time and simplicity of analysis.

- p-nitrophenyl alkyl derivatives:

One of the first assay described for *in vitro* evaluation of potential MAGL inhibitors, used *p*-nitrophenyl-alkyl derivatives[152] as chromogenic substrate: in particular the use of *p*-nitrophenyl acetate subjected to the action of MAGL led to the liberation of acetate and a molecule of *p*-nitrophenol (**scheme 5**) which is detectable at 405 nm by an UV-Vis spectrophotometer.

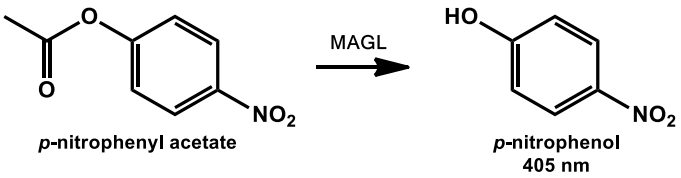

Scheme 5: Liberation of p-nitrophenol

This method is very easy to apply, having the advantages of using cheap reagents and a common instrumentation (the UV-Vis spectrophotometer); unfortunately, its specificity is very low, because *p*-nitrophenyl alkyl derivative can be hydrolysed by different lipases, due to their ability to work on and hydrolyse the simple ester bond typical of this class of compounds[153].

- 2-AG detection by mass spectrometry:

Another method[154] described the measurement of the amount of free arachidonic acid liberated by 2-AG after the action of MAGL, with an HPLC/mass spectrometry technique.

[152] Muccioli, G. G.; *ChemBioChem,* 9, **2008**, 2704-2710. CAY10499, a Novel Monoglyceride Lipase Inhibitor Evidenced by an Expeditious MGL Assay.
[153] Salameh, M. A. et al.; *Appl. Environ. Microbiol.*, 73 (23), **2007**, 7725-7731. Purification and Characterization of Two Highly Thermophilic Alkaline Lipases from Thermosyntropha lipolytica.
[154] King, A. R. et al.; *Br. J. Pharmacol.* 157, **2009**, 974-983. A critical cysteine residue in monoacylglycerol lipase is targeted by a new class of isothiazolinone-based enzyme inhibitors.

The specificity of this method is the highest among the known methods due to the measurement of the natural substrate, but it needs the use of a very expensive instrument (such as the mass spectrometer) and the set-up of the assay, which can be a long process, thus not suitable for a rapid screening.

- Glycer-2-yl-4-pyrenylbutanoate:

A third method described the use of glycer-2-yl-4-pyrenylbutanoate as MAGL substrate[155].

Similarly to the UV-based method, the enzyme works on the substrate leading to the liberation of a molecule of glycerol and one of 4-pyrenylbutanoic acid, molecule which can be detected by fluorescence (λ_{ex}.340 nm/λ_{em}.380 nm) (**scheme 6**).

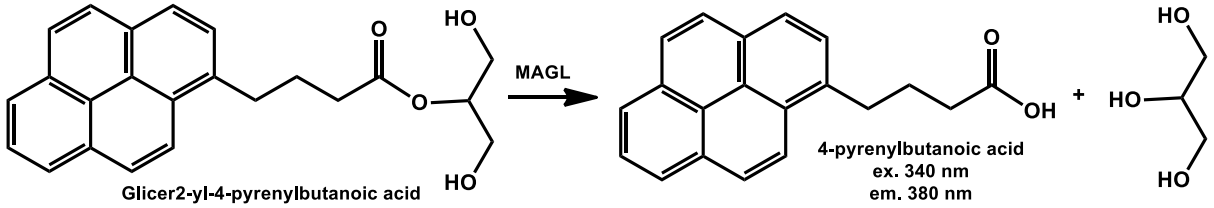

Scheme 6: Liberation of 4-pyrenylbutanoic acid

The advantages of this method are that the sensitivity of the fluorescence detector is higher than that of the UV one, and the glyceric scaffold makes the substrate more similar to the endogenous 2-AG, increasing the specificity versus the *p*-nitrophenyl alkyl method. Unlikely there are issues that have to be taken in consideration: in fact the native substrate glycer-2-yl-4-pyrenylbutanoate is detectable itself at the same wavelengths used for its metabolite 4-pyrenylbutanoic acid, so an HPLC separation is needed to distinguish the two different molecules.

This situation leads to the necessity to use a HPLC apparatus with fluorescence detector, in order to quantify the free form of 4-pyrenylbutanoic acid from its precursor, thus implying to search for the appropriate working conditions on each instrument (flow, time, etc.) and to build a calibration curve which - in HPLC technics - means the use of lot of time, solvents etc.

- [^{3}H]2-arachidonoyl glycerol:

Some assays shown the use of a tritiated derivate[156] of 2-AG (or 2-OG) such, for example [^{3}H]2-AG (**scheme 7**).

The method is based on the separation of the tritiated arachidonic acid by its precursor and the measurement of the radioactivity by scintillation.

The specificity and sensitivity are very good because of the use of the natural substrate and the high responsiveness of the radioactive signal, but it requires the handling of radioactive materials - which

[155] Holtfrerich, A. et al.; *Anal Biochem,* 399, **2010**, 218-224. High-performance liquid chromatography assay with fluorescence detection for the evaluation of inhibitors against human recombinant monoacylglycerol lipase.

[156] Matuszak, N. et al.; *J. Med. Chem.,* 52, **2009**, 7410-7420. Synthesis and in vitro evaluation of N-substituted maleimide derivatives as selective monoglyceride lipase inhibitors.

need specific instrumentations, procedures and people trained to use this kind of substances - and for these reasons not widely available.

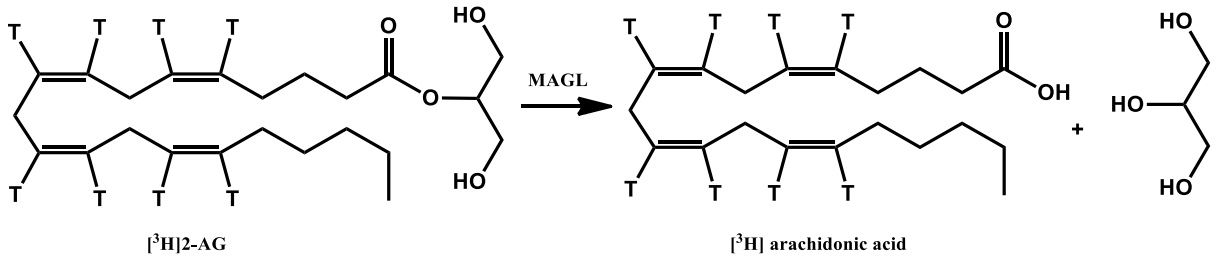

Scheme 7: Liberation of tritiated arachidonic acid

- Use of fluorogenic probe:

The last method[157] is based on the use of a fluorogenic probe, in particular 7-arachidonoyl-4-methyl-coumarin (7-HCA).

This method differs from the one using glycer-2-yl-4-pyrenylbutanoate because 7-HCA is not fluorescent itself, but once subjected to the enzyme's action, it leads to the liberation of a fluorescent molecule of 7-hydroxmethyl coumarin (7-HC), which shows a signal detectable by a fluorimeter with λ_{ex}.370 nm/λ_{em}.450 nm (**scheme 8**).

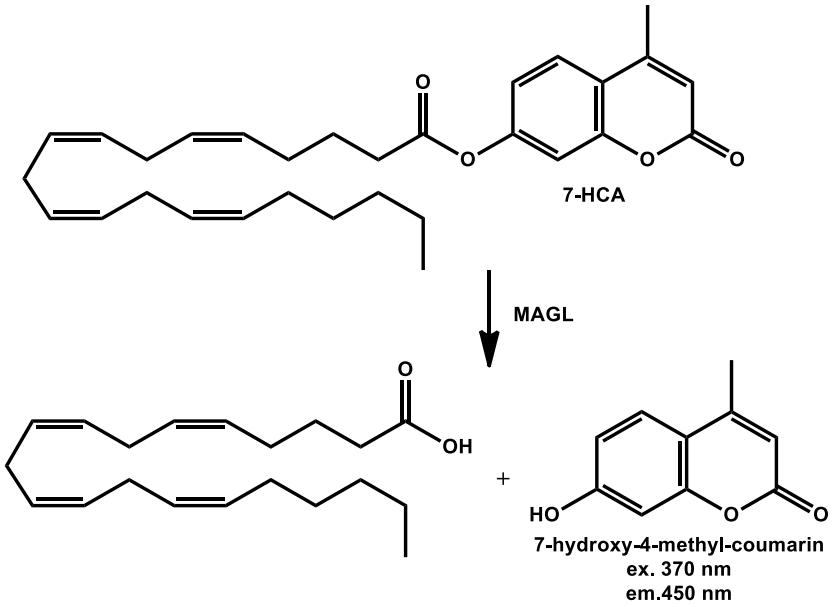

Scheme 8: Liberation of fluorescent 7-HC

The advantage of this method is that, thanks to the non-fluorescent precursor transformed in a fluorescent derivative by the action of MAGL, it is possible to obtain a value which is directly relative to the action of the enzyme (only converting the fluorescence signals through a calibration curve) without the necessity of sample treatments and separations.

[157] Savinainen, J. R. et al.; *Anal Biochem*, 399, **2010**, 132-134. Characterization of binding properties of monoglyceride lipase inhibitors by a versatile fluorescence-based technique.

For this reason the method is very fast, simple, and cheap; on the other hand, even if it is particularly potent for a rapid screening of potential inhibitors on pure MAGL, it has to be taken into account that interactions with other hydrolases using cell preparations are possible.

Moreover, cellular samples excited at 370 nm show a quite high background noise derived by the intrinsic fluorescence of tryptophan residues, and it could be a potential source of disturbance.

In addition, the assay emits blue fluorescence, which can significantly enhance interference due to compound fluorescence and dust or lint, all of which fluoresce in the blue wavelength region[158].

All the methodics have positive and negative aspects and features, in terms of costs, specificity, sensitivity or interferences; the choice has to be made basing on the type of screening needed, and the research for an assay that can be a good compromise is still going on.

[158] Fritzsche, M. et al.; *Anal Bioanal Chem,* 398, **2010**, 181-191. Fluorescent cell-based sensing approaches for toxicity testing.

2.1 Design of new fluorogenic probe 7-hydroxyresorufinylarachidonate

We decided to synthesise a new fluorogenic probe, which could overcome the problem of auto fluorescence of cell culture assays, which are the focus of inhibitors studies.

The idea was based on the use of a fluorogenic probe - which is not fluorescent by itself - that releases a high fluorescent molecule after the action of MAGL.

Fig. 14: Structure of resorufin

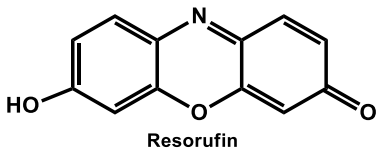

Resorufin

In the pool of potential fluorophores our choice fell on resorufin (**fig.14**): this molecule is highly fluorescent[159] at pH 7.4 (which is typical of this kind of assay) and has λ_{ex}.370 nm/λ_{em}.450 nm that are out of the field of auto fluorescence of cell cultures[158].

The fluorescence emission is due to the deprotonated anion of resorufin, since its pKa value is relatively lower than pH 5-6[160].

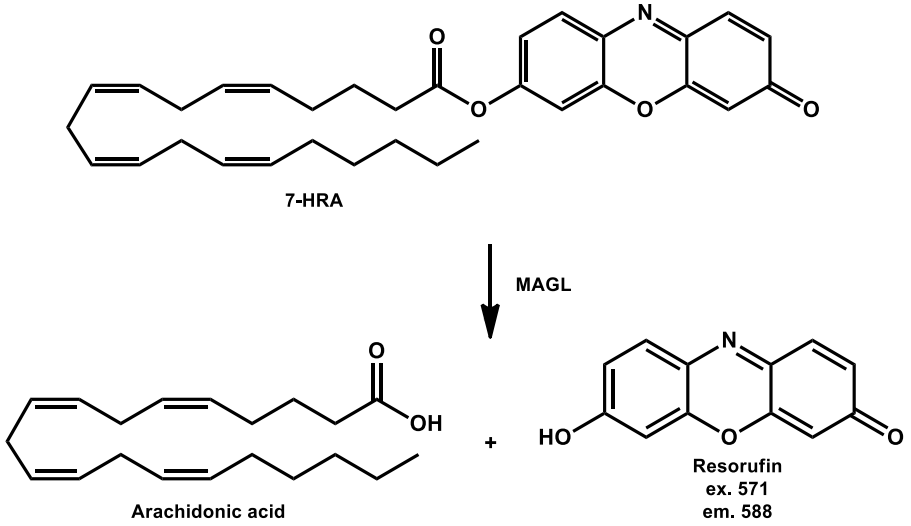

Scheme. 9: Hydrolysis of 7-HRA by MAGL

We synthesised a new long-wavelength fluorogenic substrate, 7-hydroxyresorufinyl-arachidonate (7-HRA), a highly convenient fluorogenic probe with high signal-to-noise ratio, excellent stability against non-specific degradation and which can be a useful tool in further development of MAGL inhibitors (**scheme 9**).

The new substrate was synthesised and tested to verify its stability in different conditions; it was then used for the set up and the validation of a new fluorescent assay for MAGL inhibitors screening and afterwards used for testing different synthetic molecules that were prepared in the laboratory.

[159] Myung, G. C. et al.; *Org. Lett.,* 12 (24), **2010**, 37-49. Chromogenic and Fluorogenic Signaling of Sulfite by Selective Deprotection of Resorufin Levulinate.

[160] Simpson, D. J. et al.; *J. Org. Chem.*, 56, **1991**, 5391-5396. A Mechanism-Based Fluorogenic Probe for the Cytochrome P-450 Cholesterol Side Chain Cleavage Enzyme.

2.2 Synthesis of 7-HRA

New fluorogenic probe 7-HRA was synthesised expressly to be used in the fluorescence based method for the evaluation of MAGL activity and with the purpose of obtaining a fast and reliable method for potential inhibitors screening.

The synthesis was carried out in a two steps classical coupling reaction[161] as shown in **scheme 10**: the starting arachidonic acid was dissolved in dry CH_2Cl_2 (one drop of DMF added) and activated through the addition of oxalyl chloride at 0°C; after the necessary period of time (3h) for the activation, the solvent was evaporated and the residual arachidonoyl chloride dissolved in dry CH_2Cl_2. This solution was added dropwise to an ice-cold suspension of resorufin in dry CH_2Cl_2/triethylamine, and stirred overnight at room temperature.

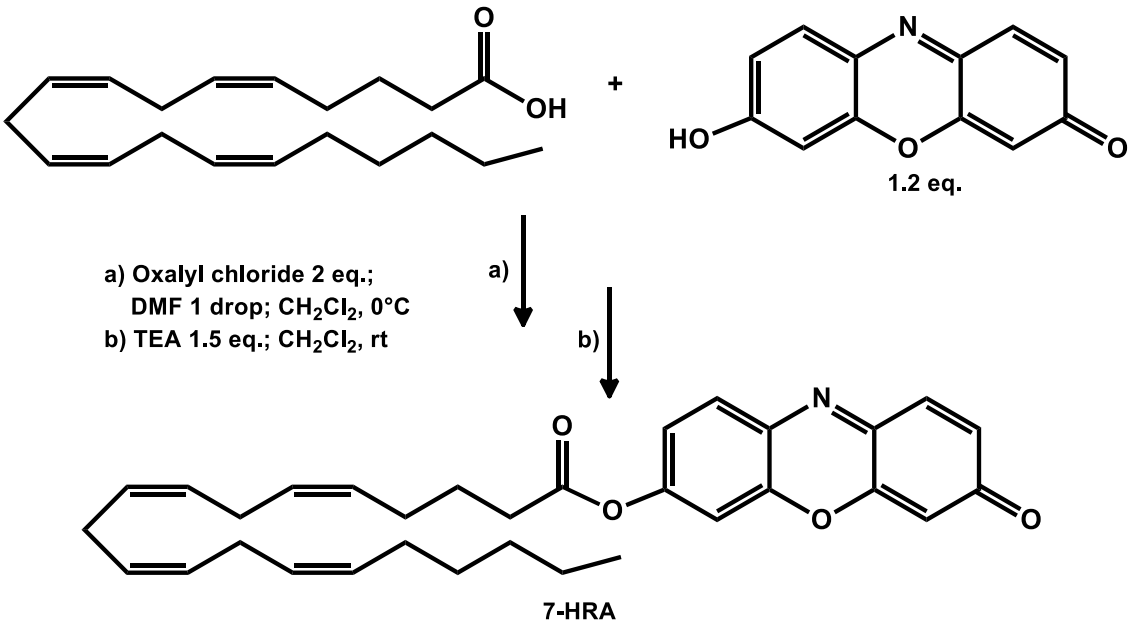

Scheme 10: Synthesis of 7-HRA

The suspension was diluted with CH_2Cl_2 and filtered for the removal of the salts.

The liquid residue was subsequently washed with 1M HCl and saturated $NaHCO_3$, dried on anhydrous sodium sulfate and purified by column chromatography on silica gel, giving the red oil product 7-HRA (62%).

[161] Mulvihill, M. M. et al.; *Life Sciences*, 92, **2013**, 506-511. Therapeutic potential of monoacylglycerol lipase inhibitors.

2.3 Method set up

- Substrate stability:

7-HRA proved to be stable for at least 6 months stored at -18°C in the dark, and dissolved (10 μM) in DMSO without TLC-noticeable decomposition.

The stability of substrate 7-HRA was tested in three different buffer solutions: 50 mM Tris–HCl (pH 7.4, 1 mM EDTA), 0.5 M Hepes (pH 7.4), and phosphate-buffered saline (PBS, pH 7.4).

To 90 μl of the selected buffer with 5 μl of DMSO, 7-HRA (10 mM in DMSO) was added, reaching the final concentration of 10 μM; after the incubation period of 3 h (darkness, room temperature), the fluorescence signal was measured at 588 nm (λ_{ex}.571 nm/λ_{em}.588 nm) by Promega-Glomax multidetection system.

Buffer	Resorufin liberation (%)
Tris-HCl	2.3 %
Hepes	2.1 %
PBS	2.3 %

Tab. 1: Resorufin liberation in three different buffers

As shown in tab. 2, Tris–HCl buffer led to the liberation of 2.3 % of total available resorufin, Hepes buffer 2.1 %, and PBS 2.3 %; the previous use of Tris–HCl buffer for our preliminary studies and the comparable results among the three different buffers, led us to continue to use Tris-HCl for further experiments.

pH 7.4 was selected for the fluorescence MAGL assay to facilitate the comparison with previous data and because typically, biochemical assays are performed near the physiological pH in attempt to mimic the intracellular environment of the natural enzyme.

To ensure solubility of the hydrophobic substrate 7-HRA the addition of 10 % DMSO in test solutions was made, since human recombinant MAGL preserves its activity up to that concentration[162]; the solubility of the substrate under these conditions appeared to be excellent, allowing to follow the reaction over many hours without precipitation's problems.

- *Kinetics of 7-HRA hydrolysis by hMAGL*:

For the setup of kinetics experiments and the determination of kinetics parameters, we used the commercially available human recombinant enzyme (hMAGL by Cayman Chemical).

[162] Wang, Y. et al.; *Assay Drug Dev Technol,* 6, **2008**, 387-393. A fluorescence based assay for monoacylglycerol lipase compatible with inhibitor screening.

Many papers describes the use of bovine serum albumin (BSA) to prevent the non-specific binding of the substrate to the walls of the tubes and assists in its solubility[163].

We decided not to use BSA because it is reported to enhance the fluorescence signal even in the absence of enzyme[163] and it is not compatible with the assay.

Different amounts of hMAGL ranging from 10 to 75 ng/well were added in each well (final volume 100 µl) to various concentrations of 7-HRA (from 0.5 to 25 µM, final concentrations) in 50 mM Tris–HCl (pH 7.4, 1 mM EDTA) with 10 % (v/v) DMSO.

The fluorescence was read every 5 min, at room temperature, for a period of 3 h using a Promega-GloMax multidetection system.

Sample	**DMSO (µl)**	**hMAGL sol. (µl)**	**Buffer sol. (µl)**	**7-HRA sol. (µl)**	**Inhibitor sol. (µl)**
Blank 7-HRA	5	-	90	5	-
Blank hMAGL	5	10	80	5	-

Tab. 2: Wells composition

The fluorescence units were converted to amount of resorufin produced basing on a calibration curve (**fig. 15**) by using standard solutions in DMSO (10 µl of standard in 90 µl of buffer).

All MAGL assays were performed in triplicate for each substrate concentration.

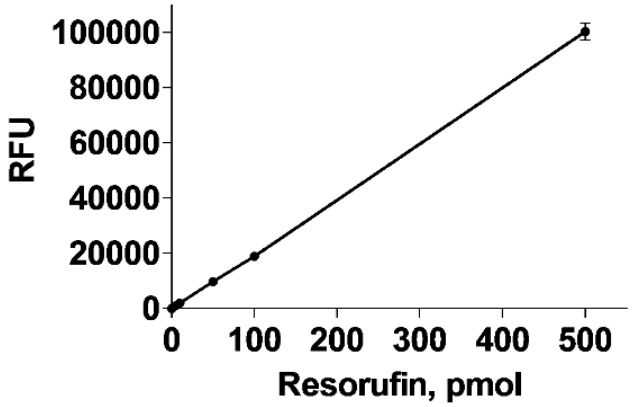

Fig. 15: Calibration curve

As shown in **fig. 16**, 7-HRA is very stable without enzyme (triangles), and leads to the liberation of a good amount of resorufin with the presence of hMAGL (circles).

[163] Savinainen, J. R. et al.; *Anal Biochem,* 399, **2010**, 132-134. Characterization of binding properties of monoglyceride lipase inhibitors by a versatile fluorescence-based technique.

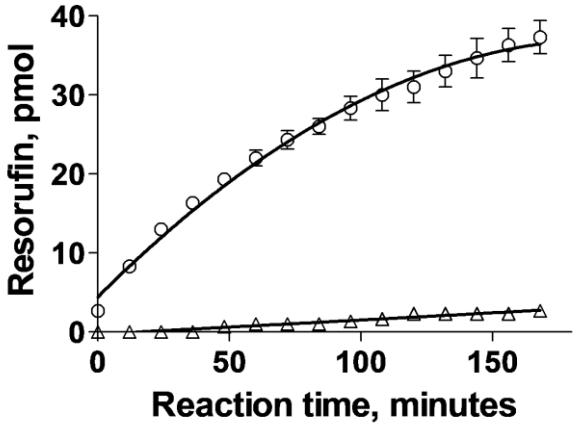

Fig. 16: 7-HRA hydrolysis with (circles) and without (triangles) MAGL

The optimal conditions for the determination of kinetic parameters were found to be 25 ng/well of MAGL with 5 μM 7-HRA (as used in fig.20); the Michaelis–Menten kinetic parameters were derived with Prism software, Version 5.0 (GraphPad, San Diego, CA) producing Km=0.87±0.13 μM and Vmax=25.84± 0.88 nmol min^{-1} mg $protein^{-1}$ (**fig. 17**).

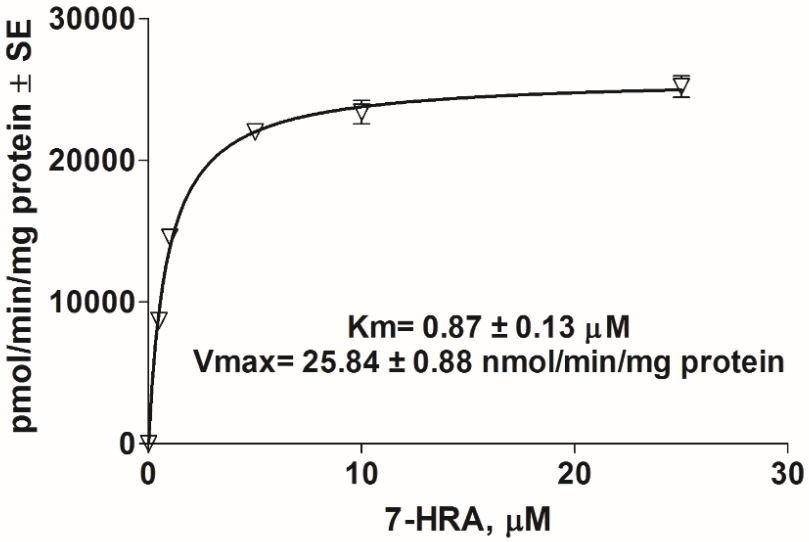

Fig. 17: Kinetics parameter of hMAGL using 7-HRA 5μM

7-HRA is particularly convenient for HTS experiments due to its low level of reactivity in the absence of enzyme. The reproducibility of the assay was given by the Z′ value of 0.80, that suggests the compatibility with HTS.

2.4 Method validation with known inhibitors

The validation of the new fluorescent method that uses 7-HRA as fluorogenic substrate for drug discovery screening, was made by studying the effect of three different known MAGL inhibitors - URB602[164], methyl arachidonyl fluorophosphonate (MAFP)[158] and JZL184 (**fig. 18**)[157] - under the standard assay conditions with 5 μM 7-HRA as substrate, DMSO as solubilizer and Tris–HCl (50mM, pH 7.4, 1 mM EDTA) as reaction buffer.

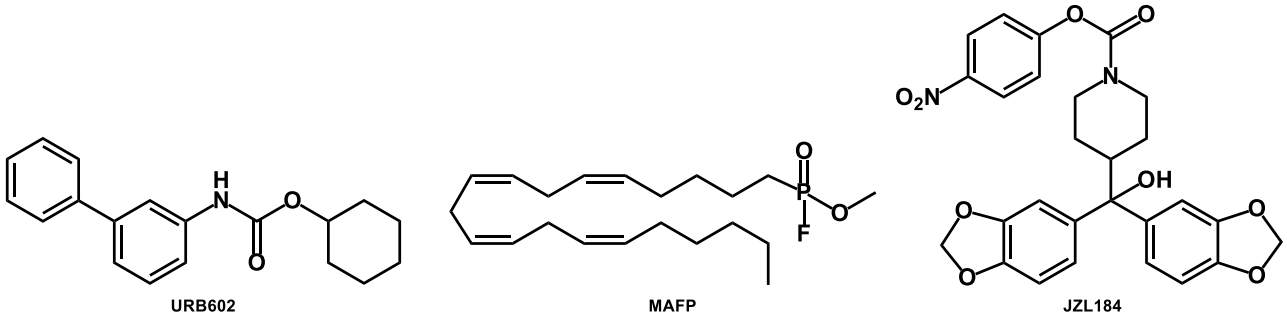

Fig. 18: Structure of known MAGL inhibitors URB602, MAFP and JZL184

25 ng/well of hMAGL was dissolved in the assay buffer and added to 80 μl of buffer solution in a 96-wells black plate; 5 μl of inhibitor solutions at different concentrations in DMSO were added and then incubated at room temperature for 60 min. For the "blank 7-HRA" well DMSO alone was added, whereas inhibitors were prepared in a range of concentration comparable to that used in literature (from nM to over μM).

After incubation, the reaction was started by the rapid addition of 5 μl of 7-HRA intermediate solution to obtain the final concentration of 5 μM, in the final volume of 100 μl.

Sample	DMSO (μl)	hMAGL sol. (μl)	Buffer sol. (μl)	7-HRA sol. (μl)	Inhibitor sol. (μl)
Blank 7-HRA	5	-	90	5	-
Blank hMAGL	5	10	80	5	-
Inhibitors	-	10	80	5	5

Tab. 3: Wells composition for blanks and inhibitors samples

The fluorescent signal was measured at different time points (every 3 minutes) for a period of 1 hour and the fluorescence unit converted to amount of resorufin basing on the calibration curve.

The IC_{50} values were calculated after 30 minutes and derived from two independent experiments performed in triplicate, calculated as nonlinear regressions using sigmoid dose–response setting with variable Hill slope by GraphPad Prism 5.0 for Windows.

Fig. 19: Inhibition of hMAGL by URB602

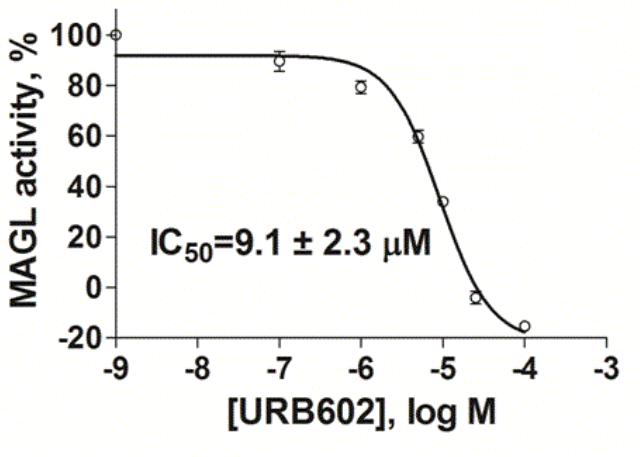

As shown in **fig. 19**, the IC_{50} value for the inhibition of hMAGL (25ng/well) is 9.1 ± 2.3 μM, which is in line with data reported in literature[164] for this first selective MAGL inhibitor.

Fig. 20: Inhibition of hMAGL by MAFP

As already known methyl arachidonyl fluorophosphonate has the lowest IC_{50} value of 5.4 ± 1.7 nM (**fig. 20**), showing a very high inhibitory potential on hMAGL, which is due to an irreversible and non-selective mechanism of action that prevents its application in therapy[158].

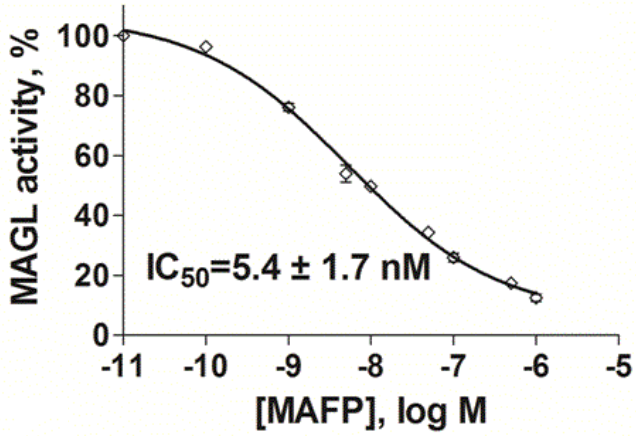

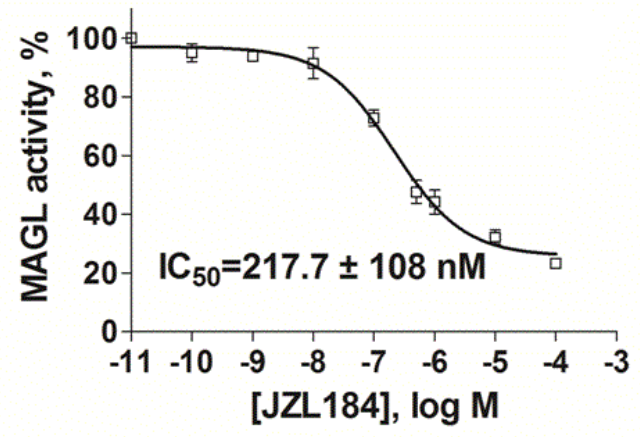

Fig. 21: Inhibition of hMAGL by JZL184

At last, JZL184 has IC_{50} value of 217 ± 108 nM (**fig. 21**) that matches what observed by *Savinainen et al*[157]; confirming the good activity described for this selective inhibitor.

[164] Matuszak, N. et al.; *J Med Chem,* 52, **2009**, 7410-7420. Synthesis and in vitro evaluation of N-substituted maleimide derivatives as selective monoglyceride lipase inhibitors.

These results proved that our fluorogenic enzyme assay, using 7-HRA as new fluorogenic substrate - and validated with the use of three known inhibitors described in literature - can be successfully applied for the identification and activity evaluation of compounds able to modulate MAGL activity. Moreover, the red fluorogenic substrate 7-HRA assay proved to be rapid, versatile and compatible with high throughput screening and led to the same sensitivity of the blue fluorogenic substrate (7-HCA), with the advantages of lower interferences on cell culture assays.

3. STRUCTURE DESIGN OF NEW POTENTIAL MAGL INHIBITORS

The beginning of the work was the selection of a reference molecule among the several that are known to be MAGL inhibitors[165].

The choice fell on molecule URB602 (**fig. 22**), which was firstly described in 2005[166] as MAGL inhibitor.

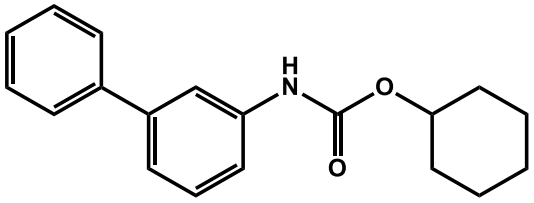

URB602

Fig. 22: URB602 molecule

Different studies have been made for the evaluation of its activity against MAGL[167],[168], and other works[169],[170] tried to evaluate which modifications could increase the selectivity and the potency against this enzyme.

In particular, the study of *Szabo et al*[169] showed the importance of different residues in the area belonging to the so called "upper active site", and confirmed the action of URB602 as a non-covalent inhibitor.

Fig. 23: Interaction between MAGL and a carbamate inhibitor (from Bioorg. Med. Chem. Lett., 21, 2011)

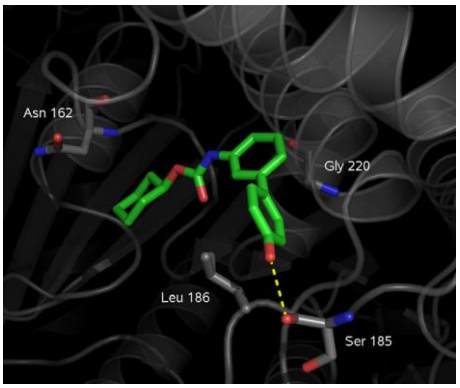

This region is characterised by the presence of a Ser-185 residue, which can make the formation of hydrogen bond interactions possible (**fig. 23**), with an appropriate substituent on the biphenyl side of the structure.

Always in this area, the presence of different hydrophobic residues - such Ala-174, Gly-220 and Leu-186 - suggest the formation of hydrophobic interactions with the cycle linked to the oxygen side of the carbamate, also suggesting that a 5- to 7-atoms ring could be the best for a correct interaction.

[165] Fowler, C. J. et al.; *Br. J. Pharmacol.,* 166, **2012**, 1568-1585. Monoacylglycerol lipase a target for drug development?

[166] Hohmann, A. G. et al.; *Nature,* 435 (23), **2005**, 326-338. An endocannabinoid mechanism for stress-induced analgesia.

[167] King, A. R. et al.; *Chem. Biol.,* 14, **2007**, 1357-1365. URB602 Inhibits Monoacylglycerol Lipase and Selectively Blocks 2-Arachidonoylglycerol Degradation in Intact Brain Slices.

[168] Comelli, F. et al.; *Br. J. Pharmacol.,* 152, **2007**, 787-794. The inhibition of monoacylglycerol lipase by URB602 showed an anti-inflammatory and anti-nociceptive effect in a murine model of acute inflammation.

[169] Szabo, M. et al.; *Bioorg. Med. Chem. Lett.,* 21, **2011**, 6782-6787. The design, synthesis and biological evaluation of novel URB602 analogues as potential monoacylglycerol lipase inhibitors.

[170] Tuccinardi, T. et al.; *Bioorg. Med. Chem.,* 22, **2014**, 3285-3291. Identification and characterization of a new reversible MAGL inhibitor.

The crystallographic structure of MAGL in complex with URB602 showed that a hydrogen bond exists between the NH-portion of Asn-162 and the oxygen belonging to the carbamate inhibitor, raising the rational for the presence of this peculiar structure.

Moreover, two other residues - Cys-201 and Cys-208 - were highlighted as very important points for the enzyme activity[171], and they are considered to be possible targets for inhibitory compounds.

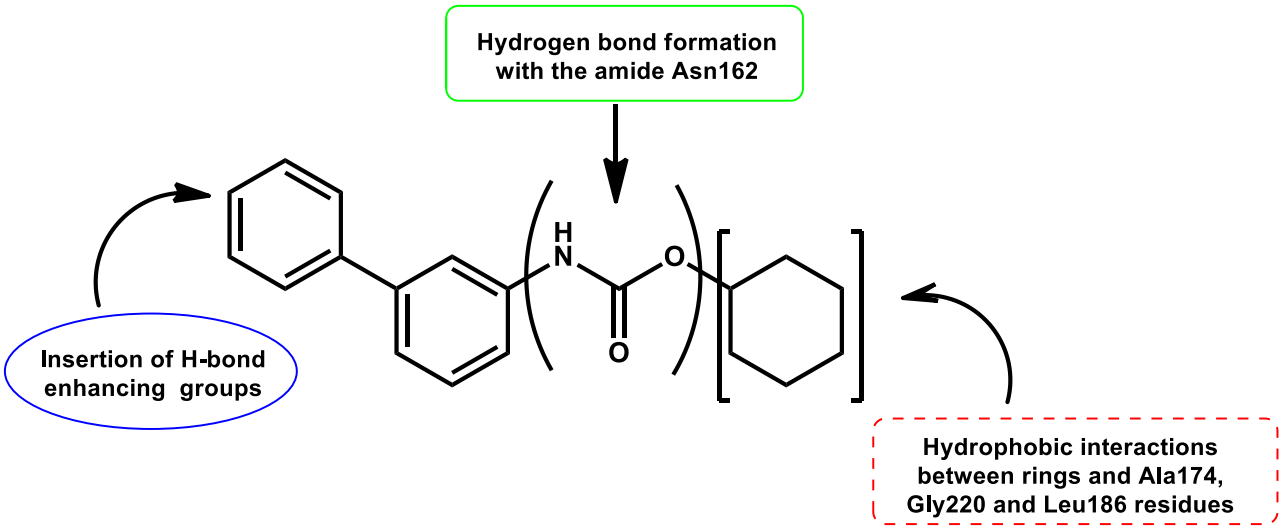

Fig. 24: URB602 modification sites

Taking into account all these considerations, during the design of new molecules (**fig. 24**), we decided to:

a) maintain the basic carbamate body;

b) insert very small groups on the biphenyl side, able to increase the possibility of H-bond interactions (-F and -CF_3 groups);

c) insert different carbocyclic or aromatic rings linked with variable - but short - spacers to the carbamate oxygen, trying to enhance the formation of hydrophobic interactions between the candidate drug and the enzyme.

[171] Bertrand, T. et al.; *J. Mol. Biol.*, 396, **2010**, 663-673. Structural Basis for Human Monoglyceride Lipase Inhibition.

3.1 Synthesis of new molecules

We decided to synthesise a small pool of potential MAGL inhibitors, basing on the structure of known URB602[169].

As shown in **fig. 25**, in these new molecules we inserted different small modifications, such as the introduction of -F or -CF_3 residues on the biphenyl side (compounds **2a** and **3a**), different carbocyclic or aromatic rings bound through short spacers (**1a**, **1b**, **1c** or **1d**), or both the things together (**2b**, **2c**, **3b**).

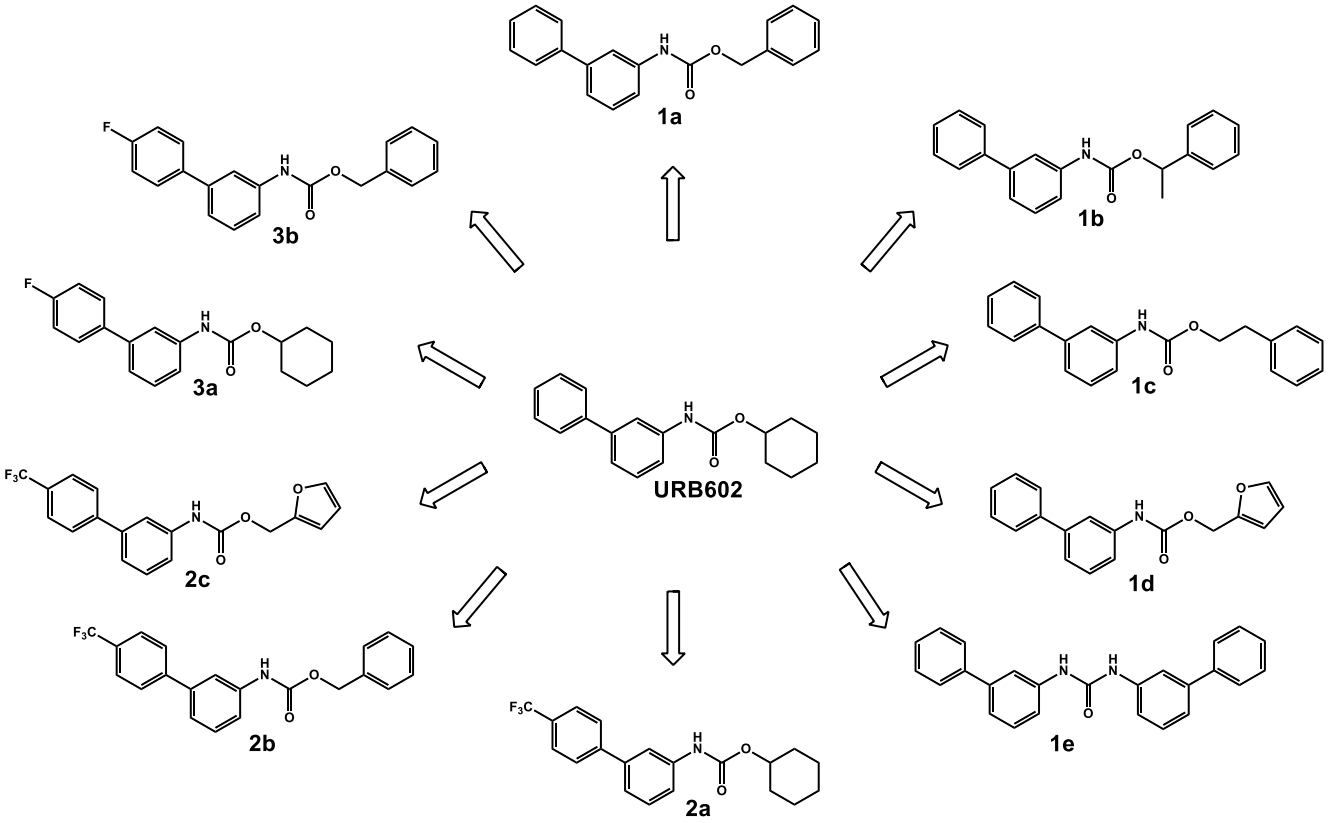

Fig. 25: Library of URB602 synthetic analogues

We also synthesised a molecule containing an ureic structure -compound **1e** - instead of the classical carbamate scaffold, to verify what happens with the substitution of the H-bond acceptor oxygen of the carbamate with the mostly H-donor nitrogen atom.

The synthesis was made using the general procedure described by *Szabo et al*[169], which consisted in a two steps process (**scheme 11**).

The first one was a Suzuki palladium tetrakis-catalysed reaction: the appropriate phenilboronic acid was reacted at reflux with *m*-bromoaniline in the presence of sodium carbonate, in dry CH_3OH, to give an intermediate biphenylamine (42 - 65% yield, **4a-c**).

The second step was the activation, at reflux, of the intermediate with carbonyl diimidazole (CDI), using DMAP as catalyst and in dry acetonitrile; the subsequent addition in the medium of the proper

alcohol and the heating for the necessary time of reaction gave the different desired products with medium to good yields (**tab. 4**).

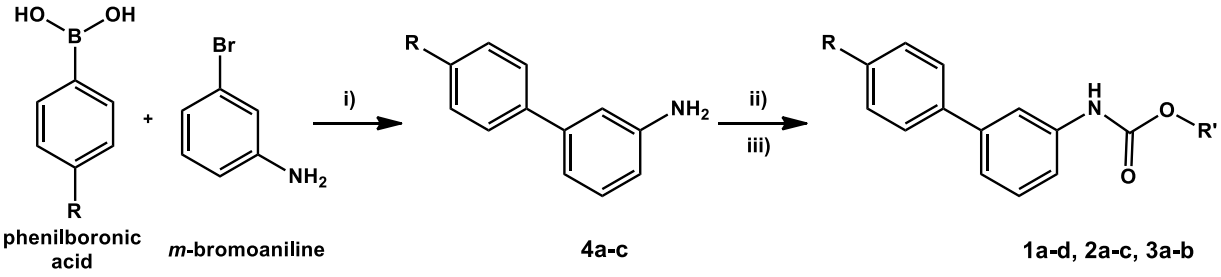

i) $Pd(PPh_3)_4$, Na_2CO_3, CH_3OH, reflux, 12 h // ii) CDI, DMAP, CH_3CN, reflux, overnight // iii) R'-OH,CH_3CN, reflux

Scheme 11: Synthetic route for URB602 analogues

Molecule	R-	R'-	Reaction iii) time	Yield
URB602	H	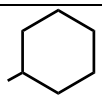	24 h	69%
1a	H	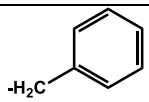	48 h	30%
1b	H	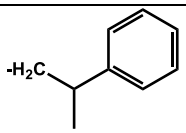	24 h	72%
1c	H	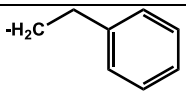	24 h	54%
1d	H	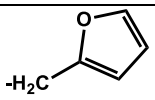	24 h	45%
2a	CF_3		24 h	58%
2b	CF_3	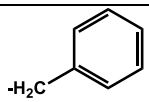	24 h	64%
2c	CF_3	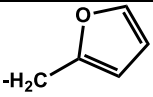	12 h	70%
3a	F		24 h	74%
3b	F	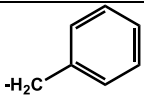	24 h	80%

Tab. 4: Reaction yields and conditions

For ureic molecule **1e**, the first step was the same previously described; otherwise, after the activation of intermediate biphenylamine with CDI, the following addition of phenol resulted in the sudden precipitation of a white solid, which resulted to be the symmetric ureic molecule **1e** and not the desired product bearing a phenolic residue directly linked on the carbamate oxygen as expected.
In this way we obtained a small stock of analogues of reference URB602, ready to be tested on their activity on hMAGL.

4. ACTIVITY EVALUATION OF NEW SYNTHETIC MOLECULES

After an initial study using the *p*-nitrophenyl alkyl esters method, synthetic molecules were studied on their potential to inhibit hMAGL using the fluorescence method developed in the laboratory[172], both on hMAGl and cellular lysates.

4.1 On human recombinant MAGL (hMAGL)

Assays were performed as described for the validation of the method, using 25ng/well of hMAGL, 5 μM 7-HRA as substrate, 10 % DMSO as solubilizer and Tris-HCl (50mM, pH 7.4, 1 mM EDTA) as reaction buffer.

All molecules were used in final concentrations that ranged from 10^{-9} M to 75 μM in order to calculate the inhibition curve against hMAGL.

The enzyme was dissolved in Tris-HCl and added to 80 μl of buffer solution in a 96-wells black plate; 5 μl of inhibitor solutions at different concentrations in DMSO were added and then incubated at room temperature for 60 min.

The reaction was started after the incubation period by the rapid addition of 5 μl of 7-HRA intermediate solution to obtain the final concentration of 5 μM, in the final volume of 100 μl. The fluorescent signal was measured at different time points (every 3 minutes) for a period of 1 hour and the fluorescence unit converted to amount of resorufin basing on the calibration curve.

The IC_{50} values were calculated after 30 minutes and derived from two independent experiments performed in triplicate, calculated as nonlinear regressions using sigmoid dose–response setting with variable Hill slope by GraphPad Prism 5.0 for Windows.

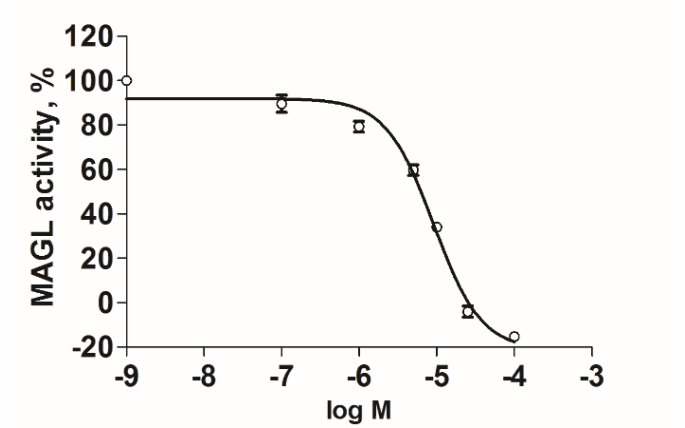

Fig. 26: Inhibition by URB602

Molecule URB602 was used as control to verify the reliability of the experiment during the different repeats and, as already shown, it gave an IC_{50}= 9.1 ± 2.3 μM

[172] Lauria, S. et al.; *Anal Bioanal Chem,* 407, **2015**, 8163-8167. Synthesis and characterization of a new fluorogenic substrate for monoacylglycerol lipase and application to inhibition studies.

Molecule **1b** could not be tested due to poor solubility, however molecule **1e**, belonging to the family of ureas, was tested but showed no activity at all as inhibitor; on the contrary, it seemed to have a positive effect on hMAGL, increasing the hydrolytic activity on the substrate, and acting as an activator of the enzyme.

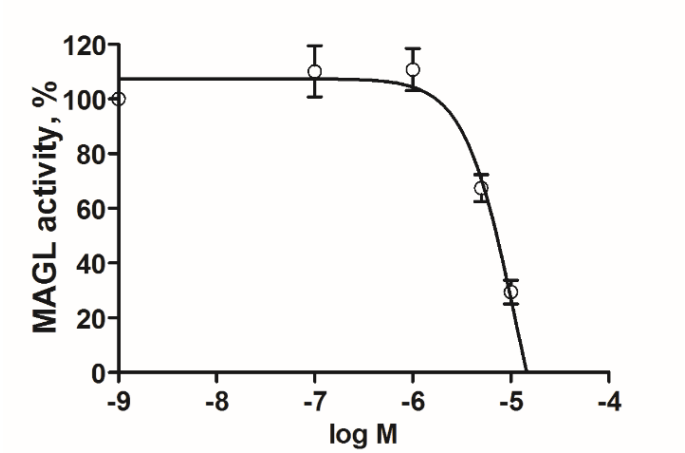

Fig. 27: Inhibition by **1a**

Molecule **1a** had an inhibition value slightly lower than URB602, with IC_{50}= 11.1 ± 2.3 μM.

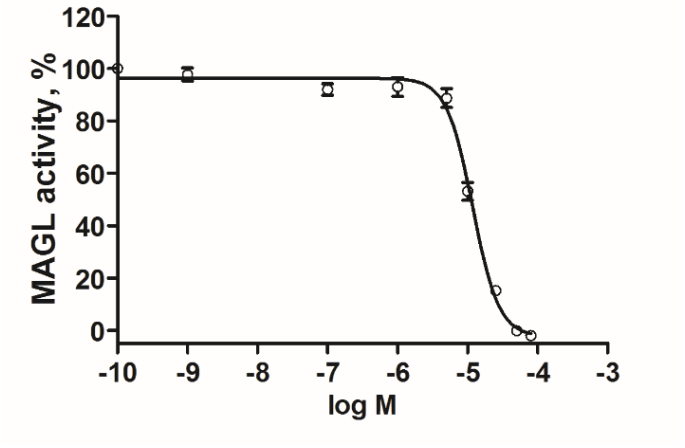

Fig. 28: Inhibition by **1c**

1c showed an IC_{50}= 11.3 ± 1.4 μM, once again comparable with that of URB602.

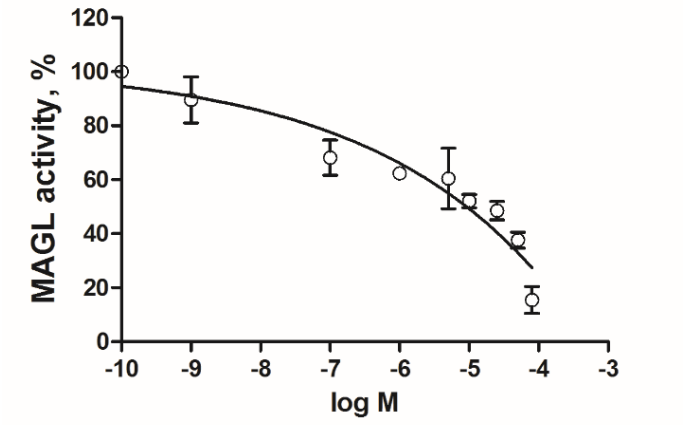

Fig. 29: Inhibition by **1d**

Molecule **1d** gave an inhibition profile very different from its analogues, with poor reliability and a too much wide range of IC_{50} values even with many repetitions of the experiment.

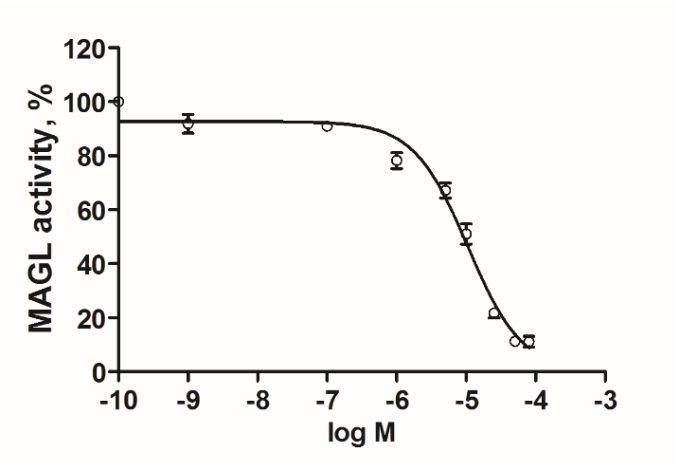

Fig. 30: Inhibition by **2a**

The same happened for molecule **2a** showing IC_{50}= 10.5 ± 2 μM, with no increasing of the activity.

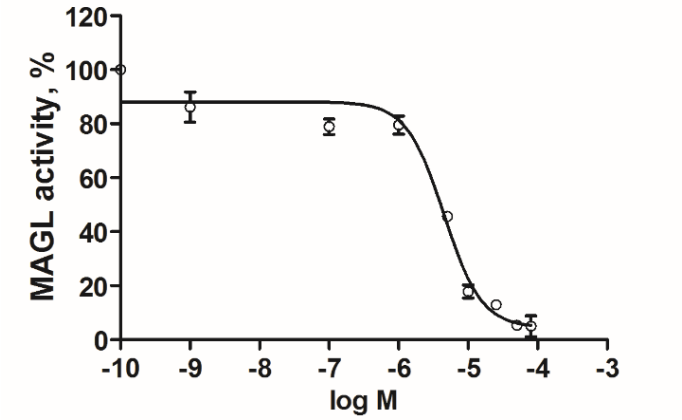

Fig. 31: Inhibition by **2b**

The best value was obtained with molecule **2b**: IC_{50}= 4.5 ± 0.7 μM, seeming to have an inhibitory activity double than URB602.

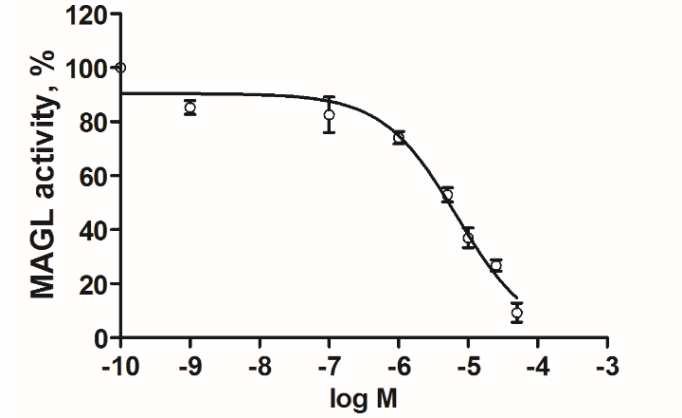

Fig. 32: Inhibition by **2c**

The furanic-fluorinated inhibitor **2c** had a slight increase of activity compared to the reference, having IC_{50}= 6.7 ± 0.7 μM.

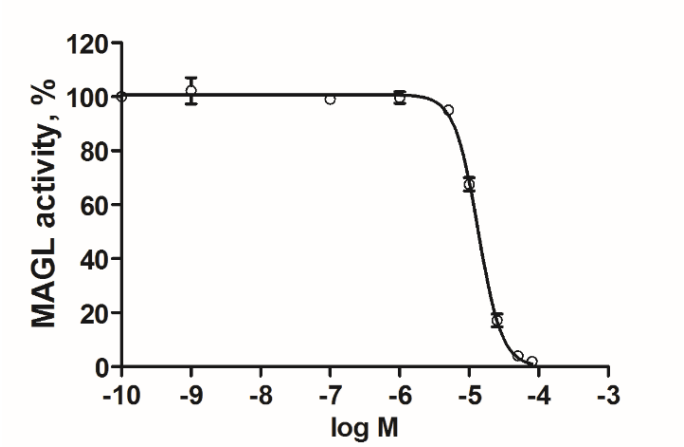

Fig. 33: Inhibition by **3a**

Molecule **3a** had IC_{50}= 13.4 ± 0.9 μM, once again comparable with reference molecule.

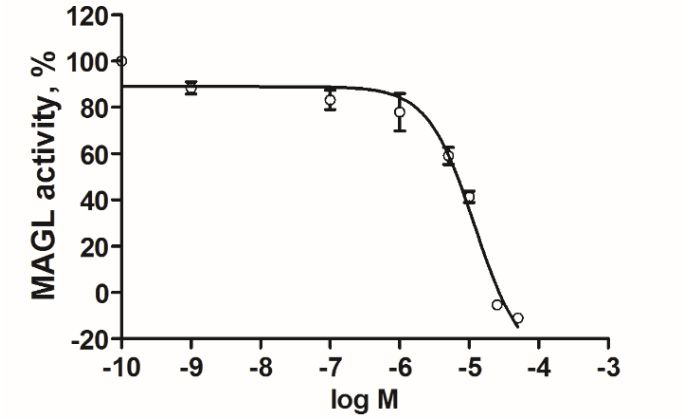

Fig. 34: Inhibition by **3b**

The analogue **3b** showed a small increase of URB602 activity, with IC_{50}= 7.9 ± 0.8 μM.

As possible to verify from the graphs, the general behaviour of all molecules is very similar to that of reference URB602.

Molecules **1a**, **1c**, **2a** and **3a** showed an IC_{50} value comparable to that of URB602, around 10 μM; molecule **1e** (not reported) demonstrated to be an activator of the enzyme, causing a huge increase of the fluorescent signal.

Better inhibition values were obtained with molecule **3b**, **2c**, and - in particular - with **2b**, which showed IC_{50}= 7.9 ± 0.8 μM, IC_{50}= 6.7 ± 0.7 μM and IC_{50}= 4.5 ± 0.7 μM respectively.

From these data, the suggestion could be that the contemporary insertion of a fluorinated residue (present in each of these molecules) on the biphenyl side and of an aromatic substituent (benzene ring for **2b**/**3b** and furanic ring for **2c**) bound through a one-carbon linker on the oxygen side of the structure, seem to be important for the interactions with the enzyme.

These interactions are favourably translated in the inhibition of MAGL (**tab. 5**), with a decrease of its activity in the assay, which is the aim of the study.

Compound	IC_{50} (μM)
URB602	9.1 ± 2.3
1a	11.1 ± 2.3
1c	11.3 ± 1.4
2a	10.5 ± 2
2b	4.5 ± 0.7
3a	13.4 ± 0.9
3b	7.9 ± 0.8
2c	6.7 ± 0.7

Tab. 5: Inhibition values of different compounds

4.2 On cancer cell lysates

The same experiment was performed *in vitro* using cancer cell lysates, in order to verify the feasibility of the new fluorescent method and to prove the eventual activity of inhibitory molecules on tissue samples.

The hydrolytic activity of MAGL on cell lysates was conducted using the fluorogenic substrate previously described.

Briefly, cells (B16-F10 melanoma cells, Lewis lung carcinoma cells, Gl261 glioma cells)[173],[174] were cultured in Dulbecco's modified medium supplemented with 10% heat-inactivated foetal bovine serum (FBS), glutamine (200 mM), penicillin/streptavidin (100 U/ml), 1% Hepes 1M pH 7.4 and grown at 37°C in a humidified atmosphere containing 5% CO2.

After 36 h of culture, cells were homogenised for 30 min at 4° C in lysis buffer (10 mM Tris, 150 mM NaCl, 1 mM EDTA, 0.1% SDS, 1% Triton X-100 with protease inhibitor mixture, pH 7.4) and lysates were then centrifuged for 5 min at 1,500 × *g*.

The assay was carried out in a 96-well format using 1 μg of cell lysate and 10 μM of substrate.

Fluorescence was measured at 588 nm (λ_{ex}.571 nm/λ_{em}.588 nm) by a Glomax-Microplate Multimode Reader (Promega) every 2 min for 2 h.

To test the inhibitors, B16-F10 melanoma cells lysate was pre-treated for 60 min with DMSO or the inhibitors at different concentrations.

Then, the substrate was added to each well and fluorescence was measured every 2 min for 2 h.

The graphs show the results after 5 min of incubation. Values are expressed as mean ± SEM (n = 3).

[173]Hamtiaux, L. et al.; *BMC Cancer.,* 12, **2012**; 92-97. The association of *N*-palmitoylethanolamine with the FAAH inhibitor URB597 impairs melanoma growth through a supra-additive action.

[174] Aaltonen, N. et al.; *Chem. Biol.,* 20, **2013**, 379-390. Piperazine and Piperidine Triazole Ureas as Ultrapotent and Highly Selective Inhibitors of Monoacylglycerol Lipase.

Each molecule was tested in a range of concentration from 0 to 75 μM, in relative high concentrations, as suggested from previous studies on URB602[175], in which it showed to have a modest activity in terms of potency when used on cells or cell lysates.

Ureic molecule **1e** (not reported) showed no activity at all as inhibitor but as already mentioned, seemed to increase the activity of the enzymatic apparatus.

Analogue **1b** was not tested due to solubility problems and molecule **1d** for the reported unrepeatability of results showed with hMAGL.

All other molecules were tested: in each graph below, relative to B16-F10 melanoma cells lysate, red lines with circles are control molecule URB602, otherwise black lines with squares are relative to test compounds.

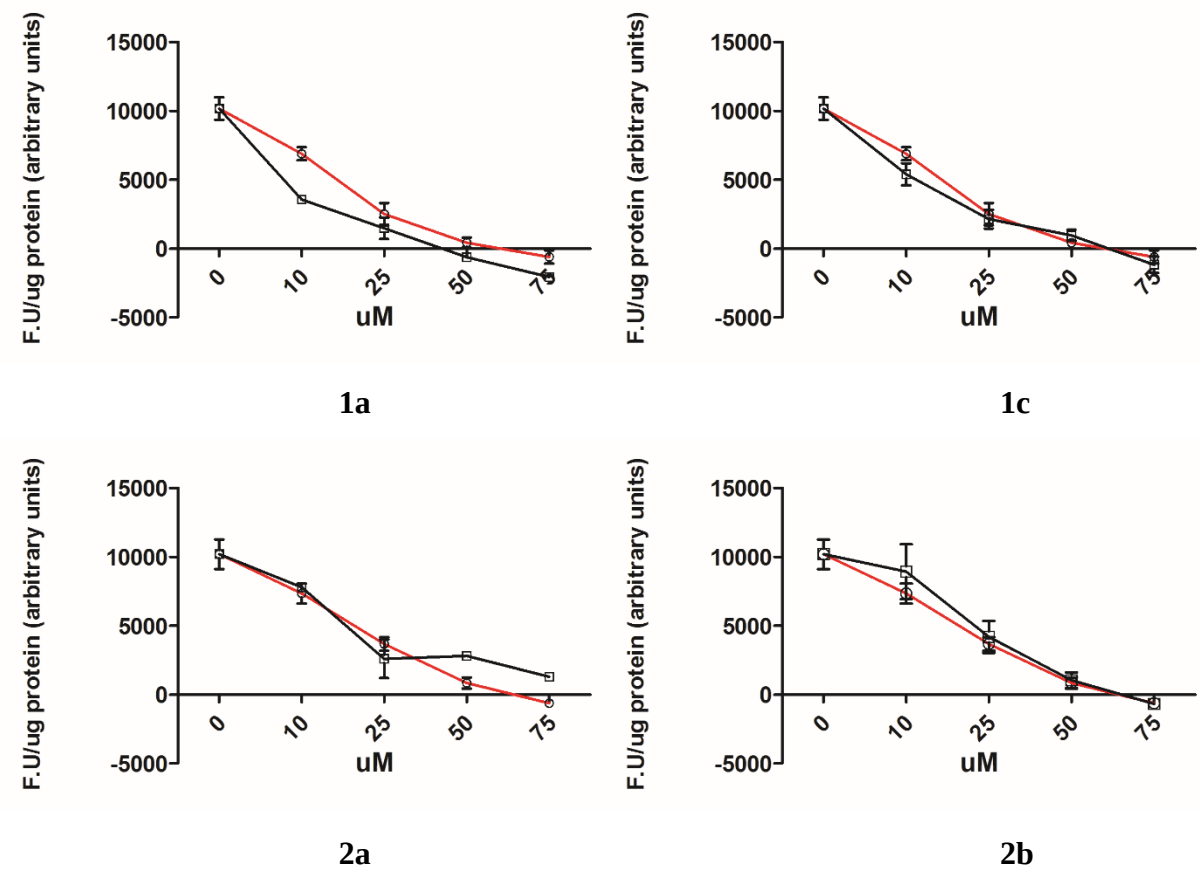

Fig. 35 (continues)

[175] King, A. et al.; *Chem. Biol.,* 14, **2007**, 1357-1365. URB602 Inhibits Monoacylglycerol Lipase and Selectively Blocks 2-Arachidonoylglycerol Degradation in Intact Brain Slices.

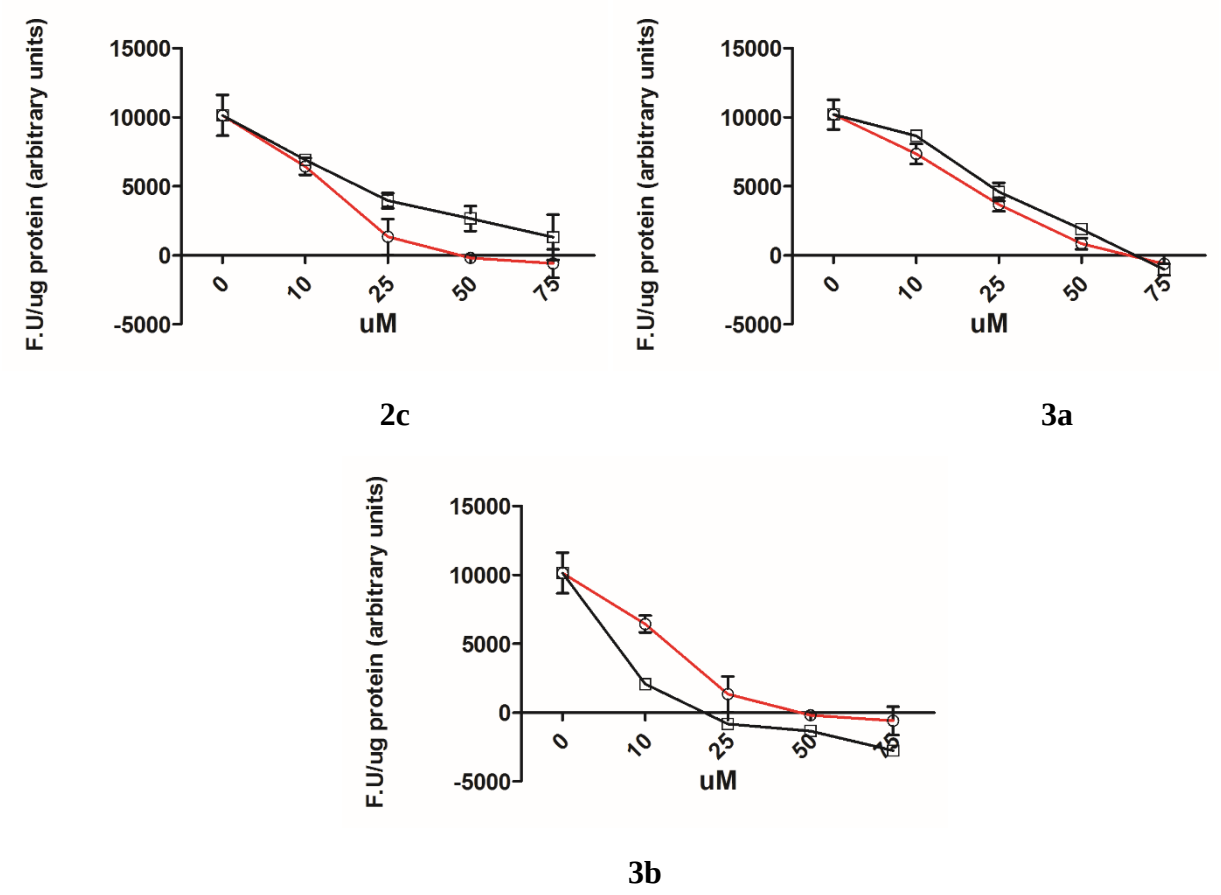

Fig. 35: Use of synthetic compounds on B16-F10 melanoma cells lysate

As possible to see from **fig. 35**, the general trend among all molecules is very similar to that of URB602: in terms of potency, all molecules have the same behaviour of the reference one, with activities that are appreciable with relatively high amount of inhibitor (in the field of μM concentrations). Only molecules **3b** and **2c** have an activity increase that is significantly different from URB602 - but however, in the field of μM concentration - too high for a direct development as possible drugs.

The essentially overlapping results between URB602 and most of the tested molecules are due to the low differences in terms of activity obtained with the fluorogenic method using hMAGL.

The small differences that spread out on the pure enzyme were not highlighted with the use of cell lysates because of the presence of all other lipases that are present in cells, and that – obviously - can produce interferences that have to be evaluated.

Anyway, the general results seemed to confirm the potential of these molecules as starting point for the development of more potent MAGL inhibitors, with perspectives in cancer-treatment applications.

5. MOLECULAR MODELLING STUDY

The in silico screening was carried out by Dr. Eberini's group, using the Dock program contained in the MOE Simulation module[176].

The full MAGL structure obtained from the Protein Data Bank (PDB code 3JW8[171]) was set as receptor.

Before starting with the placement procedure, 1.000 conformations were generated for each ligand by sampling their rotable bonds.

The selected placement methodology was Triangle Matcher, in which the poses are generated by superposing triplets of ligand atoms and triplets of receptor site points; the receptor site points are alpha spheres centres that represent locations of tight packing.

Before scoring all the generated poses, duplicate complexes were removed; poses are considered as duplicates if the same set of ligand-receptor atom pairs are involved in hydrogen bond interactions and the same set of ligand atom receptor residue pairs are involved in hydrophobic interactions.

The accepted poses were scored according to the London dG scoring, which estimates the free energy of binding of the ligand from a given pose.

$$\Delta G = c + \sum_{h-bonds} c_{HB} f_{HB} + \sum_{m-lig} c_M f_M + \sum_{atoms\_i} \Delta D_i$$

where c represents the average gain/loss of rotational and translational entropy; E_{flex} is the energy due to the loss of flexibility of the ligand (calculated from ligand topology only); f_{HB} measures geometric imperfections of hydrogen bonds and takes a value in [0,1]; c_{HB} is the energy of an ideal hydrogen bond; f_M measures geometric imperfections of metal ligations and takes a value in [0,1]; c_M is the energy of an ideal metal ligation; and D_i is the desolvation energy of atom *i*. The difference in desolvation energies is calculated according to the formula

$$\Delta D_i = c_i R_i^3 \left\{ \iiint_{u \notin A \cup B} |u|^{-6} du - \iiint_{u \notin B} |u|^{-6} du \right\}$$

where A and B are the protein and/or ligand volumes with atom *i* belonging to volume B; R_i is the solvation radius of atom *i* (taken as the OPLS-AA van der Waals sigma parameter plus 0.5 A°); and c_i is the desolvation coefficient of atom *i*. The coefficients {c, c_{HB}, c_M, c_i} have been fitted from approx. 400 x-ray crystal structures of protein–ligand complexes with available experimental pKi data. Atoms are categorized into about a dozen atom types for the assignment of the c_i coefficients. The triple integrals are approximated using Generalized Born integral formulas. Only the top scoring

[176] Eberini, I. et al.; *Cellular Signalling*, 26, **2014**, 2614-2620. Oxysterols act as promiscuous ligands of class-A GPCRs: In silico molecular modeling and in vitro validation.

solution was kept and submitted to a further refinement step, based on molecular mechanics (MM). In order to speed up the calculation, residues over a 6 A° cut-off distance away from the pre-refined pose were ignored, both during the refinement and in the final energy evaluation. All receptor atoms were held fixed during the refinement.

During the course of the refinement, solvation effects were calculated using the reaction field functional form for the electrostatic energy term.

The final energy was evaluated using the MMFF94x force field with the Generalized Born solvation model (GBIV) The estimated binding affinity and the ligand efficiency were calculated through the MOE LigX module. The pKi was computed through the binding free energy estimated with the London dG scoring function.

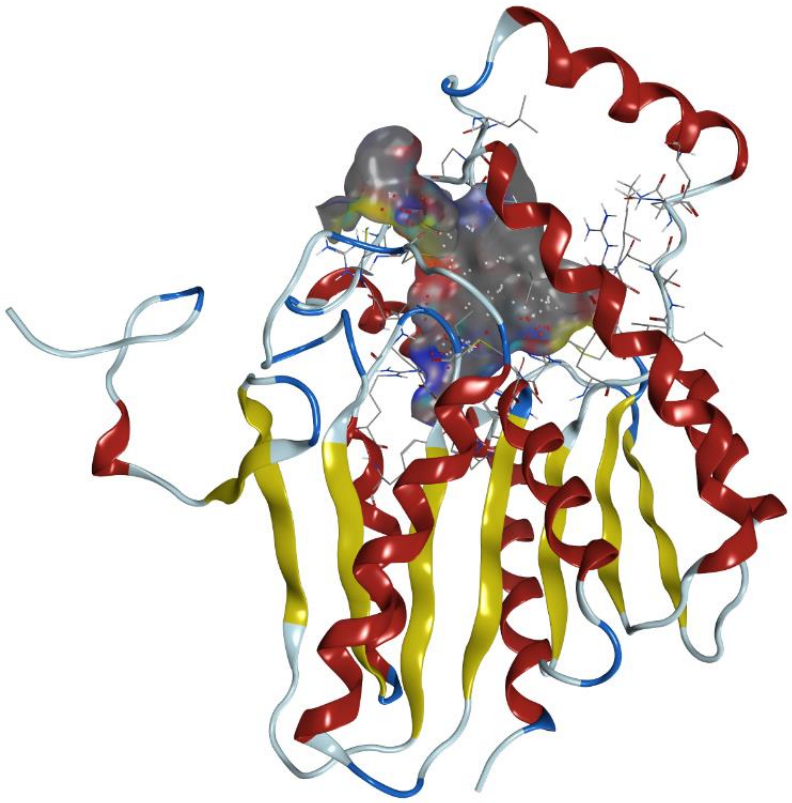

Fig. 36: MAGL's upper active site

In **fig. 36** is shown the so called "upper active site" of MAGL, a region which is in the near proximity of the catalytic active site and that has already been described by *Szabo et al*[169] as one of the top scoring area for the interaction with potential inhibitors.

This area is characterised by the presence of Cys residues which have been identified as important[171] for the activity of MAGL; in fact, the use of mercuric compounds *(p*-chloromercuribenzoic acid or mercury chloride) leads to the inactivation of the enzyme as shown by *Tornqvist and Belfrage*[177].

[177] Tornqvist, H. et al.; *J. Biol. Chem.* 251 (3), **1976**, 813-819. Purification and Some Properties of a Monoacylglycerolhydrolyzing Enzyme of Rat Adipose Tissue.

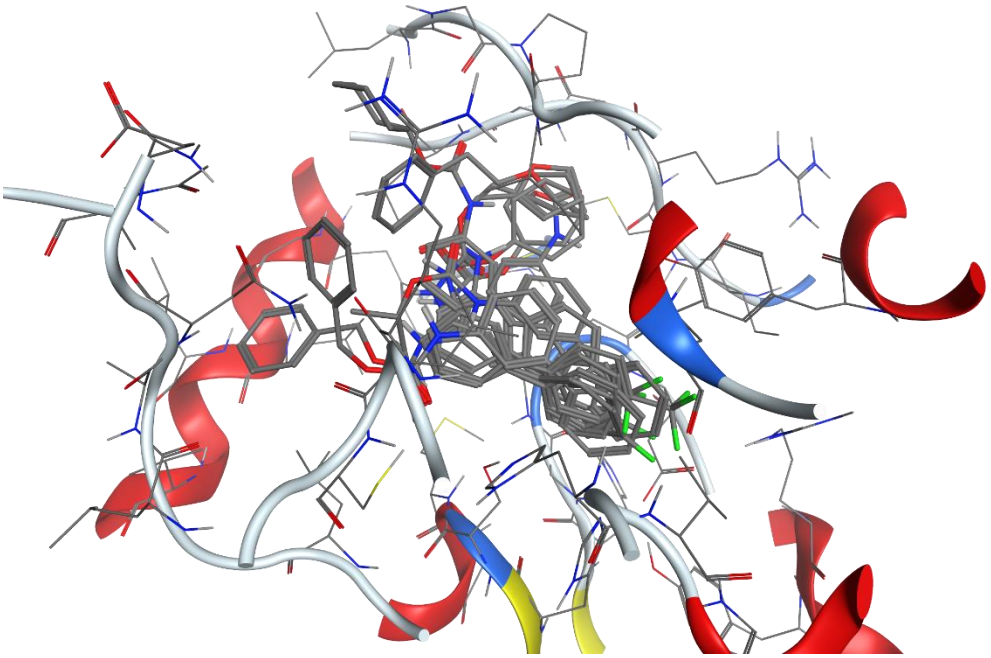

Fig. 37: Library compounds docked in the binding site

After the identification of the binding site, all molecules were docked in this area (**fig.37**) showing a good overlap with each other for what concerns the basic biphenyl-carbamate portion.

From this calculation, the parameters relative to binding scores and affinities were obtained (**tab. 6**).

Compound	S	rmsd_refine	E_conf	E_place	E_score1	E_refine	E_score2	Affinity
2b	**-5.9430838**	0.58281505	78.291893	-66.040695	-10.551647	9.3805799	-5.9430838	**-7.51**
2c	**-5.0423589**	0.7060526	61.225021	-70.984642	-11.266261	-11.543186	-5.0423589	**-7.45**
3b	**-4.8428435**	0.41026047	71.469421	-74.062782	-9.978035	9.6461573	-4.8428435	**-7.23**
2a	**-4.7799511**	0.44828889	59.427479	-92.349586	-10.491234	-5.8264842	-4.7799511	**-6.53**
1d	**-4.7777739**	0.67168045	61.030651	-78.702347	-9.6511679	-2.436954	-4.7777739	**-6.67**
1e	**-4.6375728**	0.63646847	106.74659	-84.480141	-10.593376	28.71034	-4.6375728	**-7.95**
3a	**-4.2893596**	0.63039917	56.280289	-75.822365	-10.364834	-8.0055685	-4.2893596	**-6.95**
1c	**-4.25176**	0.77640748	117.52163	-92.035095	-9.7479868	51.337315	-4.25176	**-6.65**
1b	**-4.1275358**	0.70628202	74.800369	-82.03463	-9.8570385	7.1317501	-4.1275358	**-7.10**
1a	**-4.1032023**	0.83517736	73.456062	-62.114296	-10.158004	12.805244	-4.1032023	**-6.97**
URB602	**-3.7279174**	0.67099124	56.486671	-64.88781	-9.6643295	-7.2782025	-3.7279174	**-6.86**

Tab. 6: Docking scores

From the table is possible to verify that the best “docking score” (or “binding free energy”, value S) was relative to synthetic inhibitor **2b** (-5.9430838) - which also showed the best inhibitory activity using the fluorescent method previously described.

Concerning affinities, the best value was obtained for molecule **1e** (-7.95) which had no inhibitory effect on the enzyme, but on the contrary seemed to be an activator; its activating effect on MAGL is compatible with its affinity value, but needs to be studied in more details.

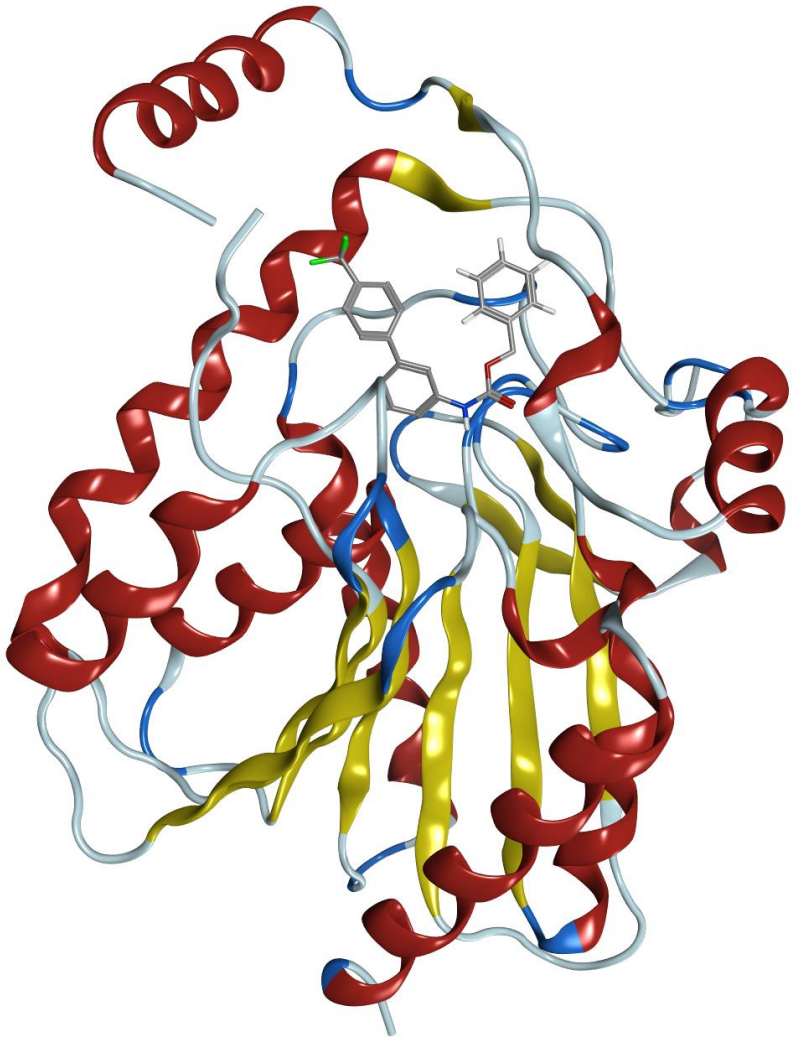

In terms of pKi values, due to the limit of this method (accuracy about one order of magnitude) there is no possibility of discrimination among the different structures, which have all (except **1e** of course) pKi=5, that is compatible with the experimental IC_{50} values, in the range of micro molar concentrations.

Fig. 38: Molecule **2b** docked to MAGL

As mentioned above, best fit values were shown by **2b**: from **fig.38** and **fig. 39** is possible to see the interactions with the upper active site of MAGL: the molecule accommodates in a pocket that is rich in hydrophobic residues, such Leu and Ile; in particular, hydrophobic interactions occur between the side chain of Ile-189 and the benzene ring present at the oxygen side of the carbamate molecule.

A ligand exposure at the level of the carbonyl oxygen takes place in proximity of Tyr-204, suggesting the possible formation of H-bond interactions.

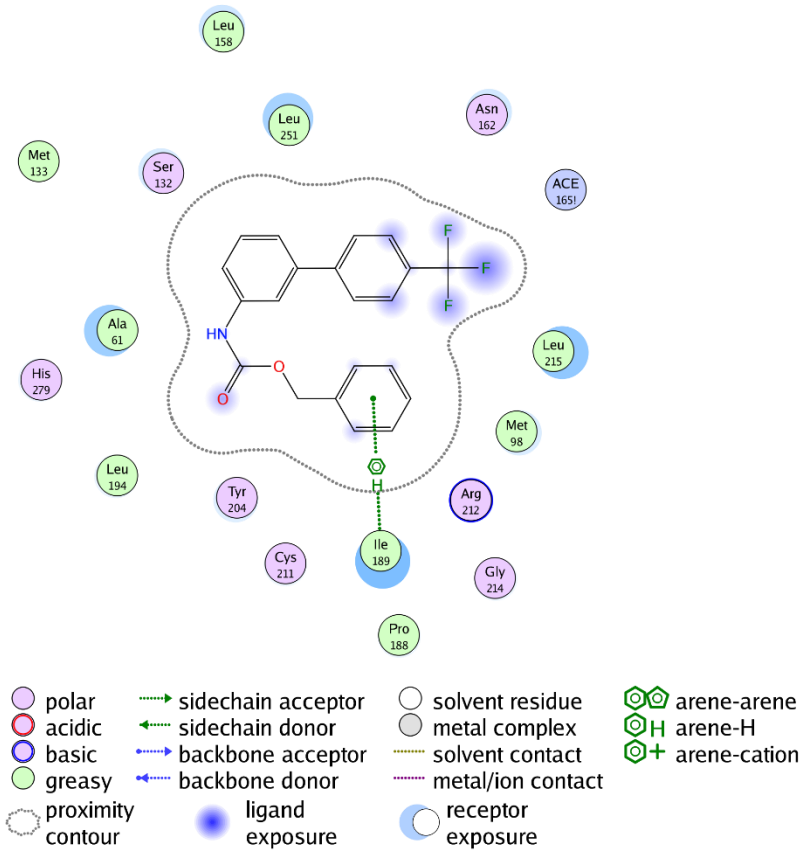

Fig. 39: 2b disposition

Another ligand exposure takes place at the trifluoromethyl residue, linked to the biphenyl portion of the molecule, which is stretched in the direction of Asn-162 and Leu-215.

Overall, these indications - docking scores and affinity values in particular - can suggest that the contemporary introduction of small polar atoms on one side and of an aromatic ring on the other produces an increase of the interactions occurring between the potential inhibitor and the enzyme.

6. CONCLUSION AND FUTURE DIRECTIONS

The endocannabinoid system (ECS) is a multifaceted entity with enormous therapeutic potential.

In the field of ECS understanding - and of MAGL in particular - a lot has to be done yet the work outlined in this thesis contributes to the advancement in MAGL knowledge.

One of the major problems in the study of possible active molecules, as MAGL inhibitors, is the availability of easy and reliable screening assays, both *in vitro* and *in vivo*.

Many methods are known, but all of them show different characteristics in terms of selectivity, sensitivity, costs of analysis and availability of the analytical equipment.

With the development of the new fluorogenic screening assay based on the use of 7-HRA, we tried to help to overcome the problems related to the sensitivity of the method and its feasibility in cellular screening assays.

In the first part of this research project, we have synthesized a red flurogenic substrate, 7-hydroxyresorufinyl-arachidonate (7-HRA), for a new assay for mammalian MAGL inhibition studies.

This assay is based on the enzymatic hydrolysis of a readily synthesized 7-HRA that results in the production of a fluorescent resorufin, with reduction of interferences due to the auto-fluorescence of cell membranes in the field of blue emitting wavelengths, giving a method useful even for *in vitro* tests on living cells.

The fluorometric method, validated using three known MAGL inhibitors, proved to be rapid, versatile, and compatible with high-throughput screening.

The assay will be applied for the development of new MAGL inhibitors as therapeutic agents that modulate the endocannabinoid system activity.

Moreover, the fluorometric assay could be a useful tool for further investigations into the relationship between MAGL inhibition and regulation of analgesia, inflammation, anxiety, and other disorders.

In the second part of this study, we have explored structural modifications of URB602 with the aim of producing inhibitors that could be more potent.

Starting from URB602 scaffold we designed and synthesized ten different new compounds carrying modifications on the three main parts of the molecule (biphenyl side, carbamate group and substituent at the oxygen side), to evaluate how these modifications (insertion of H-bond promoting groups, as -F or –NH, and/or hydrophobic interactions promoting residues) influence the inhibitory activity toward MAGL.

The synthesis of novel MAGL inhibitors was achieved with simple synthetic routes and in satisfactory yields; the molecules were tested with the new fluorogenic method on their ability to inhibit human recombinant MAGL and encouraging results were obtained.

All molecules showed a satisfactory inhibitory activity (comparable to that of reference molecule URB602) and better inhibition values were obtained with molecule **2b**, **2c**, and **3b**, which showed IC_{50}= 4.5 ± 0.7 μM, IC_{50}= 6.7 ± 0.7 μM and IC_{50}= 7.9 ± 0.8 μM, respectively.

The following modelling study helped to understand the possible role of the inserted substituents in MAGL inhibition; the contemporary insertions of –F residues on the biphenyl side and of an aromatic substituent through a one-carbon linker on the oxygen side, seem to be important for a good interaction with the enzyme.

A further step would be to verify if these new active compounds maintain their inhibitory effect *in vivo*.

Considering this work in particular, a deep study on whole cells has to be done, to evaluate the possibility to use the fluorogenic method on the constitutive MAGL enzyme in living cells.

Cancer cells could be a good model for these studies due to the naturally high expression of MAGL in cancer; consequently, we decided to optimize the conditions of the fluorogenic method on B16-F10 melanoma cell lysates.

The results obtained on cancer cell lysates seem to indicate that the potencies of the new synthetic molecules are too close one to the other to have a discrimination of their effect *in vivo*, but in any case a study on their effects on cancer cell lines is still necessary to evaluate if there a positive response to their administration.

We are still far from the definitive discover of potent, selective and safe MAGL inhibitors, but all these studies can help to trace the way to reach that goal.

7. MATERIALS AND INSTRUMENTS

7.1 Reagents

Monoacylglycerol lipase (human recombinant, 25 μg) was purchased from Cayman Chemical (Ann Arbor, MI, USA); arachidonic acid, resorufin, Tris, ethylendiaminetetraacetic acid (EDTA), Hepes, phosphate buffered saline (PBS) tablets, and all other reagents and solvents were purchased from Sigma-Aldrich (St. Louis, MO, USA).

Reaction progress was monitored by analytical thin-layer chromatography (TLC) on pre-coated aluminium foils (Silica Gel 60F254-plate, Sigma-Aldrich), and the products were visualized by UV light.

7.2 Instruments

Fluorescence signals were recorded by a Promega-GloMax multidetection system using a green fluorescence optical kit (excitation 525 nm, emission 580–640 nm) with flat bottom 96-well black plate.

IC_{50} values were calculated as nonlinear regressions using sigmoid dose–response setting with variable Hill slope by GraphPad Prism 5.0 for Windows.

NMR spectra were recorded on a Bruker AVANCE 500 spectrometer equipped with a 5mm broadband reverse probe with field z-gradient operating at 500.13 and 125.76 MHz for 1H and 13C, respectively.

NMR spectra were recorded at 298 K in $CDCl_3$ (isotopic enrichment 99.95%), *d_6*-DMSO (isotopic enrichment 99.98%) or CD_3OD (isotopic enrichment 99.96%) solutions.

The data were collected and processed by XWIN-NMR software (Bruker) running on a PC with Microsoft Windows 7.

The samples (10 mg), were dissolved in the appropriate solvent (0.7 mL) in a 5 mm NMR tube. Acquisition parameters for 1D were as follows: 1H spectral width of 5000 Hz and 32K data points providing a digital resolution of ca. 0.305 Hz per point, relaxation delay 2 s; 13C spectral width of 29,412 Hz and 64 K data points providing a digital resolution of ca. 0.898 Hz per point, relaxation delay 2 s (unless otherwise indicated).

The experimental error in the measured 1H-1H coupling constants was ±0.5 Hz.

Chemical shifts (δ) of the 1H NMR and 13C NMR spectra are reported in ppm using the signal for residual solvent protons resonance as internal standard (1H NMR: $CDCl_3$ 7.26 ppm , *d_6*-DMSO 2.49 ppm, CD_3OD 4.78 ppm, (higher field signal, central line); 13C NMR: $CDCl_3$ 77.0 ppm (central line), *d_6*-DMSO 39.50 ppm (central line), CD_3OD 49.3 (higher field signal, central line).

The splitting pattern abbreviations are as follows: s, singlet; d, doublet; t, triplet; q, quartet; m, multiplet, and bs, broad signal.

For two-dimensional experiments, Bruker microprograms using gradient selection (gs) were applied. All two-dimensional spectra (COSY, HSQC and HMBC) were acquired with 2048 data points for t2 and 256 for t1 increments.

The long-range coupling time for HMBC was 0.07 ms.

The confirmations of the structures were obtained by 500 MHz-NMR spectra, in particular through proton and carbon 1D NMR spectra, as well as by 2D NMR homo-correlation (COSY) and hetero-correlation (HSQC and HMBC) experiments.

Melting points were determined with a Stuart Scientific SMP3 melting point apparatus and left uncorrected.

8. CHEMICAL DATA

General synthetic method for new carbamate compounds

The synthesis was made using the general procedure described by *Szabo et al*[169], which consisted in a two steps process (**scheme 11**).

The first one was a Suzuki palladium tetrakis-catalysed reaction: the appropriate phenilboronic acid was reacted at reflux with *m*-bromoaniline in the presence of sodium carbonate, in dry CH_3OH, to give an intermediate biphenylamine (42 - 65% yield).

The second step was the activation, at reflux, of the intermediate with carbonyl diimidazole (CDI), using DMAP as catalyst and in dry acetonitrile; the subsequent addition in the medium of the proper alcohol and the heating for the necessary time of reaction gave the different desired products with medium to good yields.

Synthesis of 7-hydroxyresorufinyl-arachidonate (7-HRA)

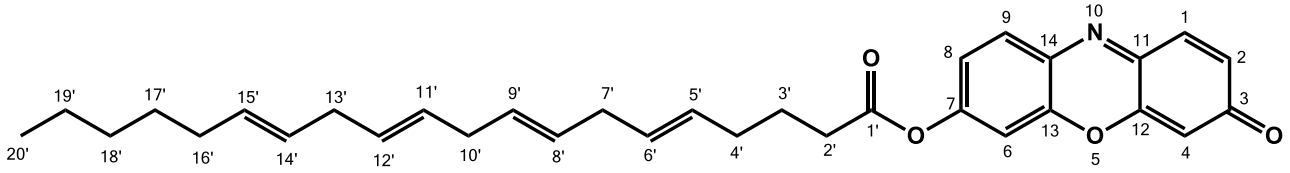

To a solution of arachidonic acid (80 mg, 0.26 mmol) in dry CH_2Cl_2 (10 ml), oxalyl chloride (45 µl, 0.53 mmol) in dry CH_2Cl_2 (1 ml) was added dropwise at 0 °C under stirring.

N,N-dimethylformamide (DMF, 1 drop) was added next. The reaction mixture was stirred at room temperature for 3 h and then concentrated under vacuum, giving crude arachidonoyl chloride.

This residue was dissolved in dry CH_2Cl_2 (5 ml) and added dropwise to an ice-cold suspension of resorufin (67 mg, 0.32 mmol) and triethylamine (55 µl, 0.39 mmol) in dry CH_2Cl_2 (15 ml) and then stirred overnight at room temperature. After dilution with CH_2Cl_2 the salts residues were removed by filtration obtaining a brick-red solution; that was washed with 1M HCl (20 ml), saturated $NaHCO_3$ (25 ml), dried on anhydrous sodium sulfate and concentrated to give the crude product. Column chromatography on silica gel (CH_2Cl_2:CH_3OH, 95:5) gave the product (80 mg, 0.16 mmol, 62%) as a red oil.

MM=499.6 g/mol

TLC (Rf=0.84, CH_2Cl_2:CH_3OH, 90:10).

^{1}H NMR ($CDCl_3$, 500 MHz): δ (ppm) 7.82 (1H, d, J=8.7 Hz, 1-H), 7.46 (1H, d, J=9.8 Hz, 9-H), 7.17 (1H, d, J=2.4 Hz, 4-H), 7.14 (1H, dd, J=8.7, 2.4 Hz, 2-H), 6.89 (1H, dd, J=9.8, 2.0 Hz, 8-H), 6.36 (1H, d, J=2.0 Hz, 6-H), 5.52-5.33 (8H, m, 5′- 6′- 8′- 9′- 11′- 12′- 14′- and 15′-CH), 2.88-2.82 (6H, m, 7′- 10′- and 13′-CH_2), 2.65 (2H, t, J=7.0 Hz, 2′-CH_2), 2.25 (2H, dt, J=7.4, 7.0 Hz, 4′-CH_2), 2.07 (2H, dt, J=7.6, 7.6 Hz, 16′-CH_2), 1.88 (2H, tt, J=7.6, 7.0 Hz, 3′-CH_2), 1.39-1.28 (6H, m, 17′-19′ CH_2), 0.91 (3H, t, J=7.6 Hz, 20′-CH_3).

^{13}C NMR: δ (ppm) 186.3 (3), 171.2 (1′), 153.6 (7), 149.4 (11), 148.3 (12), 144.4 (13), 135.2 (8), 134.8 (9), 131.3 (14), 131.2 (1), 130.6 (5′, 6′, 8′, 9′, 11′, 12′, 14′, 15′),129.5, 128.7, 128.5, 128.4, 128.1, 127.8, 127.5, 119.3 (2), 109.7 (4), 107.3 (6), 33.7 (2′), 27.2 (16′), 26.5 (4′), 25.7 (7′, 10′, 13′), 24.6 (3′), 31.5 (18′), 29.3 (17’), 22.6 (19′), 14.1 (20′).

Synthesis of intermediate [1,1'-biphenyl]-3-amine (**4a**)

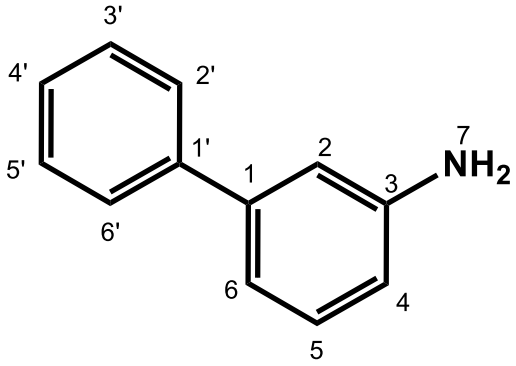

To a solution of phenylboronic acid (500 mg, 4.13 mmol) in CH_3OH (8 ml), Na_2CO_3 (911 mg, 8.6 mmol, 2 eq.) and 3-bromoaniline (414 µl, 4.13 mmol, 1 eq.) were added. After addition of $Pd(PPh_3)_4$ (160 mg, 0.139 mmol, 0.034 eq.) the reaction mixture was heated at reflux for 12 h.

The solution was cooled to r.t, diluted with methanol and filtered through celite to remove the black precipitate; water was added and the aqueous phase was washed with 2x15 ml CH_2Cl_2.

The organic fractions were combined and dried over anhydrous Na_2SO_4, filtered and evaporated to give the crude product.

The oily crude product was purified by chromatography on silica gel (petroleum ether:CH_3OH, 90:10 followed by 80:20) to give the final product **4a** (423 mg, 2.50 mmol, 65%) as a yellow oil.

MM=169.2 g/mol

TLC (Rf=0.30, petroleum ether:CH_3OH, 90:10).

^{1}H NMR ($CDCl_3$, 500MHz): δ 7.58 (2H, d, J=7.4 Hz, 2′- and 6′-H), 7.43 (2H, dd, J=8.3, 7.4 Hz, 3′- and 5′-H), 7.35 (1H, t, J=7.4 Hz, 4′-H), 7.24 (1H, dd, J=7.8, 7.6 Hz, 5-H), 7.01 (1H, ddd, J=7.6, 1.0, <1.0 Hz, 6-H), 6.92 (1H, dd, J=2.4, <1.0 Hz, 2-H), 6.69 (1H, ddd, J= 7.8, 2.4, 1.0 Hz, 4-H), 3.75 (2H, s, 7-NH_2).

^{13}C NMR: δ 146.7 (3), 142.5 (1), 141.4 (1′), 129.7 (5), 128.6 (3′ and 5′), 127.2 (4′), 127.1 (6′ and 2′), 117.7 (6), 114.1 (4), 114.0 (2).

Synthesis of cyclohexyl [1,1'-biphenyl]-3-ylcarbamate (**URB602**)

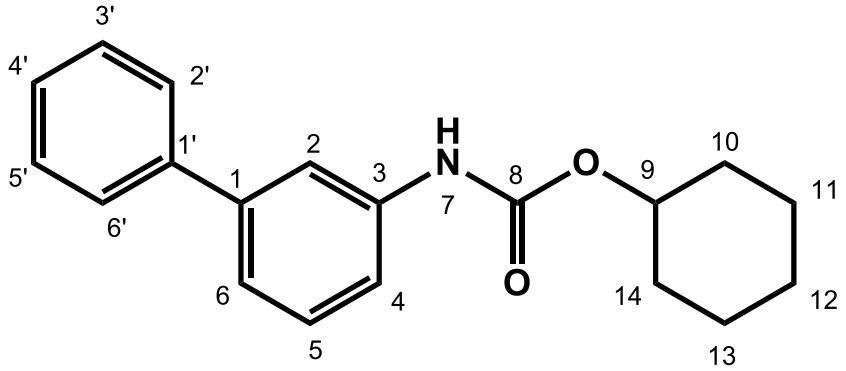

CDI (959 mg, 5.92 mmol, 4 eq.), DMAP (36.2 mg, 0.296 mmol, 0.2 eq.) and byphenyl-3-ylamine **4a** (251 mg, 1.48 mmol, 1 eq.) were mixed in dry AcCN (5 ml) and heated at reflux overnight; cyclohexanol (2.35 ml, 22.2 mmol, 15 eq.) was added to the obtained red solution and the reaction heated at 100°C for 24 h.

The reaction was cooled to r.t and evaporated *in vacuo* to give the crude product, which was then purified by chromatography on silica gel using a mixture petroleum ether:EtOAc, 95:5; the final product was then recovered by crystallisation adding cold *n*-hexane to its solution in CH_2Cl_2, obtaining 302 mg (1.02 mmol, 69%) of **URB602** as white needles.

MM=295.4 g/mol

TLC (Rf=0.22, petroleum ether:ethyl acetate, 95:5).

mp: 119.6-121.3 °C

^{1}H NMR ($CDCl_3$, 500MHz): δ (ppm) 7.70 (1H, s, 2-H), 7.62 (2H, d, J=7.2 Hz, 2'- and 6'-H), 7.45 (2H, t, J=7.6 Hz, 3'- and 5'-H), 7.42-7.34 (3H, m, 4'- 5- and 6-H), 7.32 (1H, d, J=7.1 Hz, 4-H), 6.67 (1H, s, 7-NH), 4.81 (1H, m, 9-CH), 2.03-1.92 (2H, m, 10-H_{eq} and 14-H_{eq}), 1.84-1.74 (2H, m, 11-H_{eq} and 13-H_{eq}), 1.62-1.56 (1H, m, 12-H_{eq}), 1.56-1.47 (2H, m, 10-H_{ass} and 14-H_{ass}), 1.47-1.38 (2H, m, 11- H_{ass} and 13'-H_{ass}), 1.30 (1H, m, 12-H_{ass}).

^{13}C NMR: δ (ppm) 153.2 (8), 142.2 (3), 140.8 (1), 138.5 (1'), 128.8 (5), 127.2 (2', 4' and 6'), 127.5 (3' and 5'), 122.1 (4), 117.4 (2 and 6), 73.8 (9), 32.0 (10 and 14), 25.4 (12), 23.9 (11 and 13).

Synthesis of benzyl [1,1'-biphenyl]-3-ylcarbamate (**1a**)

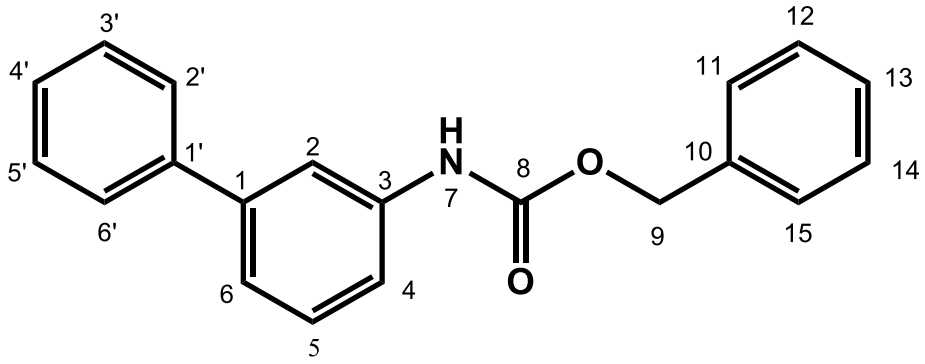

CDI (1148 mg, 7.08 mmol, 4 eq.), DMAP (43.3 mg, 0.354 mmol, 0.2 eq.) and byphenyl-3-ylamine **4a** (300 mg, 1.77 mmol, 1 eq.) were mixed in dry AcCN (8 ml) and heated at reflux overnight; phenyl methanol (917 µl, 8.85 mmol, 5 eq.) was added and the reaction heated at 100°C for 48 h obtaining a clear brown mixture.

The solution was cooled to r.t, the solvent removed by evaporation and the crude product purified by chromatography on silica gel (petroleum ether:EtOAc, 90:10); the crystallisation in CH_2Cl_2/cold *n*-hexane gave product **1a** (148 mg, 0.49 mmol, 30%) as a white powder.

MM=303.4 g/mol

TLC (Rf=0.33, petroleum ether:ethyl acetate, 95:5).

mp: 73.2-73.9 °C

^{1}H NMR ($CDCl_3$, 500 MHz): δ (ppm) 7.68 (1H, br. s, 2-H), 7.61 (2H, d, J=7.3 Hz, 2'- and 6'-H), 7.48-7.43 (5H, m, 3'- 4'- 5'- 12- and 14-H), 7.42 (1H, s, 4-H), 7.41-7.36 (4H, m, 11- 13- 15- and 6-H), 7.33 (1H, dd, J=8.7, 1.8 Hz, 5-H), 6.79 (1H, br. s, 7-NH), 5.26 (2H, s, 9-CH_2).

^{13}C NMR: δ (ppm) 153.4 (8), 142.3 (3), 140.7 (1), 138.2 (1'), 136.1 (10), 129.5 (5), 128.8 (3' and 5'), 128.7 (12 and 14), 128.4 (6, 2' and 6'), 128.4 (4), 127.5 (4' and 13), 127.2 (11 and 15), 122.4 (2), 67.1 (9).

Synthesis of 1-phenylethyl [1,1'-biphenyl]-3-ylcarbamate (**1b**)

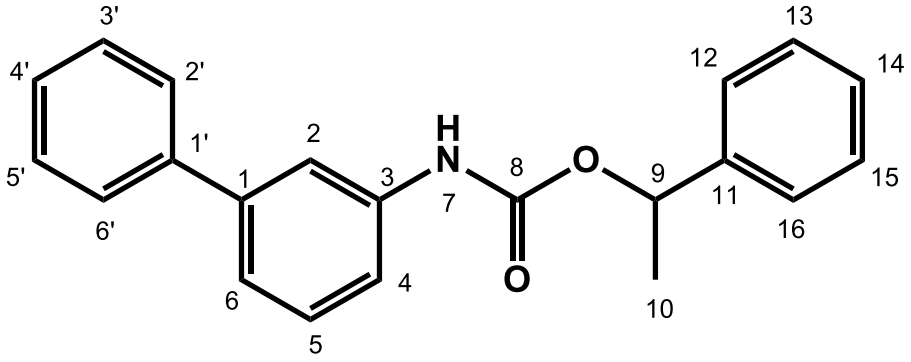

CDI (574.7 mg, 3.54 mmol, 4 eq.), DMAP (21.7 mg, 0.18 mmol, 0.2 eq.) and byphenyl-3-ylamine **4a** (150 mg, 0.88 mmol, 1 eq.) were mixed in dry AcCN (5 ml) and heated at reflux overnight; 1-phenylethanol (531 µl, 4.43 mmol, 5 eq.) was added and the reaction heated at 100°C for 24 h till the obtaining of a turbid pink solution.

After cooling to r.t, the solvent was removed by evaporation and the crude product purified by chromatography on silica gel (petroleum ether:EtOAc, 90:10), giving product **1b** (203 mg, 0.64 mmol, 72%) as a yellow oil.

MM=317.4 g/mol

TLC (Rf=0.28, petroleum ether:ethyl acetate, 90:10).

^{1}H NMR ($CDCl_3$, 500 MHz): δ (ppm) 7.68 (1H, s, 2-H), 7.59 (2H, d, J=7.8 Hz, 2'- and 6'-H), 7.48-7.42 (4H, m, 3'- 4'- 5'- and 4-H), 7.41-7.19 (7H, m, 5- 6- 12- 13- 14- 15- and 16-H), 6.75 (1H, s, 7-NH), 5.95 (1H, q, J=6.6 Hz, 9-CH), 1.65 (3H, d, J=6.6 Hz, 10-CH_3).

^{13}C NMR: δ (ppm) 153.8 (8), 144.5 (11), 143.9 (3), 143.1 (5), 131.7 (1 and 1'), 130.9 (3' and 5'), 130.3 (13 and 15), 129.8 (2'and 6'), 129.5 (4'and 14), 128.4 (12 and 16), 124.6 (6), 119.7 (2 and 4), 75.7 (9), 24.6 (10).

Synthesis of phenethyl [1,1'-biphenyl]-3-ylcarbamate (**1c**)

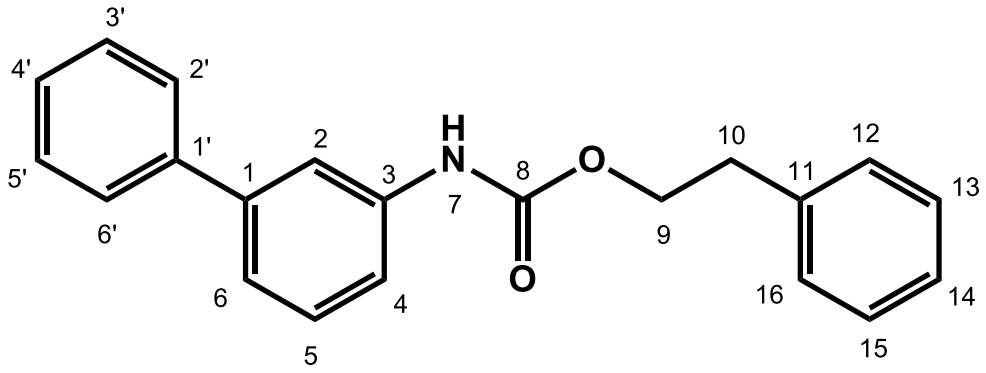

CDI (747 mg, 4.6 mmol, 4 eq.), DMAP (28.0 mg, 0.23 mmol, 0.2 eq.) and byphenyl-3-ylamine **4a** (195 mg, 1.15 mmol, 1 eq.) were mixed in dry AcCN (8 ml) and heated at reflux overnight; 2-phenylethanol (1100 µl, 9.22 mmol, 8 eq.) was added and the reaction heated at 100°C for 24 h obtaining an orange clear solution.

The reaction was cooled to r.t, the solvent was removed by evaporation and the crude product purified by chromatography on silica gel (petroleum ether, 100 followed by petroleum ether:EtOAc, 80:20); the crystallisation in CH_2Cl_2/cold *n*-hexane gave product **1c** (200.4 mg, 0.63 mmol, 54%) as a white crystalline solid.

MM=317.4 g/mol

TLC (Rf=0.41, petroleum ether:ethyl acetate, 80:20).

mp: 98.2-99.4 °C

^{1}H NMR ($CDCl_3$, 500 MHz): δ (ppm) 7.66 (1H, br. s., 2-H), 7.61 (2H, d, J=7.6 Hz, 2'- and 6'-H), 7.46 (2H, t, J=7.6 Hz, 3'- and 5'H), 7.42-7.37 (3H, m, 4- 4'- and 5-H), 7.37-7.31 (3H, m, 6- 13- and 15-H), 7.29 (3H, d, J=7.4 Hz, 12- 16- and 14-H), 6.69 (1H, br. s., 7-NH), 4.45 (2H, t, J=6.9 Hz, 9-CH_2), 3.04 (2H, t, J=6.9 Hz, 10-CH_2).

^{13}C NMR: δ (ppm) 153.5 (8), 141.9 (1'), 140.6 (1 and 3), 137.8 (11), 129.2 (4'), 128.82 (12 and 16), 128.80 (3' and 5'), 128.78 (13 and 15), 128.4 (4 and 5), 127.2 (2' and 6'), 127.22 (14), 122.3 (6), 117.5 (2), 65.7 (9), 35.5 (10).

Synthesis of furan-2-ylmethyl [1,1'-biphenyl]-3-ylcarbamate (**1d**)

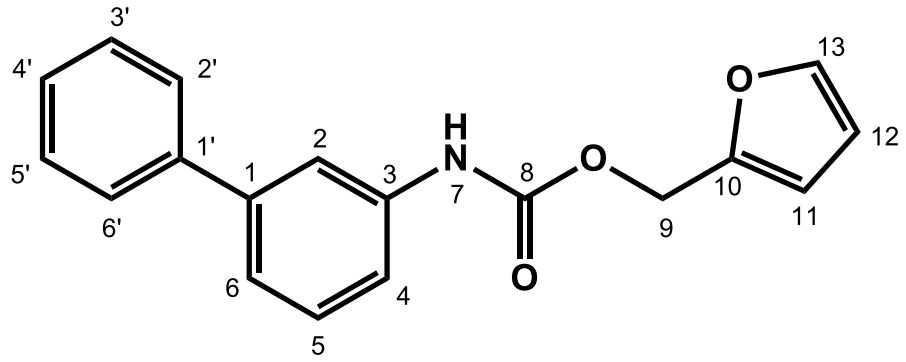

To a solution of **4a** (250 mg, 1.48 mmol, 1 eq.) in dry AcCN (10 ml) were added CDI (350 mg, 2.22 mmol, 1.5 eq.) and DMAP (90 mg, 0.74 mmol, 0.5 eq.); the mixture was heated at reflux for 24 h. Freshly distilled 2-furfuryl alcohol (767 µl, 8.88 mmol, 6 eq.) was added and the reaction heated at 100°C for 24 h giving a yellow solution.

After cooling to r.t, the solvent was evaporated and the crude product purified by chromatography on silica gel (petroleum ether:EtOAc, 90:10 followed by 70:30); giving the brown oil product **1d** in low amount (195 mg, 0.66 mmol, 45%).

MM=293.3 g/mol

TLC (Rf=0.61, petroleum ether:ethyl acetate, 75:25).

^{1}H NMR ($CDCl_3$, 500 MHz): δ (ppm) 7.67 (1H, br. s, 2-H), 7.60 (2H, dd, J=7.8, 1.3 Hz, 2'- and 6'-H), 7.49-7.46 (3H, m, 13- 3'- and 5'-H), 7.45 (1H, d, J=7.9 Hz, 4'-H), 7.41-7.35 (2H, m, 5- and 6-H), 7.35-7.30 (1H, dt, J=7.0, 1.7 Hz, 4-H), 6.77 (1H, s, 7-NH), 6.50 (1H, t, J=3.8 Hz, 11-H), 6.41 (1H, dd, J=4.1, 2.1 Hz, 12-H), 5.21 (2H, s, 9-CH_2).

^{13}C NMR: δ (ppm) 153.3 (8 and 10), 143.4 (13, 3' and 5'), 130.4 (3), 128.8 (4'), 127.5 (1 and 1'), 127.2 (5, 2' and 6'), 122.5 (4), 117.6 (2 and 6), 110.8 (11), 110.7 (12), 58.2 (9).

Synthesis of 1,3-di([1,1'-biphenyl]-3-yl)urea (**1e**)

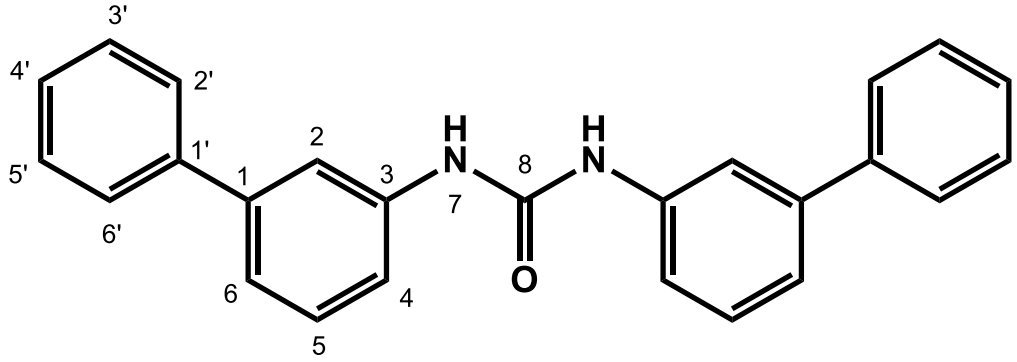

CDI (1148 mg, 7.08 mmol, 4 eq.), DMAP (43.3 mg, 0.354 mmol, 0.2 eq.) and byphenyl-3-ylamine **4a** (300 mg, 1.77 mmol, 1 eq.) were mixed in dry AcCN (8 ml) and heated at reflux overnight; phenol (777 μl, 8.85 mmol, 5 eq.) was added to the obtained red solution and the reaction heated at 100°C for 6 h obtaining a suspension of a white solid.

After cooling to r.t the solid was filtered *under vacuum*, washed with cold CH_2Cl_2/AcCN to remove the excess of CDI, and dried to obtain 255 mg (0.70 mmol, 79%) of **1e** as a white crystalline solid.

MM=364.4 g/mol

TLC (Rf=0.24, petroleum ether:ethyl acetate, 90:10).

mp: 258.2-259.0 °C

^{1}H NMR (d_6-DMSO, 500 MHz): δ (ppm) 8.85 (2H, s, 7-NH), 7.84 (2H, t, J=1.6 Hz, 2-H), 7.64 (4H, dd, J=8.2, 1.0 Hz, 2'- and 6'-H), 7.49 (4H, t, J=7.6 Hz, 3'- and 5'-H), 7.43 (2H, t, J=4.9 Hz, 4'-H), 7.39 (4H, dt, J=7.5, 1.3 Hz, 5- and 6-H), 7.28 (2H, dt, J=7.5, 1.3 Hz, 4-H).

^{13}C NMR: δ (ppm) 153.2 (8), 141.9 (1), 140.8 (1'), 140.7 (3), 129.9 (5), 129.4 (3' and 5'), 128.0 (6), 127.2 (2' and 6'), 120.9 (4), 117.9 (4'), 117.1 (2).

Synthesis of intermediate 4'-(trifluoromethyl)-[1,1'-biphenyl]-3-amine (**4b**)

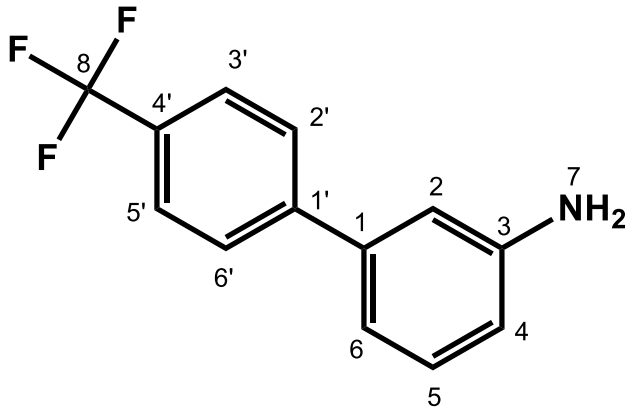

4-(Trifluoromethyl)phenylboronic acid (500 mg, 2.63 mmol, 1 eq.) was dissolved in CH_3OH (7 ml); Na_2CO_3 (558 mg, 5.27 mmol, 2 eq.) and 3-bromoaniline (430 µl, 3.95 mmol, 1.5 eq.) were added. $Pd(PPh_3)_4$ (103 mg, 0.09 mmol, 0.034 eq.) was added to the mixture under argon and the reaction was heated at reflux for 10 h, obtaining a dark suspension.

The mixture was cooled to r.t, diluted with methanol and filtered through celite to remove the black precipitate; water was added and the aqueous phase was washed with 2x15 ml CH_2Cl_2.

The organic fractions were combined and dried over anhydrous Na_2SO_4, filtered and evaporated to give an oily orange crude product; that was purified by chromatography on silica gel (petroleum ether:CH_3OH, 90:10 followed by 70:30) and crystallisation with CH_2Cl_2/cold *n*-hexane gave the final product **4b** (258 mg, 1.05 mmol, 42%) as a white crystalline solid.

MM=237.2 g/mol

TLC (Rf=0.42, petroleum ether:ethyl acetate, 70:30).

mp: 90.2-90.8 °C

^{1}H NMR (CD_3OD, 500 MHz): δ (ppm) 6.24 (2H, d, J=8.2 Hz, 3'- and 5'-H), 6.19 (2H, d, J=8.2 Hz, 2'- and 6'-H), 5.77 (1H, t, J=7.9 Hz, 5-H), 5.61 (1H, J<1 Hz, 2-H), 5.59 (1H, d, J<1 Hz, 6-H), 5.37 (1H, dd, J=11.7, 4.7 Hz, 4-H).

^{13}C NMR: δ (ppm) 144.3 (3), 140.8 (1'), 138.3 (1), 129.4 (5 and 4'), 127.5 (2' and 6'), 125.7 (3' and 5'), 122.5 (4 and 8), 118.4 (6), 117.4 (2).

Synthesis of cyclohexyl (4'-(trifluoromethyl)-[1,1'-biphenyl]-3-yl)carbamate (**2a**)

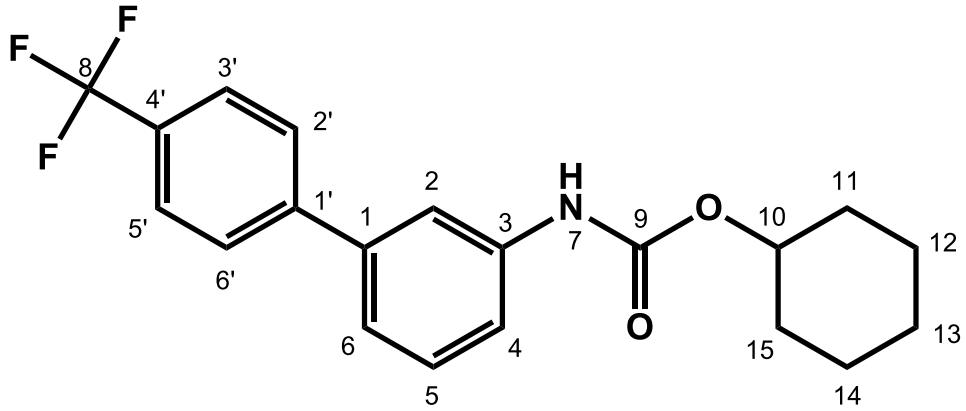

To a solution of **4b** (125 mg, 0.527 mmol, 1 eq.) in dry AcCN (8 ml), CDI (342 mg, 2.11 mmol, 4 eq.) and DMAP (12.9 mg, 0.105 mmol, 0.2 eq.) were added and the mixture heated at reflux overnight; cyclohexanol (557 µl, 5.27 mmol, 10 eq.) was added to the obtained red solution and the reaction heated at 100°C for 24 h.

The reaction was cooled to r.t, the solvent was removed by evaporation and the crude product purified by chromatography on silica gel (petroleum ether:EtOAc, 90:10 followed by 80:20); the crystallisation in CH_2Cl_2/cold *n*-hexane gave product **2a** (111.3 mg, 0.31 mmol, 58%) as a fine white solid.

MM=363.4 g/mol

TLC (Rf=0.62, petroleum ether:ethyl acetate, 80:20).

mp: 124.8-126.2 °C

^{1}H NMR ($CDCl_3$, 500 MHz): δ (ppm) 7.78 (1H, s, 2-H), 7.74-7.67 (4H, t, J=9.6 Hz, 2'- 3'-5' and 6'-H), 7.42 (1H, t, J=7.8 Hz, 5-H), 7.36 (1H, d, J=7.9 Hz,4-H), 7.31 (1H, d, J=7.5 Hz, 6-H), 6.69 (1H, s, 7-NH), 4.84-4.74 (1H, m, 10-CH), 1.97 (2H, dd, J=8.0, 2.3 Hz, 11-H_{eq} and 15-H_{eq}), 1.79 (2H, dd, J=10.1, 4.4 Hz, 12-H_{eq} and 14-H_{eq}), 1.61 (1H, s, 13-H_{eq}), 1.49 (2H, dd, J=12.4, 10.4 Hz, 11-H_{ass} and 15-H_{ass}), 1.42 (2H, dd, J=12.7, 10.9 Hz, 12-H_{ass} and 14-H_{ass}), 1.33-1.27 (1H, m, 13-H_{ass}).

^{13}C NMR: δ (ppm) 153.2 (9), 146.3 (1), 144.3 (1'), 140.7 (4'), 138.8(3), 129.6 (5), 127.5 (2' and 6'), 125.7 (3' and 5'), 122.1 (6), 118.2 (4), 117.4 (2), 73.9 (10), 32.0 (11 and 15), 25.4 (13), 23.8 (12 and 14).

Synthesis of benzyl (4'-(trifluoromethyl)-[1,1'-biphenyl]-3-yl)carbamate (**2b**)

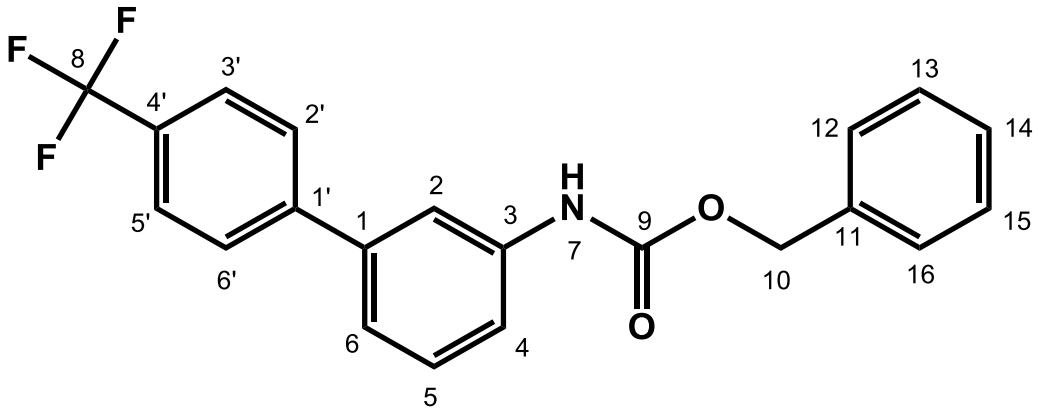

CDI (342 mg, 2.11 mmol, 4 eq.), DMAP (12.9 mg, 0.105 mmol, 0.2 eq.) and **4b** (125 mg, 0.527 mmol, 1 eq.) were mixed in dry AcCN (8 ml) and heated at reflux overnight; phenyl methanol (546 µl, 5.27 mmol, 10 eq.) was added and the reaction heated at 100°C for 24 h obtaining a yellow solution.

The reaction was cooled to r.t, the solvent was removed by evaporation and the crude product purified by chromatography on silica gel (petroleum ether, 100 followed by petroleum ether:EtOAc 80:20); the crystallisation with CH_2Cl_2/cold *n*-hexane gave product **2b** (126 mg, 0.34 mmol, 64%) as a white crystalline solid.

MM=371.4 g/mol

TLC (Rf=0.59, petroleum ether:ethyl acetate, 80:20).

mp: 114.6-116.0 °C

^{1}H NMR ($CDCl_3$, 500 MHz): δ (ppm) 7.75 (1H, s, 2-H), 7.70 (4H, s, 3'- 5'- 4- and 5-H), 7.49-7.35 (7H, m, 2'- 6'- 12- 13- 14- 15- and 16-H), 7.33 (1H, dt, J=7.4, 1.5 Hz, 6-H), 6.80 (1H, s, 7-NH), 5.27 (2H, s, 10-CH_2).

^{13}C NMR: δ (ppm) 153.3 (9), 144.3 (1), 140.8 (1'), 138.5 (3), 135.9 (11), 129.7 (4'), 128.7 (13 and 15), 128.5 (2' and 6'), 128.4 (12 and 16), 127.5 (14), 125.9 (3' and 5'), 122.5 (6), 118.3 (4), 117.6 (2), 67.2 (10).

Synthesis of furan-2-ylmethyl 4'-(trifluoromethyl)biphenyl-3-ylcarbamate (**2c**)

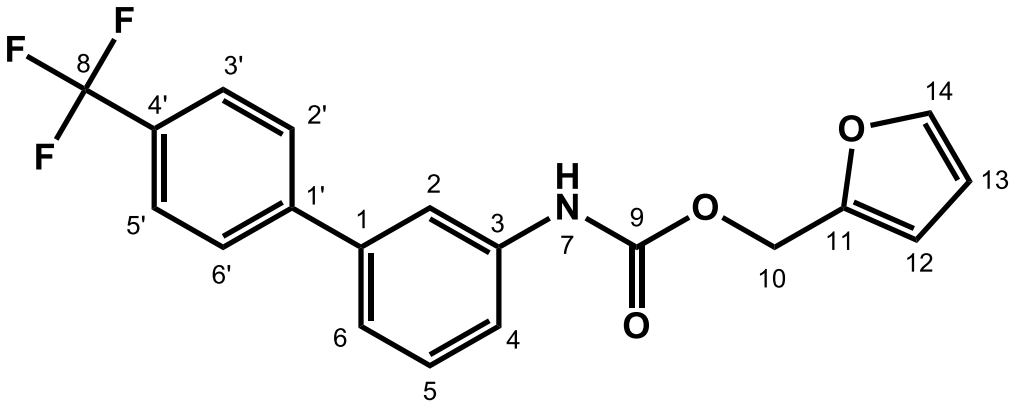

CDI (273 mg, 1.68 mmol, 2 eq.), DMAP (51.0 mg, 0.42 mmol, 0.5 eq.) and **4b** (200 mg, 0.843 mmol, 1 eq.) were mixed in dry AcCN (8 ml) and heated at reflux for 24 h; Freshly distilled 2-furfuryl alcohol (437 µl, 10.1 mmol, 6 eq.) was added and the reaction heated at 100°C overnight.

After cooling to r.t, the solvent was removed by evaporation and the crude product purified by chromatography on silica gel (petroleum ether:EtOAc, 85:15 followed by 70:30); the obtained yellow solid was dissolved in CH_2Cl_2 and crystallised adding cold *n*-hexane giving the white crystalline product **2c** in poor yeld (213 mg, 0.59 mmol, 70%).

MM=361.3 g/mol

TLC (Rf=0.63, petroleum ether:ethyl acetate, 80:20).

mp: 119.2-120.0 °C

^{1}H NMR ($CDCl_3$, 500 MHz): δ (ppm) 7.74 (1H, br.s, 2-H), 7.72-7.67 (4H, m, 2'- 3'- 5' and 6'-H), 7.48 (1H, dd, J=1.7, <1 Hz, 14-H), 7.42 (1H, t, J=7.8 Hz, 5-H), 7.36 (1H, d, J=8.0 Hz, 6-H), 7.32 (1H, dt, J=7.4, 1.4 Hz, 4-H), 6.78 (1H, br.s, 7-NH), 6.51 (1H, d, J=3.2 Hz, 12-H), 6.41 (1H, dd, J=5.9, 2.7 Hz, 13-H), 5.21 (2H, s, 10-H).

^{13}C NMR: δ (ppm) 153.0 (9), 149.5 (11), 144.3 (3), 143.5 (14), 140.8 (1'), 138.3 (1), 129.4 (5 and 4'), 127.5 (2' and 6'), 125.7 (3' and 5'), 122.5 (4 and 8), 118.4 (6), 117.4 (2), 110.9 (12), 110.7 (13), 58.8 (10).

Synthesis of intermediate 4'-fluoro-[1,1'-biphenyl]-3-amine (**4c**)

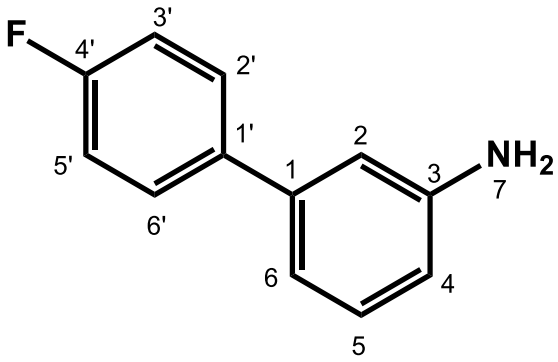

4-Fluorophenylboronic acid (500 mg, 3.57 mmol, 1 eq.), Na_2CO_3 (758 mg, 7.15 mmol, 2 eq.) and 3-bromoaniline (584 µl, 5.36 mmol, 1.5 eq.) were mixed in CH_3OH (8 ml). $Pd(PPh_3)_4$ (140 mg, 0.12 mmol, 0.034 eq.) was added under argon and the reaction was heated at reflux for 10 h, obtaining a dark suspension.

After cooling to r.t, the mixture was diluted with methanol and filtered through celite to remove the black precipitate; water was added and the aqueous phase was washed with 2x15 ml CH_2Cl_2.

The organic fractions were combined and dried over anhydrous Na_2SO_4, filtered and evaporated to give a black oil; the crude product was purified by chromatography on silica gel (petroleum ether:CH_3OH, 90:10 followed by 75:15) and crystallisation with CH_2Cl_2/cold *n*-hexane gave rise to the final product **4c** (436 mg, 2.32 mmol, 65%) which is an ochre powder.

MM=187.2 g/mol

TLC (Rf=0.46, petroleum ether:ethyl acetate, 80:20).

mp: 63.6-64.9 °C

^{1}H NMR (CD_3OD, 500 MHz): δ (ppm) 7.58 (2H, m, 2'- and 6'-H), 7.19-7.12 (3H, m, 5- 3'- and 5'-H), 6.96 (1H, t, J=1.9 Hz, 2-H), 6.93-6.8 (1H, m, J=7.0 Hz, 6-H), 6.72 (1H, ddd, J=7.9, 2.2, <1 Hz, 4-H).

^{13}C NMR: δ (ppm) 163.4 (4'), 147.8 (3), 140.9 (1), 137.9 (1'), 129.2 (5), 128.3 (2' and 6'), 116.5 (6), 116.5 (6), 114.9 (3' and 5'), 114.2 (4), 113.6 (2).

Synthesis of cyclohexyl (4'-fluoro-[1,1'-biphenyl]-3-yl)carbamate (**3a**)

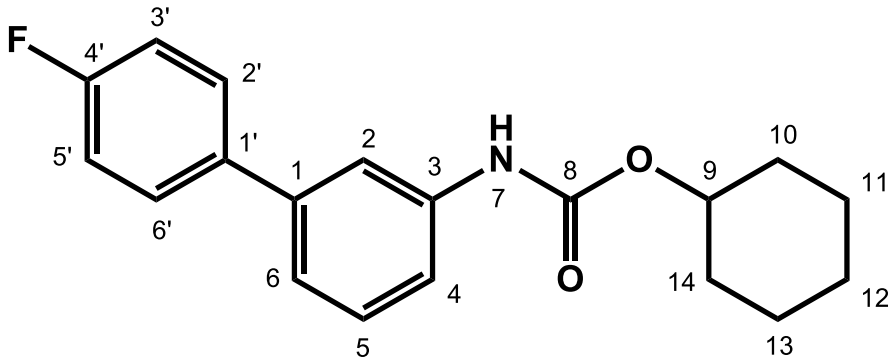

To a solution of **4c** (200 mg, 1.07 mmol, 1 eq.) in dry AcCN (8 ml), CDI (693 mg, 4.27 mmol, 4 eq.) and DMAP (27.0 mg, 0.214 mmol, 0.2 eq.) were added and the mixture heated at reflux overnight; cyclohexanol (1.13 ml, 10.7 mmol, 10 eq.) was added to the obtained red solution and the reaction heated at 100°C for 24 h.

After cooling to r.t, the solvent was removed and the crude product purified by chromatography on silica gel (petroleum ether:EtOAc, 90:10 followed by 80:20) giving a colourless oil; that was treated with cold *n*-hexane to give final product **3a** as a white powder (247.8 mg, 0.79 mmol, 74%).

MM=313.4 g/mol

TLC (Rf=0.59, petroleum ether:ethyl acetate, 80:20).

mp: 124.6-125.0 °C

^{1}H NMR ($CDCl_3$, 500 MHz): δ (ppm) 7.70 (1H, s, 2-H), 7.57 (2H, dd, J=8.7, 5.3 Hz, 2'- and 6'-H), 7.38 (1H, t, J=7.8 Hz, 5-H), 7.32 (1H, d, J=8.3 Hz, 4-H), 7.25 (1H, d, J=7.6 Hz, 6-H), 7.13 (2H, t, J=8.7 Hz, 3'- and 5'-H), 6.68 (1H, s, 7-NH), 4.83-4.75 (1H, m, 9-CH), 2.01-1.94 (2H, m, 10-H_{eq} and 14-H_{eq}), 1.80-1.75 (2H, m, 11-H_{eq} and 13-H_{eq}), 1.64-1.55 (1H, m, 12-H_{eq}), 1.53-1.46 (2H, m, 10-H_{ass} and 14-H_{ass}), 1.46-1.38 (2H, m, 11-H_{ass} and 13-H_{ass}), 1.33-1.25 (1H, m, 12-H_{ass}).

^{13}C NMR: δ (ppm) 163.6 (4'), 153.2 (8), 141.2 (1), 138.6 (1'), 136.9 (3), 129.5 (2' and 6'), 128.8 (5), 121.9 (6), 117.3 (2), 115.7 (3' and 5'), 115.5 (4), 73.9 (9), 32.0 (10 and 14), 25.4 (12), 23.8 (11 and 13).

Synthesis of benzyl (4'-fluoro-[1,1'-biphenyl]-3-yl)carbamate (**3b**)

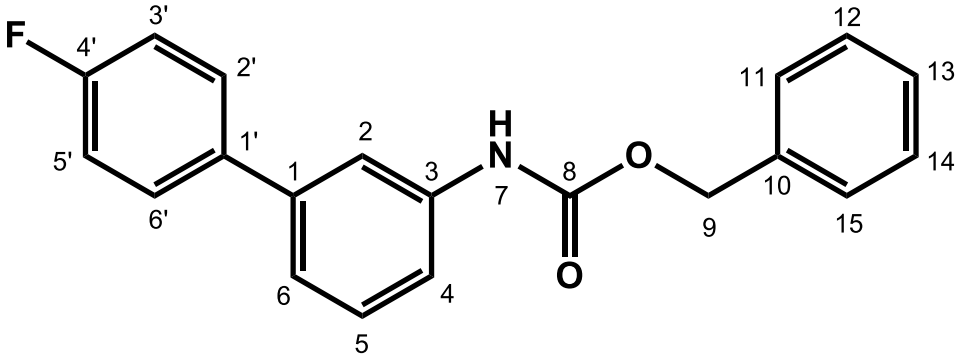

CDI (693 mg, 4.27 mmol, 4 eq.), DMAP (27.0 mg, 0.23 mmol, 0.2 eq.) and **4c** (200 mg, 1.07 mmol, 1 eq.) were mixed in dry AcCN (8 ml) and heated at reflux overnight; phenyl methanol (1100 µl, 10.68 mmol, 10 eq.) was added and the reaction heated at 100°C for 24 h.

The reaction was cooled to r.t, the solvent was removed by evaporation and the crude product purified by chromatography on silica gel (petroleum ether:EtOAc 85:15) giving a white semisolid; this was dissolved in CH_2Cl_2 and crystallised by adding cold *n*-hexane leading to product **3b** (273.3 mg, 0.85 mmol, 80%) as a white powder.

MM=321.3 g/mol

TLC (Rf=0.55, petroleum ether:ethyl acetate, 80:20).

mp: 82.2-82.8 °C

^{1}H NMR ($CDCl_3$, 500 MHz): δ (ppm) 7.64 (1H, d, 2-H), 7.55 (2H, t, J=5.8 Hz, 2'- and 6'-H), 7.47-7.40 (3H, t, J=9.2 Hz, 11- 13- and 15-H), 7.39 (3H, m, 5- 12- and 14-H), 7.33 (1H, d, J=7.3 Hz, 4-H), 7.27 (1H, d, J=7.5 Hz, 6-H), 7.14 (2H, t, J=8.5 Hz, 3'- and 5'-H), 6.79 (1H, br.s, 7-NH), 5.25 (2H, s, 9-CH_2).

^{13}C NMR: δ (ppm) 163.6 (4'), 153.6 (8), 141.3 (1), 136.9 (3), 136.5 (1'), 136.0 (10), 129.6 (5), 128.9 (2' and 6'), 128.7 (12 and 14), 128.5 (13), 128.4 (11 and 15), 122.3 (6), 117.5 (4), 117.3 (2), 115.5 (3' and 5'), 67.2 (9).